Dissertation zur Erlangung des Doktorgrades
der Fakultät für Chemie und Pharmazie
der Ludwig-Maximilians-Universität München

Regulation of Integrin-linked Kinase (ILK) Stability

Korana Radovanac

aus

Belgrad, Serbien

2012

Erklärung

Diese Dissertation wurde im Sinne von § 7 der Promotionsordnung vom 28. November 2011 von Herrn Prof. Dr. Reinhard Fässler betreut.

Eidesstattliche Versicherung

Diese Dissertation wurde eigenständig und ohne unerlaubte Hilfe erarbeitet.

München, 11.06.2012

(Unterschrift des Autors / der Autorin)

Dissertation eingereicht am 11.06.2012

1. Gutachterin / 1. Gutachter: Prof. Dr. Reinhard Fässler

2. Gutachterin / 1. Gutachter: Prof. Dr. Christian Wahl-Schott

Mündliche Prüfung am 05.07.2012

Table of Contents

Acknowledgements

The work presented in this thesis was performed at Max Planck Institute of Biochemistry in Martinsried, a stimulating place both intellectually and culturally, with a help and support of the wonderful people around me, to only some of whom is possible to give a special gratitude here.

First and foremost I owe my sincerest gratitude to my supervisor Prof. Dr. Reinhard Fässler whose expertise and vast knowledge were instrumental for carrying out this project and my thesis. I am truly thankful to Dr. Sara A. Wickström for supporting me throughout my entire doctoral work, patiently reviewing my thesis and for starting this project in the first place, together with Dr. Anika Böttcher.

To Dr. Anika Böttcher, Dr. Aurelia Raducanu and Dr. Esra Karaköse I am eternally grateful both for all the helpful scientific discussions and ``therapy´´ needed to cope with the everyday stress of PhD work.

I am thankful to Dr. Julien Polleux for all the great discussions on cell migration and his student Zhu Min for producing those wonderful micropatterns.

I would also like to express my gratitude to Misha Hildegard Reiter, Michal Grzejszczyk and Ushi Ursula Kuhn for taking care of all of us PhD students and passing on their admirable knowledge and experience.

Last but not least I have to thank my family and my best friends who had stood by me all this time. To Ivanka Ješić and Tamara Osoba, my oldest friends, I am grateful for always giving me a perspective of the rest of the world, which might have gotten lost during hard work in the lab. To Raphael Ruppert for going through this with me, always keeping me grounded. Finally, I am thankful to my family who has supported me my whole life and encouraged me to pursue my dreams and interests even when it meant moving 1000 km away from them. The notion of having somebody to turn to, to count on in every moment of my life both happy and hard, has given me the strength and courage I need in life. Thank you.

Abbreviations

AdMIDAS adjacent to MIDAS

ADP adenosine diphosphate

Akt RAC-alpha serine/threonineprotein kinase

AP-2 adaptor protein-2

APC adenomatous polyposis coli

Arp2/3 actin related protein 2/3complex

BrdU Bromodeoxyuridine

Cdc42 cell division cycle 42

CH calponin homology

CHIP C-terminal of Hsp70 interacting protein

CMA chaperone-mediated autophagy

CPZ chlorpromazine

Cre cyclization recombinase

Dab-2 Disabled

DAG diacylglycerol

ECM extracellular matrix

EGF epidermal growth factor

EGFR epidermal growth factor receptor

ERK extracellular signal-regulated kinase

FA focal adhesion

FAK focal adhesion kinase

FGF fibroblast growth factor

FGFR fibroblast growth factor receptor

FN fibronectin

FRAP fluorescence recovery after photobleaching

GAP GTP-ase activating protein

GDF growth and differentiation factor

GDP guanosine diphosphate

GEF guanine nucleotide exchange factor

GFR growth factor receptor

GPCRs G proteins coupled receptors

GSK3β glycogen synthase kinase 3β

GTP guanosine trisphosphate

Hsp40 Heat shock protein 40

Hsp70 Heat shock protein 70

Hsp90 Heat shock protein 90

HIP Hsc70- interacting protein

HOP Hsc70-Hsc90 organizing protein

ICAMs intercellular adhesion molecules

I_f immobile fraction

Ig immunoglobulin

IGF-1 insulin growth factor-1

ILK integrin linked kinase

ILKAP integrin-linked kinase-associated serine/threonine phosphatase

IPP ILK-PINCH-Parvin

IP3 inositol triphosphate

JAK Janus kinase

JNK c-jun N-terminal kinase kDa kiloDaltons

LAP latency-associated peptide

LEF lymphoid enhancer-binding factor

LGN leucine, glycine, asparagine

LTBP latent TGFβ binding protein

MAPK mitogen-activated protein kinase

MEVs multivesicular endosomes

M_f mobile fraction

MHC-I class I major histocompatibility complex

MIDAS metal-ion-dependent adhesion site

MLC myosin light chain

MMP matrix metalloproteinase

MVB multi-vesicular bodies

Nck2 noncatalytic region of tyrosine kinase adaptor protein 2

pFAK phosphoFAK

PI3-K phosphatidylinositol 3-kinase

PINCH Particularly interesting new Cys-His protein

PK Prickle

PKC protein kinase C

PKCζ protein kinase C ζ

PH pleckstrin homology

PLC phospholipase C

PSI plexin, semaphorins, and integrins

PtdIns phosphatidylinositol

PtdIns-4,5-P2 PtdIns4,5-bisphosphate

PYK2 pyruvate kinase 2

Rab5 Rab protein 5

Rac1 ras-related C3 botulinum toxin substrate 1

Rap1 RAS-related protein-1

Ras rat sarcoma viral oncogene homolog

RGD arginine, glycine, aspartate

RhoA ras homolog gene family, member A

RIAM Rap1-interacting adaptor molecule

ROCK Rho-associated protein kinase

RSU1 Ras suppressor protein 1

Runx runt-related transcription factor

Smad Similar to mothers against decapentaplegic

Src Rous sarcoma oncogene

STAT signal transducer and activator of transcription

SUMO small ubiquitin-like modifier

SyMBS synergistic metal ion binding site

TCF T cell-specific transcription factor

TGF-β transforming growth factor β

TESK1testis-specific kinase 1

Ub ubiquitin

UBDs ubiquitin binding domains

UIM ubiquitin interacting motif

VCAMs vascular cell-adhesion molecules

VEGF vascular endothelial growth factor

WASp Wiscott-Aldrich Syndrome protein

WAVE WASP-family verprolin homologue

Wnt wingless-type MMTV integration site family member

Summary

Integrins are heterodimeric transmembrane receptors that mediate cell adhesion through their interaction with the extracellular matrix (ECM). Remarkably, integrins are also signal transduction receptors regulating a wide range of cellular processes such as proliferation, survival, differentiation and migration despite lacking enzymatic activity. Integrins accomplish this function by recruitment of various adaptor, scaffolding and signaling molecules to their short cytoplasmic tails. Through extensive intracellular interactions integrins assemble large signaling hubs known as focal adhesions to couple to the cytoskeleton and to transduce signals. Integrin-linked kinase (ILK) is a central constituent of β1 and β3 integrin adhesions. ILK is composed of three structurally distinct domains: five ankyrin repeats, a pleckstrin homology (PH) domain and kinase-like domain, and it forms an obligatory trimeric protein complex with two other focal adhesion proteins, PINCH and parvin (IPP complex). ILK functions as an adaptor protein downstream of integrins, but in addition it was proposed to possess kinase activity (Hannigan, Leung-Hagesteijn et al. 1996). However, recent structural and genetic studies clearly demonstrate that ILK, despite its homology to serine/threonine kinases, does not possess catalytic activity (Lange, Wickstrom et al. 2009; Fukuda, Knight et al. 2011). *In vivo* studies have shown that the adaptor function of ILK is essential for normal development in the worm, fly and mouse (Zervas, Gregory et al. 2001; Mackinnon, Qadota et al. 2002; Sakai, Li et al. 2003).On the cellular level ILK is required for cell spreading, focal adhesion formation and migration (Grashoff, Aszodi et al. 2003; Sakai, Li et al. 2003). Interaction of ILK and α-parvin is essential for maturation of focal adhesions into fibrillar adhesions and subsequent fibronectin matrix deposition in fibroblasts (Stanchi, Grashoff et al. 2009). In addition, altered ILK protein levels have been shown to play a role in the pathophysiology of several cancers, heart disease, and fibrosis (Li, Yang et al. 2003; Zhang, Ikegami et al. 2006; Hannigan, Coles et al. 2007; Schmidmaier and Baumann 2008; Kavvadas, Kypreou et al. 2010).

C-terminal of Hsp70 interacting protein (CHIP) is an Ubox E3/E4 ubiquitin ligase (Ballinger, Connell et al. 1999; Nyamsuren, Faggionato et al. 2007) consisting of a N-terminal tetratricopeptide domain (TRP) and C-terminal U-box domain (Schulman and Chen 2005). While the TPR domain mediates interaction of CHIP with chaperones such

as hsp70 and hsp90, the U box domain executes ubiquitin ligase activity (Schulman and Chen 2005). These two features present in one protein make CHIP an important player in protein quality control by integrating the ubiquitin proteasome system (UPS) with the chaperone machinery. CHIP is also involved in the cellular stress response by controlling the transcription of heat shock factor 1 (HSF-1) as well as by regulating hsp70 levels via ubiquitination and proteasomal degradation (Min, Whaley et al. 2008). As an important regulator of cellular proteostasis CHIP plays a role in many neurodegenerative diseases that arise as a consequence of accumulation of abnormal proteins, such as Alzheimer´s, Parkinson´s, Huntington`s disease as well as several spinocerebellar ataxias and spinal and bulbar muscular atrophy (Dickey, Patterson et al. 2007).

In this study we have analyzed the molecular mechanisms by which ILK levels are adjusted in the cell. We demonstrate that CHIP is capable of regulating ILK levels through ubiquitination and proteasomal degradation. Furthermore we show that under basal conditions, ILK is protected from CHIP-mediated ubiquitination and proteasomal degradation through its interaction with the chaperone Hsp90. As a consequence, blocking the chaperone activity of Hsp90 by the inhibitor 17AAG leads to rapid degradation of ILK and concomitant inhibition of cell migration. As ILK is upregulated in various cancer cells that show cell adhesion-mediated drug resistance (CAM-DR), 17AAG-induced degradation of ILK represents a potential approach for the treatment of different drug resistant tumors (Schmidmaier and Baumann 2008). In addition, 17AAG could potentially have anti-fibrotic activity through its effect on ILK protein levels, as ILK has been implicated in fibrosis development in kidney, liver and lung (Li, Yang et al. 2003; Zhang, Ikegami et al. 2006; Kavvadas, Kypreou et al. 2010).

Aim of the Thesis

ILK is an essential scaffold linking integrins and the actin cytoskeleton in β1 and β3 integrin-containing adhesions. It has essential cellular functions in focal adhesion formation, cell spreading and migration. This study was directed to understand how ILK is regulated on the molecular level and how this regulation impacts the role of ILK as an essential downstream target of integrins. Therefore we were prompted to:

1. Identify posttranslational modifications of ILK and find novel interacting partners responsible for these modifications.
2. Investigate how these posttranslational modifications regulate the turnover and function of ILK.

1. Introduction

1.1. The integrin receptor family

Tissue integrity in all multicellular organisms depends on intercellular cohesion as well as communication. While cadherins and immunoglobulin superfamily proteins are the two largest groups of proteins involved in cell-cell interaction, integrins are the largest family of proteins involved in cell-matrix as well as cell-cell adhesion (Hynes and Zhao 2000). Integrins are heterodimeric type I transmembrane receptors consisting of non-covalently linked α and β subunits (Hynes 2002). They are expressed in all metazoans from sponges and coelenterates to insects, nematodes and vertebrates (Hynes and Zhao 2000). While C. elegans expresses 1 β and 2 α subunits, D. melanogaster has 2 β and 5 α subunits (Johnson, Lu et al. 2009). In mammals there are 8 β and 18 α subunits that can combine to form a total of 24 heterodimers (Hynes 2002). Different integrin heterodimers are expressed in different tissues, during different developmental stages and have different ligand binding properties (Bokel and Brown 2002; Humphries, Byron et al. 2006). Integrins mediate bidirectional mechanical and chemical signaling and by this regulate various cellular processes such as cell adhesion, proliferation, survival, differentiation and cell shape (Giancotti and Ruoslahti 1999) in physiological as well as in pathological conditions (Margadant, Monsuur et al. 2011). Remarkably, integrins do not posses intrinsic enzymatic activity and do not connect directly to cytoskeleton, but accomplish their function through recruiting intracellular adaptor proteins.

1.1.1. Integrins and their ligands

In mammals 24 integrin heterodimers can be detected at the protein level (Hynes 2002). The dimerization of integrin subunits occurs intracellularly prior to their transport to the cell surface (Humphries 2000) (Fig.1.1.1.). β subunits are present in excess, and so the amount of the α subunit expressed in the cell determines which heterodimers are present at the cell surface (Santala and Heino 1991). Integrins can be categorized according to the subunit composition and ligand binding properties. β1 (12), β2 and αV (5) containing integrin heterodimers are the three most represented groups of integrins (Barczyk,

Carracedo et al. 2010). Integrin receptors bind a wide range of extracellular ligands and many of these ligands can bind different integrin heterodimers. This promiscuity occurs due to the mechanism of interaction, which is similar between different integrins and their ligands (Humphries, Byron et al. 2006).

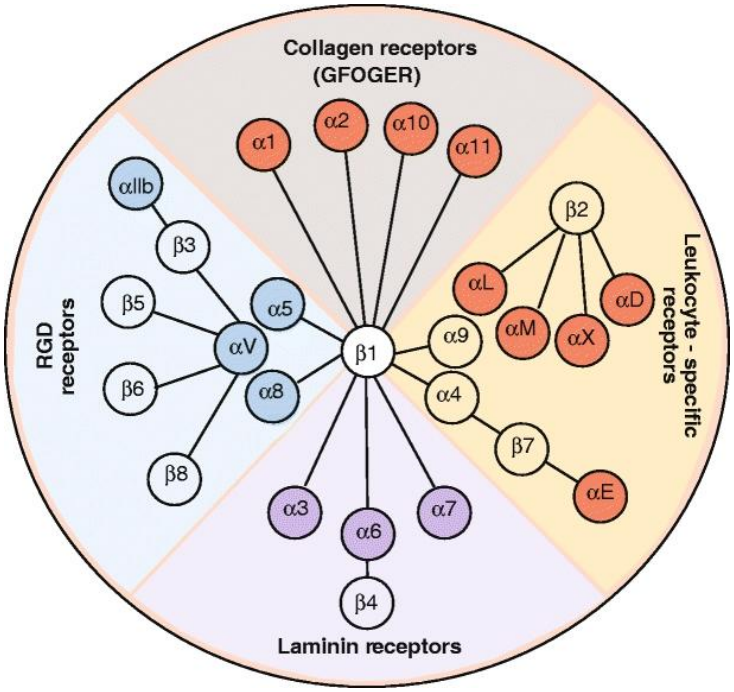

Figure 1.1.1. The integrin family: *The integrin family in vertebrates contains 24 heterodimers. Some isolated species that went through genome duplication (e.g., Danio rerio) have more integrin family members. (Barczyk, Carracedo et al. 2010).*

All five αV subunit-containing integrins, α5β1 and α8β1 as well as αIIbβ3 integrins recognize ligands that contain a RGD (arginine, glycine, aspartate) tripeptide motif. The RGD tripeptide is a minimal recognition sequence found in fibronectin, vitronectin, tenascin, osteopontin and fibrinogen. It is important to note that large macromolecules can contain other integrin binding sites besides the RGD sequence. One such example is the fibronectin synergy site that can bind to the α5 subunit. α4β1, α4β7 and α9β1 bind to the LDV (lysine, aspartate, valine) motif that is functionally related to RGD. Fibronectin contains the prototype LDV motif in its type III connecting segment region. Other ligands such as VCAM-1 and MadCAM-1 contain sequences related to LDV. The mode of interaction of the LDV sequence with integrin heterodimers is most probably similar to the one of RGD, at the interface of the α and β subunits. β2 integrins interact with their ligands in a similar mode, but involving an I domain inserted into the α subunit as a

major interaction interface. However, the ligand sequence that is recognized by β2 containing integrins is structurally similar to the LDV motif. Four α-subunits that contain an α-I-domain (α1, α2, α10, α11) combined with β1, form a distinct laminin/collagen-binding subfamily. Finally, three β1 containing integrins (α3β1, α6β1 and α7β1) as well as α6β4 present the group of integrins that are highly selective laminin receptors that lack an α-I-domain. However, they most probably bind to a different region of laminin (Campbell and Humphries 2011). In addition to these major ligand groups integrins can bind to other ligands such as milk fat globule-EGF factor 8 (MFGE8) and complement factor iC3b, which facilitate phagocytosis of apoptotic cells and pathogens, respectively; the latency-associated peptide of transforming growth factor β (TGFβ) that regulates the activation of TGFβ as well as some of the ADAM (a disintegrin and metalloproteinase) family members as well as matrix metalloproteinase-2 (MMP-2) which participate in ECM remodeling during cell adhesion and migration (Humphries, Byron et al. 2006; Legate and Fassler 2009). Some integrin ligands are generated by proteolysis, the best known examples being endostatin (derived from collagen XVIII), endorepellin (derived from perlecan) and tumstatin (derived from collagen α3) (Bix and Iozzo 2005). In addition, integrins can bind snake toxins as well as certain pathogens like viruses and bacteria. Some of these interactions occur outside the regular ligand-binding sites in the integrins and display distinct binding characteristics when compared to the binding of physiological ligands (Barczyk, Carracedo et al. 2010).

Additional complexity to the integrin receptor family comes from existence of alternatively spliced isoforms. Different variants of both the extracellular and cytoplasmic domains have been reported. Alternative extracellular domains and cytoplasmic domains may account for different ligand-binding affinities or variations in the state of activation as well as variation in downstream integrin activity, cytoskeletal associations and/or signaling events respectively (van der Flier and Sonnenberg 2001). The best known example is the β1 subunit with four known cytoplasmic variants (β1A, β1B, β1C and β1D). These variants have tissue-specific expression patterns. For example the β1A subunit is present in all tissues except mature cardiac and skeletal muscle; these tissues instead express the highly homologous β1D variant. These two variants of β1 subunit are not functionally equivalent in embryonic development. The replacement of β1A by β1D results in embryonic lethality in mice, whereas replacement of β1D with β1A does not lead to severe abnormalities in striated muscles *in vivo* (Baudoin, Goumans et al. 1998).

Genetic studies employing single integrin subunit-deficient mice have demonstrated that all 24 vertebrate integrins are not redundant and have a specific function. The phenotypes of these mice range from a complete block of embryo implantation (β1) through major developmental defects (α4, α5, αV, β8) to perinatal lethality (α3, α6, α8, αV, β4, β8) and defects in leukocyte function (αL, αM, αE, β2, β7), inflammation (β6), haemostasis (αIIb, β3, α2), bone remodeling (β3), and angiogenesis (α1, β3), reflecting the different functions of individual integrins (Bouvard, Brakebusch et al. 2001). Further insights to function of the integrins that give rise to severe phenotypes during embryonic development have been accomplished by generating tissue-specific integrin knockout mice.

1.1.2. Structural features of integrins

Integrin α and β subunits have a large extracellular domain (approximately 800 amino acids), a single transmembrane domain of around 20 amino acids and a short cytoplasmic tail (10-70 amino acids). The exception here is β4 integrin that has an unusually long cytoplasmic tail of approximately 1000 amino acids (Hynes 2002).

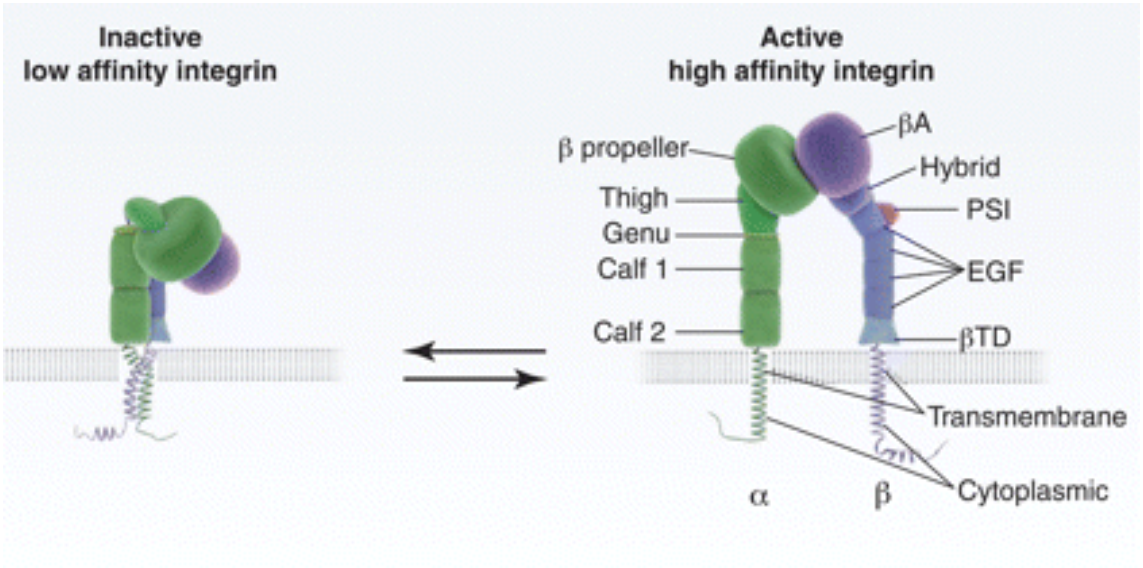

Figure 1.1.2. Schematic representation of integrin domain structure and integrin activation. *Integrin is kept in a bent inactive conformation via a specific interaction between the ectodomains, the transmembrane domain, and the cytoplasmic domains. During integrin activation the separation of integrin legs, transmembrane domain and cytoplasmic domains occurs leading to the extended integrin conformation The α subunit is shown in green and the β subunit in purple (Moser, Legate et al. 2009).*

The extracellular, N-terminal domains of α and β subunits within a heterodimer adopt a head on stalks conformation. Most of our knowledge about the structure of integrins comes from the crystal structure of the αvβ3 and more recently the αIIbβ3 (Xiong, Stehle et al. 2001; Zhu, Luo et al. 2008). We cannot, however, be certain if these concepts can be applied to all other integrin heterodimers. The extracellular domain of the α subunit contains a β propeller domain followed by an Ig-like (thigh) and two β sandwich domains (calf1 and calf2) (Fig. 1.1.2.). Half of the known α subunits (the collagen-binding and leukocytes-specific integrins) contain an I/A domain inserted into the larger β propeller domain. When present, the I/A domain participates in ligand binding (Hynes 2002). The extracellular domain of the β subunit consists of a βI/A domain, which is inserted into an immunoglobulin (Ig)-like "hybrid" domain preceded by an N-terminal 54-residue PSI (plexin, semaphorins, and integrins) domain, four tandem cysteine-rich EGF-like repeats and a β-tail domain. The PSI domain forms a disulfide bond with the distal I-EGF domain (Hynes 2002; Arnaout, Mahalingam et al. 2005). The head domain of the integrin heterodimer comprises of the β propeller of the α subunit and the βI/A and the "hybrid" domains of the β subunit. The ligand-binding pocket is formed by the interface between the β propeller and the βI/A domain. Integrin ligand binding depends on divalent cations. There are three metal binding sites essential for ligand binding in the βI/A domain: a central Mg^{2+} binding site called MIDAS (metal-ion-dependent adhesion site) flanked by two Ca^{2+} sites, the SyMBS (synergistic metal ion binding site) and the AdMIDAS (adjacent to MIDAS) (Zhu, Luo et al. 2008).

The best characterized structures of transmembrane domains of integrins are the ones of αIIb and β3 subunits. The β3 transmembrane domain has 30 amino acids that form an α helix. The length of this structure is longer than an average thickness of a lipid bilayer, suggesting that it is probably tilted within the membrane (Lau, Partridge et al. 2008). The αIIb transmembrane domain has only 24 amino acid residues forming an α helix followed by a backbone reversal and therefore does not display the tilt within the membrane (Lau, Dua et al. 2008).

The cytoplasmic tails of α and β subunits contain several well conserved features: the GFKKR motif in the α subunit has been proposed to be important for interaction with the β tail HDRRE motif (Vinogradova, Haas et al. 2000; Vinogradova, Velyvis et al. 2002). This data is, however, still controversial (Wegener and Campbell 2008). Moreover, the β

tail contains two NPXY motifs, a membrane proximal and a membrane distal one, that are a part of a canonical recognition sequence for phosphotyrosine-binding (PTB) domains. The phosphotyrosine-binding (PTB) domains are present in a large number of proteins, enabling them to interact with β tail of integrins (Calderwood, Fujioka et al. 2003).

1.1.3. Integrin signaling

Integrins are remarkable in their ability to transduce signals across the plasma membrane in a bidirectional manner. Upon ligand binding, integrins cluster and various adaptor and signaling molecules are recruited to integrin tails. As many of these adaptors are actin-binding proteins, this leads to the establishment of a connection to the actin cytoskeleton. In addition, recruitment of signaling proteins leads to activation of various signal transduction pathways important for cellular processes such as spreading, migration, and proliferation. Collectively this process is referred to as "outside-in" signaling. On the other hand, non-integrin mediated signaling pathways can lead to binding of regulatory proteins to integrin cytoplasmic tails inducing changes in integrin activity and ligand binding affinity. This is referred to as "inside-out" signaling.

1.1.3.1. Inside-out signaling

The first studies on the regulation of integrin activation were done in platelets that express αIIbβ3 integrin. After vascular injury, presence of insoluble proteins such as collagen and von Willebrand factor as well as soluble agonists like ADP, thrombin and thromboxane A2, can activate platelets (Li, Delaney et al. 2010). These signals act through receptors coupled to heterotrimeric G proteins (GPCRs) or through receptors that are not directly coupled to G proteins such as the collagen receptor GPVI. These initial signaling events will almost always lead to activation of phospholipase C (PLC). Consequently, PLC will hydrolyse phosphatidylinositol to produce the secondary messengers inositol trisphosphate (IP3) that increases cytoplasmic [Ca^{2+}], and diacylglycerol (DAG) that activates protein kinase C as well as a Ca^{2+} and DAG-dependent guanine nucleotide exchange factor (Cal-DAG-GEF) for the Ras-like small GTPases Rap1 (Li, Delaney et al. 2010). Activated Rap1 binds to its effector RIAM that in turn binds to talin (Fig. 1.1.3.). This interaction leads to unmasking of the integrin binding site on the adaptor protein talin, allowing integrin activation (Han, Lim et al. 2006). Furthermore, another central adaptor Kindlin-3, like talin, can bind β1 and β3 integrin tail resulting in integrin activation (Moser, Nieswandt et al. 2008). In lymphocytes, chemokines can trigger some

additional signaling pathways. These involve activation of PI3K and small GTPases RhoA and possibly Rac1 that in turn can trigger downstream PIP2 generating kinases like PIPKIα, β, γ, leading to local increase of PIP2 and activation of talin (Alon and Ley 2008). As illustrated by the above examples, all of these pathways ultimately lead to activation of talin that can be considered the major activator of integrins. It has been proposed that binding of talin to membrane-proximal residues in the β integrin tail can lead to disruption of a salt bridge between an Asp residue within the β-tail HDRK motif and an Arg residue in the GFFKR motif within the α-tail (Wegener, Partridge et al. 2007).

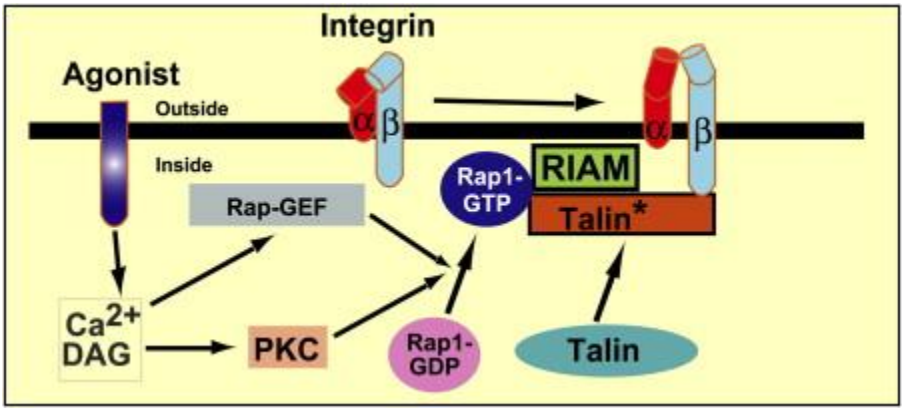

Figure 1.1.3. Connection between agonist stimulation and integrin activation. *Agonist receptors such as G protein-coupled receptors, tyrosine-kinase-coupled receptors induce the formation of diacylglycerol (DAG) and increased* Ca^{2+}*. This leads to the activation and/or translocation of active GTP bound Rap1 to the plasma membrane via activation of protein kinase C (PKC) or a Rap guanine nucleotide exchange factor (Rap-GEF). At the plasma membrane, activated Rap interacts with RIAM. This in turn leads to the recruitment of talin to form the integrin activation complex, by unmasking the integrin binding site in F3 domain of talin leading to integrin activation (Han, Lim et al. 2006).*

However, talin alone seems not be sufficient for full activation of integrins and the kindlin family of proteins has been shown to play a central role in integrin activation (Montanez, Ussar et al. 2008; Moser, Bauer et al. 2009). Talin and kindlin binding induces a conformational change of integrin tails that is propagated through the transmembrane domains to the extracellular domains of the integrins. In inactive integrins the transmembrane domains of α and β subunit interact through GxxxG dimerization motifs and in order for integrin activation to occur, the transmembrane domains have to be separated. It is still unclear if these changes take place through piston-like movement

or tilting of the transmembrane domain (Moser, Legate et al. 2009). The integrin heterodimer can then switch to an active state by switching from a low affinity bent conformation to a high affinity extended conformation. The structural changes that occur in the transmembrane domain during activation of the extracellular domain are still controversial. Two main competing models have been proposed for integrin activation: The switchblade model states that the separation of the cytoplasmic tails and TM domains of the inactive bent integrin causes knee extension and opening of the ligand binding pocket. The deadbolt model does not require unbending. It proposes that a change in the transmembrane domains leads to a conformational change within the head domain to reveal the ligand binding site and extension occurs only after the ligand binding (Arnaout, Mahalingam et al. 2005). Upon ligand binding, integrins initiate clustering and recruitment and activation of other integrin binding molecules thus strengthening the interaction with the ECM and activating intracellular signaling pathways also known as outside-in signaling (Arnaout, Mahalingam et al. 2005).

1.1.3.2. Outside-in signaling

As already mentioned, integrins possess no enzymatic activity. They therefore depend on interactions with a large group of accessory proteins to transduce signals. The most recent studies based mainly on large scale mass spectrometry analyses show that there are approximately 180 proteins associated both directly and indirectly with integrins (Zaidel-Bar and Geiger 2010). Downstream signaling events that occur upon integrin activation can be divided in three temporal stages (Legate, Wickstrom et al. 2009) (Fig. 1.1.4.). One of the immediate effects is up-regulation of lipid kinase activity that subsequently leads to an increase in the local concentration of phosphoinositide second messengers PtdIns-4,5-P2 and PtdIns-3,4,5-P3 as well as rapid phosphorylation of specific proteins. On the scale of several minutes these changes lead to activation of various signaling pathways. The central event in integrin-mediated signaling is cell adhesion-dependent phosphorylation of Focal Adhesion Kinase (FAK) and Src kinases.

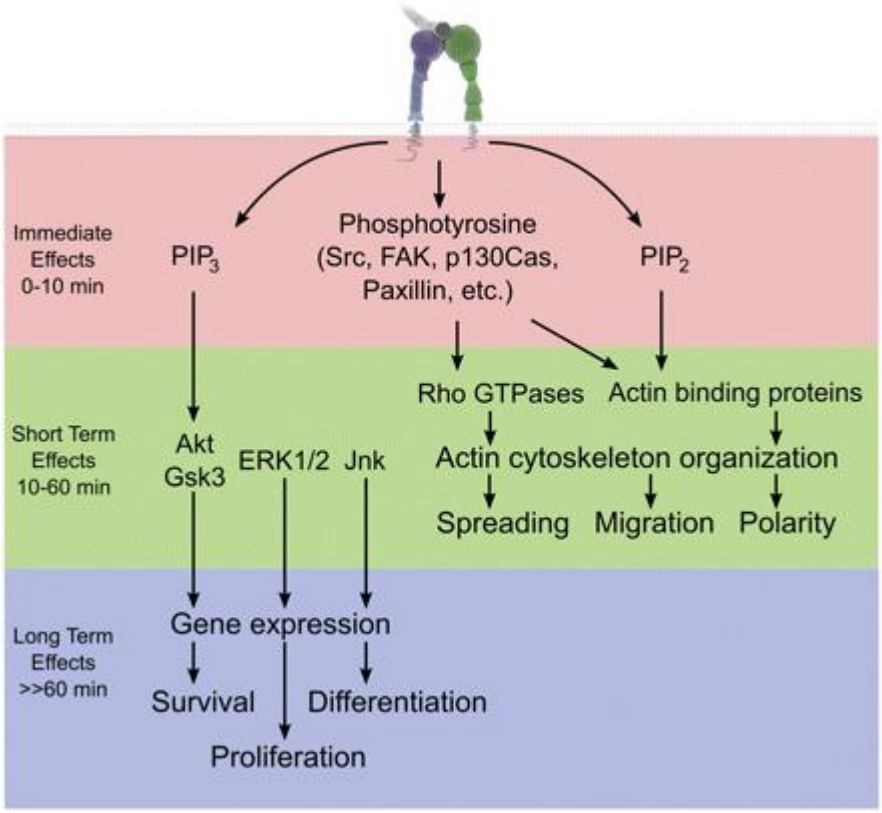

Figure 1.1.4. Three temporal stages of integrin signaling. *Downstream signaling events initiated upon integrin ligand binding can be divided into three temporal stages. The immediate effects: up-regulation of lipid kinase activity increases the concentrations of phosphoinositide second messengers PtdIns-4,5-P_2 and PtdIns-3,4,5-P_3, as well as the rapid phosphorylation of specific protein substrates. Short term effects: induction of signaling pathways such as activation of Rho family GTPases and other actin regulatory proteins. This drives the reorganization of the actin cytoskeleton. Long-term consequences: activation of proliferation and survival pathways as well as the induction of genetic programs to regulate cell fate* (Legate, Wickstrom et al. 2009).

Phosphorylation of FAK at the tyrosine-397 enables the interaction with Src family kinases by creating a docking site for the SH2 domain of Src. This interaction in turn releases an autoinhibitory interaction thus activating Src. The activated FAK/Src complex in turn phosphorylates other focal adhesion proteins such as FAK, paxillin and p130Cas. This results in the recruitment of intermediate signaling molecules including Grb2 as well as activation of downstream signaling pathways such as the Ras/MAPK signaling pathway.

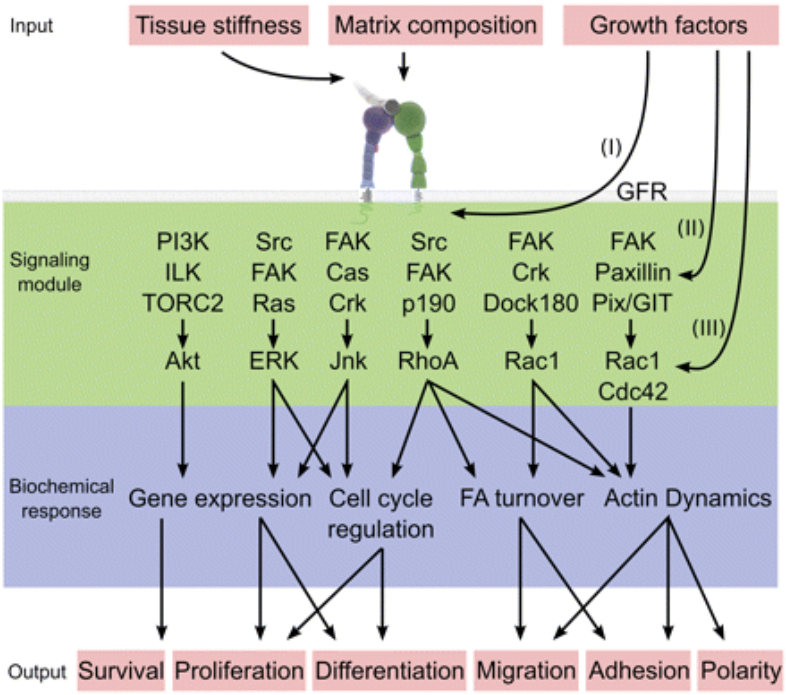

Figure 1.1.5. Examples of signaling pathways downstream of integrin activation. *The growth factor receptors (GFR) and the growth factor environment in cooperation with components and mechanical properties of the extracellular matrix regulate outside-in signaling of integrins. Integrin-mediated signaling interacts with growth factor signaling on multiple levels: integrin affinity for ligands (I), the activity of the integrin-associated signaling proteins (FAK, Src, and PI3K) (II), and the activity of the downstream effectors (ERK, Akt, JNK, and the Rho GTPases) (III). The central signaling module downstream of integrins is the Src/FAK complex that activates ERK and JNK to regulate cell survival, proliferation, and differentiation. In addition to this, the Src/FAK complex regulates Rho GTPase activity through activation of Crk/Dock180 or PIX/GIT pathways, resulting in cytoskeletal reorganization and leading to regulation of migration, adhesion, and polarity. An additional signaling event is activation of PI3K, which in collaboration with mTOR and possibly ILK regulates cell survival through Akt. The alternative activation pathways and cross-talk between the various depicted pathways are not presented. (GFR) Growth factor receptor; (PI3K) PI-3-kinase; (ILK) integrin linked kinase; (TORC) mammalian target of rapamycin complex; (FAK) FA kinase; (ERK) extracellular signal-regulated kinase; (Cas) Crk-associated substrate; (JNK) Janus kinase; (DOCK180) dedicator of cytokinesis 1; (PIX) PAK interactive exchange factor; (GIT) G protein-coupled receptor kinase-interacting protein (Legate, Wickstrom et al. 2009).*

Activation of Rho family GTPases and other actin regulatory proteins is another important event of integrin signaling. It drives the reorganization of the actin cytoskeleton leading to changes in cell shape and initiation of cell migration. On a long-term scale integrin outside-in signaling leads to activation of proliferation and survival pathways and to induction of genetic programs that control cell fate (Legate, Wickstrom et al. 2009).
It is important to note that integrin signaling operates partly through extensive cross-talk with other signaling pathways such as the EGF, IGF, PDGF and TGF-β pathways (Fig. 1.1.5.). This crosstalk is regulated on multiple levels and is relevant both under physiological and pathophysiological conditions (Schwartz and Ginsberg 2002; Cabodi, Moro et al. 2004; Beattie, McIntosh et al. 2010; Margadant and Sonnenberg 2010).

1.1.4. Assembly of integrin dependant adhesion structures

Upon activation integrins respond not only by increasing their affinity towards ligand but also by increasing their avidity by clustering. Integrin clustering is important for pulling together thousands of weak interactions thus establishing a strong adhesive structure with the ECM. The smallest integrin-containing structures that can be observed by light microscopy are focal complexes and nascent adhesions (Nobes and Hall 1995; Geiger, Bershadsky et al. 2001; Alexandrova, Arnold et al. 2008; Choi, Vicente-Manzanares et al. 2008). These early integrin-based adhesions are approximately 100 nm in diameter, and they are composed of a few thousand protein molecules including integrins, talin and paxillin (Zaidel-Bar, Ballestrem et al. 2003; Ponti, Machacek et al. 2004; Giannone, Dubin-Thaler et al. 2007; Alexandrova, Arnold et al. 2008; Choi, Vicente-Manzanares et al. 2008). They are positioned close to the leading edge of a migrating cell, forming the contact between the lamellipodium, a flat and ribbon-shaped actin-based protrusion at the edge of the cell, and the matrix. The forces that are generated through actin flow drive growth of nascent adhesions to form bigger focal complexes (Alexandrova, Arnold et al. 2008; Choi, Vicente-Manzanares et al. 2008). The link between the moving actin cytoskeleton and integrins is described as a molecular clutch that enables movement of the cell body in respect to stationary cell-matrix adhesions (Huttenlocher and Horwitz 2011) (Fig. 1.1.6.). As the edge of the moving cell is advancing, the growing adhesions remain attached to the matrix and mature in a process which is characterized by changes in their protein composition (e.g., the recruitment of zyxin), tyrosine phosphorylation (e.g., of paxillin), dynamics (e.g., enhanced exchange rate) and association with actin stress fibers (Ballestrem, Hinz et al. 2001; Cluzel, Saltel et al. 2005; Ballestrem, Erez et

al. 2006; Zaidel-Bar, Milo et al. 2007; Zamir, Geiger et al. 2008). Maturation of focal complexes to focal adhesions is also accompanied by changes in length and size of the adhesions (Berrier and Yamada 2007).

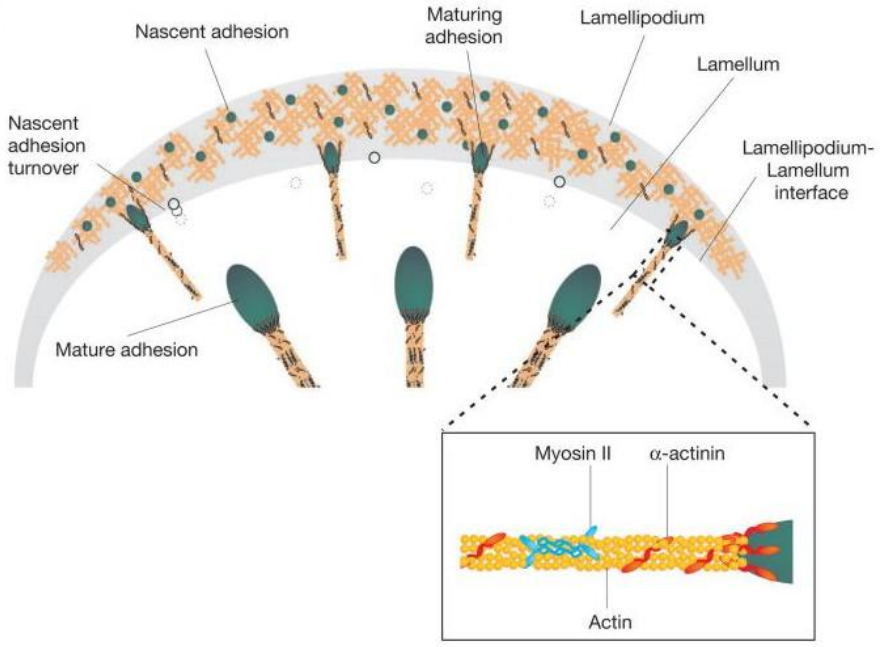

Figure 1.1.6. Adhesion assembly, turnover and maturation *In the course of cell protrusion, adhesions initially assemble as puncta (blue circle) in the lamellipodium (gray band); this process is driven by or linked to actin polymerization. These nascent adhesions remain small and stable within the lamellipodium. The stability of these adhesions is linked to the integrity of the actin cytoskeleton network; the nascent adhesions turn over (clear circle) after the depolymerizing dendritic actin at the rear of the lamellipodium has passed them. Myosin II activity is not required for the formation and turnover of nascent adhesions. Maturing adhesions are formed as nascent adhesions that grow along the actin template, which elongates centripetally at the lamellipodium-lamellum interface. For the initial elongation of adhesions both myosin II and α-actinin cross-linking activities, possibly in conjunction with contraction, are necessary. For the proper positioning of the adhesions on actin filaments α-actinin is required. Further development and maturation of adhesions is mediated by the cross-linking of actin by myosin II and α-actinin most likely working in synergy with contraction. (Choi, Vicente-Manzanares et al. 2008).*

In certain cell types like fibroblasts adhering to a fibronectin matrix, focal adhesions will mature into so called fibrillar adhesions (Hynes and Destree 1978; Chen and Singer 1982; Chen, Hasegawa et al. 1985; Zamir, Katz et al. 2000). Fibrillar adhesions are elongated adhesion structures located in the central region of the cell. Maturation of focal adhesions to fibrillar adhesions is followed by increased recruitment of tensin and a change in integrin content. While focal adhesions contain both $\alpha5\beta1$ and $\alpha V\beta3$, fibrillar adhesions are rich in $\alpha5\beta1$ integrin. Maturation of fibrillar adhesion is tightly connected to the formation of fibronectin fibrils (Pankov, Cukierman et al. 2000; Zamir, Katz et al. 2000; Baharloo, Textor et al. 2005). Certain highly migratory and invasive cell lines such as v-Src transformed fibroblasts, osteoclasts, macrophages and dendritic cells, form special integrin adhesion structures called podosomes (Tarone, Cirillo et al. 1985; Linder, Nelson et al. 1999). Invadopodia are found in invasive cancer cells and are related protrusive structures. Both podosomes and invadopodia have the ability to degrade cell matrix, however the relation between podosomes and invadopodia is not clearly defined (Huttenlocher and Horwitz 2011).

It is important to note that most of the studies on different types of adhesive integrin structures as well as their dynamics were done in cell culture on rigid 2D surfaces. In recent years there has been some controversy on the existence of such structures in vivo or in 3D model systems. Observing cells embedded in 3D cell-derived matrices as well as in collagen gels or 3D systems derived from other extracellular matrix molecules has, however, allowed the conclusion that most cells do form distinct adhesion structures also in 3D, and that these structures contain a similar set of molecules that are present in 2D adhesions, including integrins, vinculin and paxillin (Harunaga and Yamada 2011). It has been shown that 3D adhesions are similar to fibrillar adhesions in respect to their $\alpha5\beta1$ integrin content, but also similar to focal adhesions in regard to the presence of vinculin, a-actinin and phosphorylated paxillin (Zamir and Geiger 2001; Yamada, Pankov et al. 2003; Berrier and Yamada 2007) (Fig. 1.1.7.).

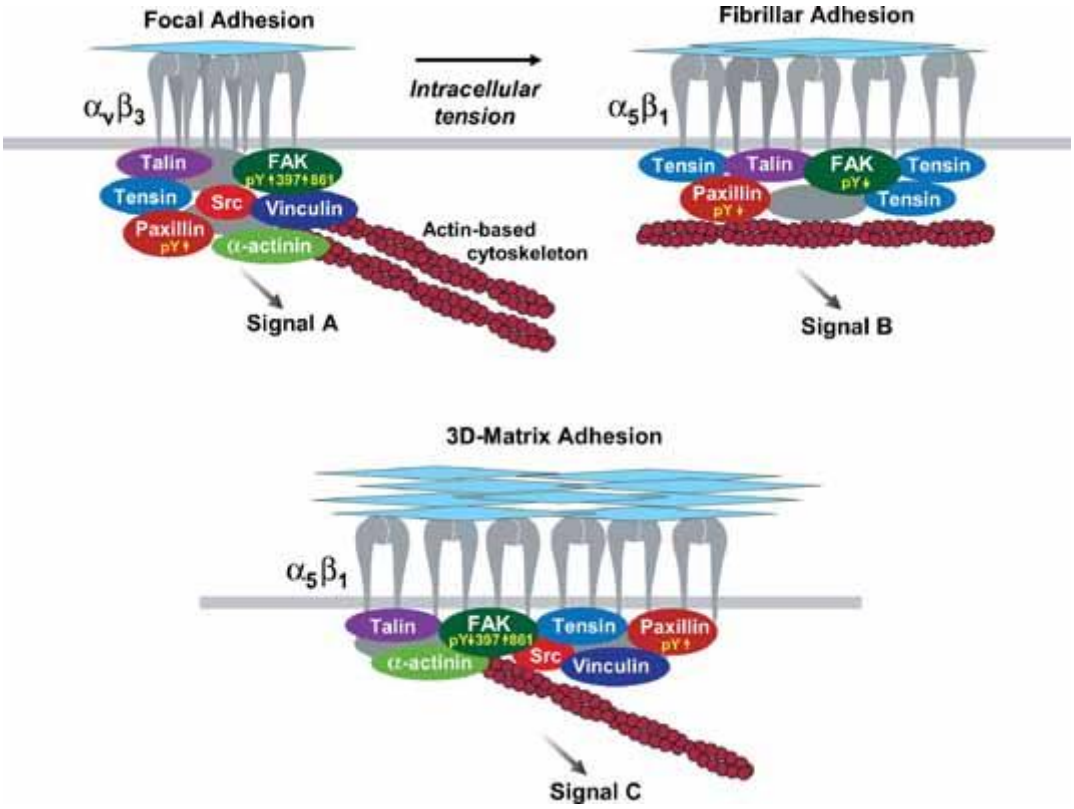

Figure 1.1.7. Differences between focal adhesions, fibrillar adhesions, and 3D-matrix adhesions. *The various matrix adhesion structures differ in the levels of protein tyrosine phosphorylation (pY)and of adaptor and signaling protein composition. In focal adhesions as opposed to fibrillar and 3D-matrix adhesions, levels of phosphorylated FAK, particularly tyrosine (Y) 397 are high. Both focal adhesions and 3D-matrix adhesions in contrast to fibrillar adhesions have high levels of phosphorylated paxillin (particularily pY 31) and FAK (pY 861). Distinct protein complexes are likely to form within each type of matrix adhesion leading to the activation of specific signaling pathways* (Berrier and Yamada 2007).

1.1.5. Mechanisms of cell motility

In order for the cell to successfully migrate through a given environment, tight regulation of adhesion assembly and disassembly is necessary. At the leading edge of a migrating cell nascent adhesions are formed, and they can either mature into focal adhesions or be turned over. This allows the cell to generate pulling force that is necessary for motility. At the cell rear, disassembly of focal adhesions is necessary for detachment and retraction of the trailing edge. This allows net forward motion of the cell. Two major cellular processes are important for adhesion dynamics: actin polymerization and myosin II-generated

tension (Parsons, Horwitz et al. 2010). The remodeling of the actin cytoskeleton is driven by Rho GTPases that are in turn regulated by a complex signaling network arising from integrin adhesions. The best studied examples are paxillin and FAK that can either directly or indirectly bind various GEFs and GAPs, thus influencing the activity of Rho GTPases (Brown and Turner 2004; Huttenlocher and Horwitz 2011). Rho GTPases Rac and cdc42 drive polymerization of actin within the lamellipodium through downstream effectors WASP (Wiscot Aldrich syndrome protein) and WAVE (WASP-family verprolin homologue) that activate the Arp2/3 complex. Arp2/3 in turn induces actin polymerization to form a specific branched structure. The plasma membrane at the leading edge provides resistance to actin polymerization, resulting in retrograde flow of actin.

Within the structure directly behind the lamellipodium, the lamella, actin gets organized in thick bundles, so called stress fibers that undergo much slower retrograde flow. Here the retrograde flow is mainly regulated by myosin II contraction that pulls antiparallel actin fibers past each other, thus creating the force that rearranges the actin cytoskeleton. (Parsons, Horwitz et al. 2010). Myosin II activity (ATP hydrolysis and actin filament formation) depends on the reversible phosphorylation of two tyrosine residues Thr18 and Ser19. This phosphorylation is regulated by Rho GTPases via activation of Rho kinase and inhibition of myosin phosphatases (Parsons, Horwitz et al. 2010; Huttenlocher and Horwitz 2011). Myosin activity can also be regulated by Rac/Cdc42 via inhibition of myosin light chain kinase or phosphorylation of the regulatory light chain of myosin directly (Vicente-Manzanares, Koach et al. 2008; Huttenlocher and Horwitz 2011). Tension generated by myosin is essential for adhesion maturation. This might occur for example by inducing conformational changes in focal adhesion proteins such as talin and vinculin. This results in exposure of additional actin binding sites of vinculin, thereby strengthening the integrin-actin linkage. On the other hand it has also been shown that the actin bundling activity of myosin plays an important role in adhesion maturation (Vicente-Manzanares, Koach et al. 2008; Parsons, Horwitz et al. 2010).

Disassembly of focal adhesion is thought to be driven by microtubule targeting of focal adhesions as well as by cleavage of certain adhesion components by calpain (Rinnerthaler, Geiger et al. 1988; Zhong, Chrzanowska-Wodnicka et al. 1998; Small and Kaverina 2003; Geiger and Yamada 2011). Microtubule targeting of focal adhesions might lead to local modulation of Rho GTPase signaling, thereby regulating adhesion

turnover (Broussard, Webb et al. 2008). On the other hand it has been reported that microtubules regulate disassembly of focal adhesions through the FAK/dynamin pathway by inducing clathrin mediated integrin endocytosis, independently of Rho and Rac (Ezratty, Partridge et al. 2005; Ezratty, Bertaux et al. 2009; Huttenlocher and Horwitz 2011).

Mechanisms of focal adhesion disassembly at the rear of a migrating cell are less well understood. It is, however, likely that mechanisms that destabilize focal adhesions at the trailing edge are similar to those that act at the cell front during focal adhesion turnover. A specific feature of the trailing edge is that actomyosin stress fiber contraction driven by Rho activity and subsequent retraction of the cell rear can lead to formation of so called footprints. In response to rapid detachment of the rear, molecular bonds can be broken at the level of the integrin-actin linkage, resulting in a large part of the adhesion, including the integrins and part of the membrane, being left behind in a form of a footprint (Broussard, Webb et al. 2008). In certain cell types such as neutrophils, Ca++/calmodulin-activated integrin $\alpha V\beta 3$ endocytosis also plays role in rear end detachment (Lawson and Maxfield 1995; Huttenlocher and Horwitz 2011). In fibroblasts calpains, calcium-dependent proteases acting downstream of microtubules, play a role in destabilizing focal adhesion at the rear. The best described targets of calpains are FAK, paxillin and talin (Huttenlocher, Palecek et al. 1997; Carragher, Levkau et al. 1999; Dourdin, Bhatt et al. 2001; Glading, Lauffenburger et al. 2002; Franco, Rodgers et al. 2004; Huttenlocher and Horwitz 2011).

Cell adhesion, spreading and migration in adherent cells is regulated by integrin trafficking. This can occur through regulation of focal adhesion disassembly, ECM turnover or integrin redistribution to new adhesion sites at the leading edge of migrating cell (Caswell, Vadrevu et al. 2009; Margadant, Monsuur et al. 2011). Integrin trafficking includes several aspects of targeted protein transport such as the cell surface delivery of newly synthesized integrins by biosynthetic-secretory pathways, integrin internalization, and recycling. Integrin internalization may occur both through clathrin-independent and clathrin-dependent pathways, and many integrins can follow more than one pathway. In recent years clathrin-dependent integrin endocytosis has emerged as a mechanism important in the process of focal adhesion disassembly during cell migration. Most integrins require adaptor proteins such as Disabled (Dab-2) and adaptor protein-2 (AP-2) to recruit them to clathrin-coated pits (Margadant, Monsuur et al. 2011). It has been

demonstrated that the β integrin tails can bind the adaptors such as Numb and Dab-2 through their NPxY motifs, the canonical signal for clathrin-mediated endocytosis (Calderwood, Fujioka et al. 2003). Triggering focal adhesion disassembly, for example by inducing the microtubule-dependent FA disassembly using nocodazole, results in dynamin-dependent integrin internalization and transport along microtubules to Rab5-positive endosomes (Ezratty, Bertaux et al. 2009). Depletion of dynamin 2, clathrin or its adaptors Dab-2 and AP-2 leads to increased integrin surface expression and reduced cell migration (Chao and Kunz 2009; Ezratty, Bertaux et al. 2009). In addition, *in vivo* studies performed on D. melanogaster embryos and larvae have demonstrated the importance of clathrin-dependent and particularly Rab5-dependent integrin turnover for maintenance of the myotendinous junction (Yuan, Fairchild et al. 2010).

Integrins can also be internalized by the clathrin-independent pathway. For example, integrin α5β1 has been shown to be endocytosed via a caveolin-mediated pathway and that this is relevant for turnover of fibronectin and collagen (Shi and Sottile 2008; Shi, Harman et al. 2010). The internalized integrins can be recycled back to the plasma membrane or degraded via the lysosome (Margadant, Monsuur et al. 2011).

1.1.6. The ILK/PINCH/parvin (IPP) complex

The molecular composition of adhesion structures creates an additional level of complexity to integrin signaling. Alternative components of adhesion complexes can lead to activation of different signaling pathways. The central constituent of at least β1 integrin- and possibly also β3 integrin-containing adhesions is the Integrin-linked kinase (ILK)/PINCH/parvin (IPP) complex. This ternary complex serves as a signaling hub downstream of integrins but most importantly it couples integrins to actin cytoskeleton providing mechanical support to adhesion structures (Fig. 1.1.8.).

1.1.6.1. The molecular composition of the IPP complex

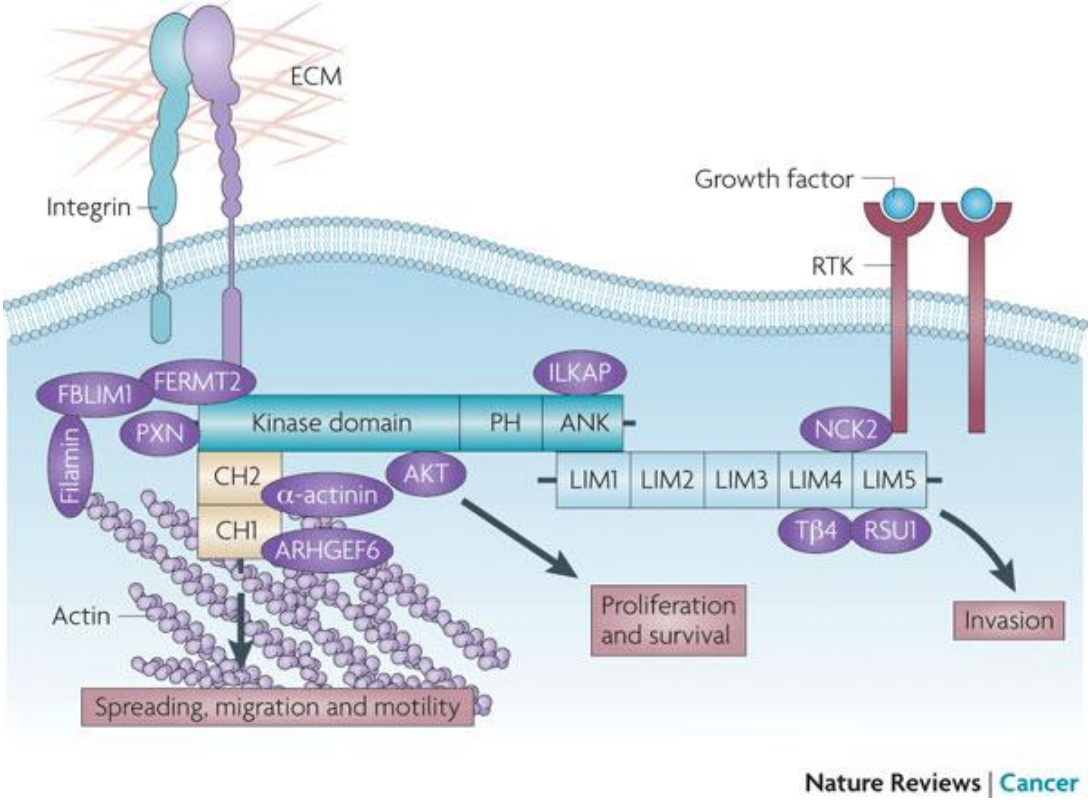

Figure 1.1.8. The IPP complex. *The integrin-linked kinase –pinch–parvin (IPP) complex is formed by ILK, PINCH1/PINCH2 and α-parvin/β-parvin/γ-parvin. Depicted are the central interactions of the IPP complex. ILK associates with the cytoplasmic tails of β1 integrin. Pinch isoforms can in addition bind to receptor tyrosine kinases (RTKs) through the NCK adaptor protein 2 (NCK2). This leads to coupling of growth factor signaling to integrin signaling. PINCH1 interacts with Ras suppressor protein 1 (RSU1) and thymosin-β4 (Tβ4) leading to the activation of JUN N-terminal kinase (JNK) signaling and cell migration and survival, respectively. a-parvin and β-parvin bind to F-actin directly and indirectly, through the interaction with paxillin (PXN) or α-actinin. ANK, ankyrin repeat domain; CH, charged amino acid-rich domain; ECM, extracellular matrix; FBLIM1, filamin binding LIM protein 1; FERMT2, fermitin family member 2; ILKAP, integrin-linked kinase-associated serine/threonine phosphatase 2C; PH, pleckstrin homology domain (Cabodi, del Pilar Camacho-Leal et al. 2010).*

ILK is a ubiquitously expressed protein that is essential for vertebrate and invertebrate development (Legate, Montanez et al. 2006; Hannigan, McDonald et al. 2011). Structurally it consists of three different domains: five ankyrin repeats at N-terminus followed by a pleckstrin homology (PH)-like domain and a putative kinase domain at C-

terminus (Hannigan, Leung-Hagesteijn et al. 1996). ILK was discovered in a yeast-two hybrid screen as a protein that binds β1 and β3 integrin tails (Hannigan, Leung-Hagesteijn et al. 1996). Although the interaction of ILK with β tails has been shown in vitro to be direct, it is possible that recruitment of ILK may depend, at least in some cell types, on kindlin-2 (Montanez, Ussar et al. 2008) and/or paxillin (Nikolopoulos and Turner 2001; Nikolopoulos and Turner 2002). ILK is the central constituent of a ternary complex with the LIM only domain-containing protein PINCH and the calponin homology (CH) domain-containing protein parvin (Zhang, Guo et al. 2002). Formation of the ILK-PINCH-parvin (IPP) complex precedes cell adhesion, implying that the complex is preassembled in the cytoplasm. Assembly of the IPP complex is essential for the stability of the individual components and their recruitment to FAs, at least in mammals (Fukuda, Chen et al. 2003).

In mammals there are two PINCH and three parvin isoforms. Both PINCH1 and PINCH2 consist of five LIM domains and contain a nuclear export signal. The first LIM domain of PINCH binds to the groove formed between the second and fifth ankyrin repeat of ILK (Chiswell, Zhang et al. 2008; Yang, Wang et al. 2009). α-parvin is ubiquitously expressed, β-parvin is enriched in heart and skeletal muscle, and γ-parvin is only found in hematopoietic cells (Nikolopoulos and Turner 2000; Olski, Noegel et al. 2001; Tu, Huang et al. 2001; Yamaji, Suzuki et al. 2001; Chu, Thievessen et al. 2006). Structurally parvins are comprised of an N-terminal polypeptide followed by two C-terminal CH domains, where the second CH domain binds the kinase-like domain of ILK (Tu, Huang et al. 2001; Fukuda, Gupta et al. 2009).

1.1.6.2. The biological function of the IPP complex

Mice lacking ILK die during peri-implantation around embryonic day (E) 5.5-6.5, due to a failure of cells within the embryo proper to organize their F-actin cytoskeleton and to polarize (Sakai, Li et al. 2003). In addition, *in vitro* studies showed that ILK is required in fibroblasts and chondrocytes for cell spreading, focal adhesion formation and migration (Grashoff, Aszodi et al. 2003; Sakai, Li et al. 2003). ILK-deficient fibroblasts show defective maturation of focal adhesions into fibrillar adhesions resulting in the loss of their ability to deposit fibronectin matrix (Stanchi, Grashoff et al. 2009). Interestingly, this function requires the interaction of ILK with α-parvin but not with PINCH-1 (Stanchi, Grashoff et al. 2009). The importance of ILK as a scaffold between integrins

and the actin cytoskeleton has been further studied and confirmed in several cell types as well as different tissues (McDonald, Fielding et al. 2008). Recent studies have also demonstrated the involvement of ILK in the regulation of the microtubule network and mitotic spindle orientation (Dobreva, Fielding et al. 2008; Fielding, Dobreva et al. 2008). In keratinocytes, ILK acts in a complex with IQGAP-1 and mDia1, thereby stabilizing microtubules and their interaction with the cortical actin cytoskeleton. This function allows specific vesicular carriers containing the scaffold protein caveolin-1 to switch from microtubule-based motility to actin-based motility (Wickstrom, Lange et al. 2010).

PINCH-1 is ubiquitously expressed throughout mammalian development and adult life, whereas PINCH-2 expression starts during the second half of embryonic development and has a slightly more restricted expression pattern (Braun, Bordoy et al. 2003). Ablation of PINCH-2 does not affect mouse development, but loss of PINCH-1 results in abnormal epiblast polarity, impaired cavitation, and detachment of endoderm and epiblast from basement membranes (Li, Bordoy et al. 2005). PINCH1 null mice also show an increase in endodermal cell apoptosis, which demonstrates that PINCH1 regulates cell survival (Li, Bordoy et al. 2005; Legate, Montanez et al. 2006). PINCH1 null embryos die at E6.5-7.5. Delayed mortality compared to ILK null embryos cannot be a consequence of expression of the PINCH2 since this isoform is expressed later on during embryonic development (Braun, Bordoy et al. 2003; Legate, Montanez et al. 2006). PINCH2 null mice are viable probably due to compensation by PINCH1 isoform (Legate, Montanez et al. 2006; Stanchi, Grashoff et al. 2009).

α-Parvin null mice die around the embryonic day E11.5-E14.5 due to vascular defects, whereas β-parvin and γ-parvin null mice show no obvious phenotypes. Delayed lethality compared to ILK and PINCH1 null mice suggests that there might be functional compensation between different parvin isoforms (Chu, Thievessen et al. 2006; Montanez, Wickstrom et al. 2009). It has been shown that parvins play a role in modulating cell spreading as well as actin organization; however the exact role of each of parvin isoform in these processes is not yet clear. All three parvin isoforms contain two CH-domains. *In vitro* studies have demonstrated that the CH-domains of parvin can bind F-actin, even though these domains have a significantly different sequence from typical actin-binding CH-domains (Olski, Noegel et al. 2001; Yamaji, Suzuki et al. 2001; Gimona, Djinovic-Carugo et al. 2002; Yamaji, Suzuki et al. 2002). In addition, α-parvin can interact with paxillin. Since the CH-domains are highly conserved between all parvin isoforms it is

highly likely that all three isoforms can bind paxillin, as well as its homolog Hic-5 (Nikolopoulos and Turner 2000; Lorenz, Vakonakis et al. 2008; Wang, Fukuda et al. 2008).

Binding of the two PINCH and three parvin isoforms to ILK gives rise to molecularly distinct IPP complexes with differential binding partners. One example is the interaction of PINCH1 with Ras suppressor protein 1 (RSU1) which is important for integrin-mediated cell adhesion and spreading (Ito, Takahara et al. 2010)(Ito et al., 2010). While RSU1, a known regulator of growth factor induced Jun N-terminal kinase (JNK), binds to LIM 5 domain of PINCH1 it does not bind to PINCH2 (Kadrmas, Smith et al. 2004; Ito, Takahara et al. 2010). Through its interaction with Nck2, an adaptor protein that interacts with receptor tyrosine kinases (RTKs), PINCH might couple integrin signaling to the growth factor signaling (Vaynberg, Fukuda et al. 2005). Parvin isoforms on the other hand have differential effects on the actin cytoskeleton. Parvins not only passively crosslink integrins with actin, but also actively regulate actin remodeling through interaction with various actin regulatory proteins. For example α-parvin, through of its interaction with testis-specific kinase 1 (TESK1), promotes F-actin polymerization through cofilin phosphorylation (LaLonde, Brown et al. 2005). β-parvin in turn interacts with α-Pix, a guanidine exchange factor (GEF) for Rac1 and cdc42, two major regulators of actin dynamics (Mishima, Suzuki et al. 2004; Legate, Wickstrom et al. 2009). α-parvin can also recruit CdGAP to focal adhesions, resulting in inhibition of G-proteins (LaLonde, Grubinger et al. 2006). Furthermore, α-Parvin functions as a negative regulator of RhoA/ ROCK driven contractility in vascular smooth muscle cells (Montanez, Wickstrom et al. 2009).

In summary, ILK plays an important role as a scaffold protein within the IPP complex, providing an important link between integrin and the actin cytoskeleton. However, the molecular details of this regulation remain partly unclear.

1.1.6.3. The ILK kinase controversy

Since its discovery as a serine (Ser)/threonine (Thr) kinase in 1996 by Hannigan and co-workers, the potential kinase activity of ILK has been hotly debated. In this initial study it was shown that ILK possesses a high degree of sequence homology to Ser/Thr kinases (Hannigan, Leung-Hagesteijn et al. 1996). However, it was obvious that ILK lacks several sequence motives that are highly conserved among eukaryotic kinases, including

sequences within the active loop and the DXG motif (Hanks and Hunter 1995). Despite a large number of studies claiming kinase activity in vitro and in cell culture systems, a significant body of recent work demonstrates that ILK does not possess kinase activity. It has was initially shown that bacterially expressed recombinant ILK can phosphorylate β1 integrin as well as the model substrate myelin basic protein in an in vitro kinase assay (Hannigan, Leung-Hagesteijn et al. 1996). These studies were followed by identification of numerous ILK kinase targets including myosin light chain kinase, β-parvin, GSK3b and Akt/PKB (Legate, Montanez et al. 2006). These studies were convincingly disproved by Fukuda et al. who demonstrated that ILK kinase activity is a result of impurities of purified recombinant ILK and thereby a laboratory artefact (Fukuda, Knight et al. 2011).

In vivo studies in invertebrates had already earlier substantiated the role of ILK as a scaffold protein with no requirement for kinase activity (Zervas, Gregory et al. 2001; Mackinnon, Qadota et al. 2002). Deletion of ILK in Drosophila could be completely rescued by re-expression of a kinase dead mutant (K220M) (Zervas, Gregory et al. 2001). Following studies in mouse fibroblasts showed that the same kinase dead ILK mutant could rescue the actin reorganization defects of ILK-deficient cells (Sakai, Li et al. 2003). Finally, studies using various knock-in mutants of ILK demonstrated the both kinase-dead and kinase-hyperactive mutations of ILK allow normal development and adult life in mice. Interestingly, these studies also showed that the K220M mutation thought to affect the kinase activity actually destabilizes the interaction between ILK and α-Parvin. This mutation results in a severe defect in kidney development, a phenotype also found in the α-parvin -/- mice (Legate, Wickstrom et al. 2009).

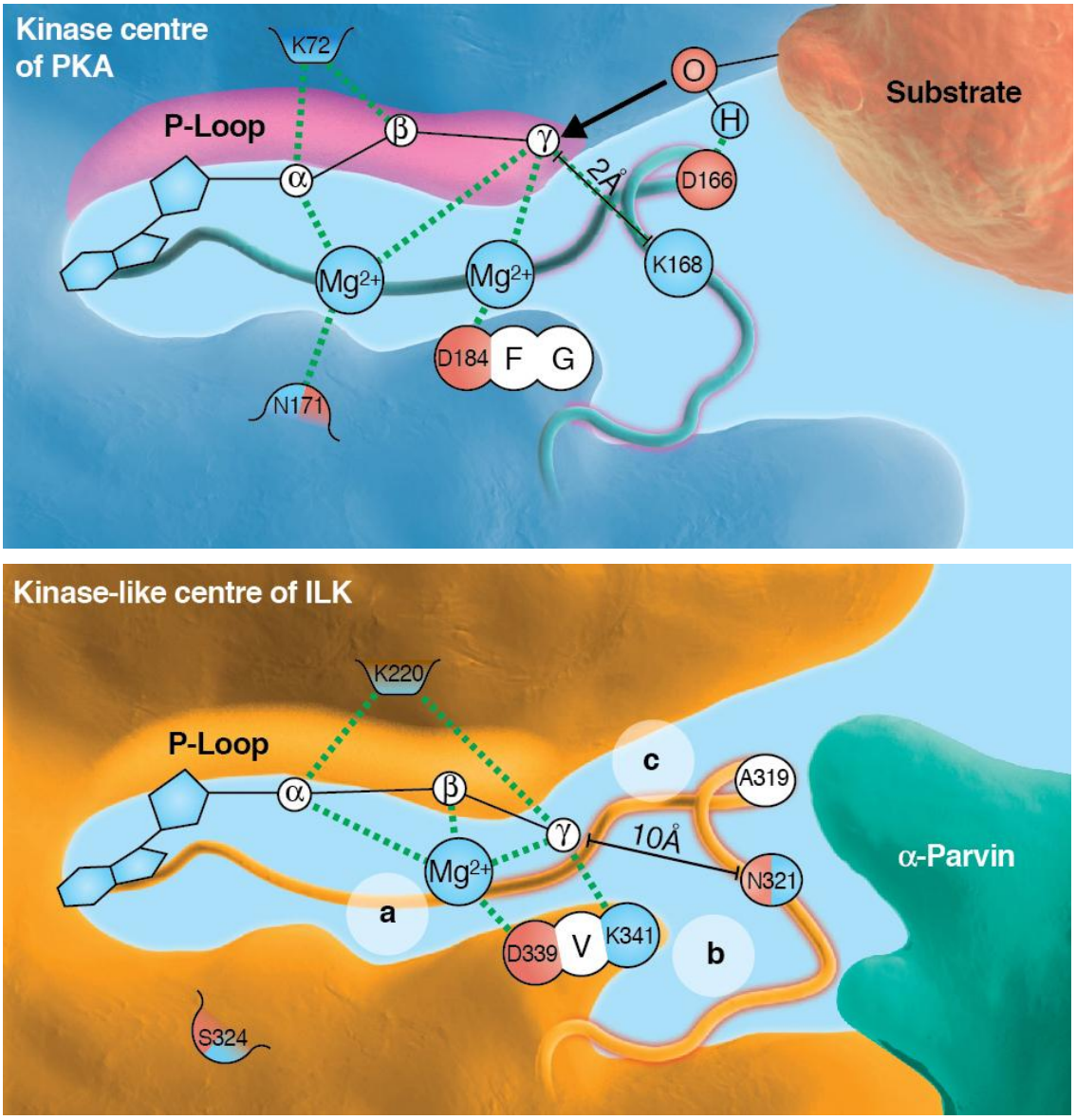

Figure 1.1.9. Schematic representation and comparison of ILK and PKA kinase domains. *The ATP coordination in the ILK kinase-like center is defective; ILK orientates ATP with single Mg^{2+} or Mn^{2+}; increased distance between the γphosphate of the ATP and the catalytic loop (Widmaier, Rognoni et al. 2012).*

Resolving the crystal structure of ILK kinase domain allowed mechanistic insight into the function of the K220 residue. This residue plays a crucial role in stabilizing the global structure of ILK in the ATP unbound state. Therefore mutations in this residue lead to a similar effect as partial or complete loss of ILK (Fukuda, Knight et al. 2011). Furthermore, the crystal structure allows the conclusion that ILK is a pseudo-kinase by demonstrating that important regulatory structures are locked in an ``active´´ state (activation loop, DFG-motive and p-loop) and the kinase domain therefore lacks the

structural flexibility essential for kinase activity (Fukuda, Gupta et al. 2009). Surprisingly, the strongly degraded p-loop indeed can coordinate ATP with moderate affinity. The ATP γ-phosphate, however, is far away from the putative active center (10Å) and its access to the substrate is partially blocked by the γ-phosphate coordinating residue K321 (Fukuda, Gupta et al. 2009; Fukuda, Knight et al. 2011) (Fig. 1.1.9.). Finally, the acidic residue of the catalytic core that polarizes the substrate hydroxyl group is exchanged to alanine and no other residue in structural vicinity can compensate for this. Therefore ILK was not able to hydrolyze ATP in the crystal, allowing full resolution of the ATP conformation (Fukuda, Gupta et al. 2009).

In conclusion, the in vivo studies together with the crystal structure demonstrate that ILK does not possess kinase activity and support previous work showing that ILK functions as a scaffold protein in integrin adhesions.

1.2. Ubiquitin

Functional diversity and dynamics of the eukaryotic proteome is accomplished by a variety of different posttranslational modifications; attachment of small molecule groups such as phosphorylation, acetylation, methylation, and glycosylation but also attachment of small proteins such as ubiquitin, a small 76 amino acids polypeptide chain, or ubiquitin like proteins such as SUMO, Nedd8, Atg8, and ISG15 (Kerscher, Felberbaum et al. 2006; Hochstrasser 2009). Ubiquitination, the covalent attachment of ubiquitin, of target proteins has been shown to be one of the most prevalent posttranslational modifications (Strieter and Korasick 2012). Proteins can be modified by monoubiquitin or polyubiquitin chains of different architecture. These various ubiquitin modifications allow differential recognition of the targets by regulatory proteins harboring ubiquitin binding domains (UBDs). In this way ubiquitination is involved in various cellular processes including transcription, autophagy, DNA repair, signal transduction and cell cycle control (Kerscher, Felberbaum et al. 2006). As ubiquitination is essential for normal cellular physiology it is not surprising that dysregulation of this process plays a central role in a number of pathological conditions such as cancer, immune disorders, neurodegenerative diseases, and congestive heart failure (Strieter and Korasick 2012).

1.2.1. Ubiquitination cascade

The ubiquitination cascade is a three-step enzymatic process in which the carboxylic acid of the terminal glycine from the di-glycine motif in the activated ubiquitin forms an amide bond with the ε amine of the lysine in the target protein. In the first step ubiquitin is activated in an ATP-dependent manner by the E1 ubiquitin activating enzyme. The E1 enzyme uses energy from ATP hydrolysis to adenylate ubiquitin at its C-terminus in order to create a ubiquitin-adenylate intermediate. Subsequently the C-terminal carboxyl group of ubiquitin forms a high-energy thioester bond with the cysteine sulfhydryl group of the E1 enzyme, while releasing AMP. In the second step activated ubiquitin is passed on to the active site of the E2 ubiquitin conjugating enzyme by a trans(thio)esterification reaction. Finally, in the third step ubiquitin is conjugated to the substrate protein with the help of an E3 enzyme, the ubiquitin ligase. This results in the covalent isopeptide linkage of the C-terminus of ubiquitin with the ε-amino group of lysine in the substrate (Kerscher, Felberbaum et al. 2006) (Fig. 1.2.1). Recently it has been demonstarated that ubiquitin can also be attached to cysteine, serine and threonine residues in the substrate (Cadwell and Coscoy 2005; Ravid and Hochstrasser 2007; Wang, Herr et al. 2007; Hochstrasser 2009). After attaching the first ubiquitin the entire process can be paused creating a monoubiquitin modification on the substrate. It can also proceed by attaching another ubiquitin molecule via its C-terminal glycine to one of the seven lysine residues (Lys6, Lys11,Lys27, Lys29, Lys33, Lys48, Lys63) or the N-terminal methionine (Met1) in the previous ubiquitin (Hochstrasser 2009; Behrends and Harper 2011).

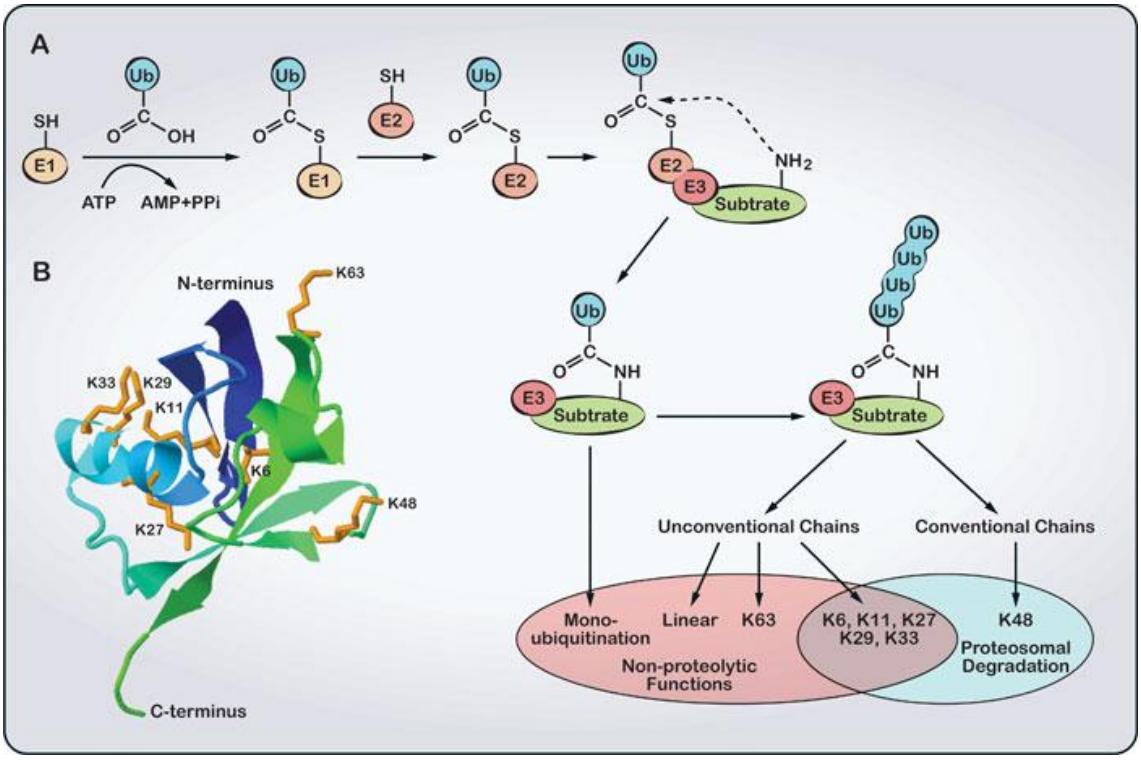

Figure 1.2.1. The ubiquitin cascade and consequences of ubiquitination on protein function. ***(A)*** *Schematic illustration of the three-step ubiquitination cascade. Monoubiquitination and K63 polyubiquitination generally serve non-proteolytic functions, while polyubiquitin chains of other linkages have a proteolytic function.* ***(B)*** *Structure of ubiquitin (PDB code: 1UBQ), the seven lysine residues in ubiquitin protein are indicated (Liu and Chen 2011).*

In this way polyubiquitine chains of different architecture are created. Substrates can also be decorated by several single monoubiquitins attached within close proximity thus creating an atypical multivalent ubiquitin signal (Ikeda and Dikic 2008). The specificity of the chain type depends on the E3 ligase as well as on the E2 enzyme (Ikeda and Dikic 2008). Collectively monoubiquitination and different polyubiquitin chains are able to create around ten different signals.

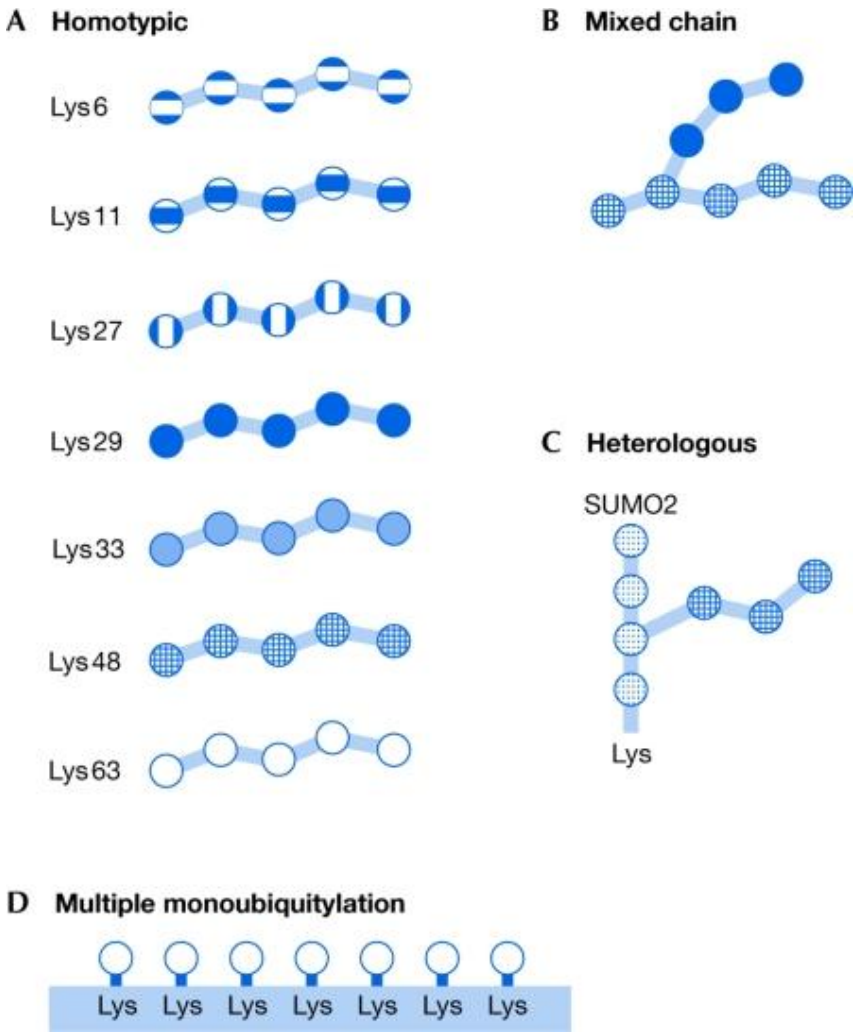

Figure 1.2.2. Possible formations of ubiquitin chains on a target protein. (A) *Homotypic typical and atypical chains include lysine 6 (Lys 6)-, Lys 11-, Lys 27-, Lys 29- , Lys 33-, Lys 48- and Lys 63-linked ubiquitin (Ub) chains.* ***(B)*** *Mixed-linkage atypical chains can be formed by the use of different lysines for sequential Ub conjugation. This leads to the formation of bifurcated chains, such as Lys 48/Lys 29 forks.* ***(C)*** *Heterologous chains can be formed between Ub and Ub-like proteinssuch as the small ubiquitin-like modifier (SUMO) 2.* ***(D)*** *Multiple multiple mono-Ub molecules attached to the substrate can be regarded as a subtype of multivalent chain-like Ub signals (Ikeda and Dikic 2008).*

However, taking into account the fact that the chains can be of different lengths as well as the posibility of heteromeric chains containing for example two different types of linkages such as Lys 6/11, Lys 27/29, Lys 29/48 or Lys 29/33, one can apreciate the vast complexitiy of ubiquitin signalling (Ikeda and Dikic 2008; Ikeda, Crosetto et al. 2010) (Fig. 1.2.2.).

1.2.2. Ubiquitin the modifier of many faces

The ground breaking observations on ubiquitin and its biological role were made in the late 1970´s and early 1980´s and resulted in the Nobel Prize for chemistry being awarded to Aaron Ciechanover, Avram Hershko and Irwin Rose in 2004 for their discovery of ubiquitin-mediated protein degradation. Today it is textbook knowledge that covalently attached K48-linked polyubiquitin chains target proteins to the proteasome for degradation. However, in recent years it has become clear that ubiquitin has a much broader role in cellular physiology and pathology than just disposing of cellular ``junk´´.

Involvement of ubiquitin in DNA repair is a good example of how different ubiquitin modifications can change the function of a protein. PCNA (proliferating cell nuclear antigen) is a DNA polymerase processivity factor that trimerizes around a DNA strand and serves as the platform for binding of accessory factors. In case of DNA damage, the DNA polymerase is unable to proceed with replication. Monoubiquitination of PCNA at K164 leads to error prone DNA lesion bypass by allowing a switch to a specialized translesion synthesis (TLS) polymerase, that is able to insert nucleotides opposite to damaged bases (Kannouche, Wing et al. 2004; Pickart and Fushman 2004). The extension of this monoubiquitin to a K63-linked polyubiquitin chain leads to an error-free mode of lesion bypass probably by allowing the switch to the unaffected sister chromatid DNA strand (Hoege, Pfander et al. 2002; Pickart and Fushman 2004). In addition to ubiquitination PCNA can be modified by SUMO (small ubiquitin related modifier) leading to inhibition of its role in DNA repair, probably allowing normal DNA replication (Hoege, Pfander et al. 2002; Pickart and Fushman 2004).

Ubiquitin is involved in regulation of transcription in multiple ways. One way is through monoubiquitination of histones of which the best studied are histone H2B and H2A. Monoubiquitination of histone H2B at K123 mediates the methylation of histone H3 at K4 and this in turn regulates transcription. On the other hand monoubiquitination of histone H2A at K119 is associated with gene silencing rather than gene activation (Welchman, Gordon et al. 2005; Osley 2006). Another way by which ubiquitin controls transcription is through ubiquitin-dependent proteasomal degradation of transcription factors. The best example of this is the regulation of p53 by Mdm2, a RING finger E3 ligase (Conaway, Brower et al. 2002). On the other hand the 26S proteasome can interact with RNA polymerase II to facilitate termination as well as with stalled elongation complexes to allow degradation of proteins in these stalled complexes (Welchman,

Gordon et al. 2005). Another example of regulation of transcription by ubiquitination is estrogen receptor degradation by the 26S proteasome as a part of the cyclical regulation of estrogen-sensitive promoters (Welchman, Gordon et al. 2005).

Ubiquitination also regulates various signaling pathways; the best studied example is the NF-kB signaling pathway. On the one hand the p105 and p100 precursors of the NF-kB1 complex are processed into the active NF-kB p52 and p50 subunits by ubiquitination and cleavage by the proteasome (Conaway, Brower et al. 2002). On the other hand activation of NF-κB signaling requires degradation of IκB, which is regulated by phosphorylation and subsequent K48-linked polyubiquitination and proteasomal degradation (Liu and Chen 2011). Also the phosphorylation of IκB depends on ubiquitination. Upon binding of an immunostimulative ligand to the receptor such as TNFα to TNFR1, the receptor trimerizes and recruits the E3 ligase TRAF2 (depending on the stimulus signal it can also be TRAF6) that attaches a K63 polyubiquitin chain to RIP (receptor- interacting protein) and to itself. The recruitment of TAK1-TAB1-TAB2 complex to the membrane is accomplished by binding to the K63 polyubiquitin chain of RIP. Once membrane-bound, TAK1 is activated and phosphorylates IKKβ subunit of IKK that in turn phosphorylates IκB. Additional level of control is added by CYLD (cylindromatosis) which has the ability to cleave polyubiquitin chain from TRAF6, as well as by A20 that can edit the K63 chain on RIP to a K48 chain, leading to its proteasomal degradation (Ravid and Hochstrasser 2004; Welchman, Gordon et al. 2005).

In addition to regulation of DNA repair, transcription and signaling, ubiquitination is also involved in endocytosis and sorting and of course in proteasomal and lysosomal degradation of proteins. The role of ubiquitin in protein turnover will be discussed in more detail in the next chapter.

1.2.2.1. Ubiquitin in different degradation pathways

The entire cellular machinery including proteins and organelles is kept in a state of self-renewal through constant degradation and synthesis of new components. In order for cells to maintain their proteome, constant quality control of the individual proteins is carried out. This quality control results from cooperation between chaperones and the proteolytic systems. The task of chaperones is to assist in the folding of polypeptides into their 3-dimensional conformations. If the chaperones fail in this process, the misfolded protein is recognized and sent to one of the two major degradation pathways for proteolysis. These

are the lysosome pathway and ubiquitin-proteasome pathway (Wong and Cuervo 2010). Proteins that enter the cell from the extracellular environment are generally degraded in a nonselective manner by the lysosome. The same is true for the proteolysis during cellular stress, whereas cytosolic proteins are degraded in a highly selective manner by the 26S proteasome. However, in recent years it has become clear that both endocytosis of extracellular proteins and autophagy of both large non-hydrophobic proteins and cellular organelles can also be performed in a very selective manner. Furthermore, the mutual dependence and integration of all cellular proteolytic systems has become evident

1.2.2.1.1. Ubiquitin-proteasome system

Degradation of proteins by the ubiquitin proteasome system is a two-step process. The first step involves covalent attachment of multiple ubiquitin molecules that are recognized by the proteasome that degrades the modified protein in the second step (Ciechanover 1994). Most commonly a polyubiquitin chain of K48 linkage targets the proteins for proteasomal degradation. Recently it has been shown that some of the atypical chains such as K6, K11, K27, K29, monoubiquitin and multiple monoubiquitins can play a proteolytic role as well (Adhikari and Chen 2009). Studies with the K48 polyubiquitin chain have shown that affinity of the chain for the proteasome increases with chain length and that the minimal signal contains 4 ubiquitins in the chain. By increasing the number of ubiquitin moieties from two to four the affinity for the proteasome increases 100 fold (Thrower, Hoffman et al. 2000). Other atypical proteolytic signals may also involve heterogeneous (branched) chains of mixed linkage and heterologus chains between ubiquitin and other ubiquitin-like molecules such as SUMO (Kravtsova-Ivantsiv and Ciechanover 2012).

The specificity for a substrate is determined by cooperation between E3 and E2 enzyme in the ubiquitination cascade. Typically, ubiquitination occurs on one of the lysine residues in the substrate protein, but in rare cases also cysteine, serine and threonine can serve as ubiquitin acceptors (Kravtsova-Ivantsiv and Ciechanover 2012). The 26S proteasome is a large multicatalytic protease composed of a 20S core particle with proteolytic activity and a 19S regulatory particle (Fig. 1.2.3.). The 20S core particle is barrel shaped and contains two outer α rings and two inner β rings. Each ring has seven subunits termed α1-7 and β1-7. The 19S regulatory subunit is placed on one or both ends of the core subunit. The 19S regulatory particle is responsible for the recognition of the

polyubiquitin signal and it further facilitates the entry of the substrate into the proteasome by opening the orifice of the α ring and unfolding the substrate. This particle is composed of 17 different subunits forming the so-called base and lid. Six of the subunits have ATPase activity allowing energy-dependent processes like α ring opening and substrate unfolding to take place. The end products of proteasomal degradation are short peptides and reusable ubiquitin that is cleaved prior to substrate degradation (Ciechanover 2005).

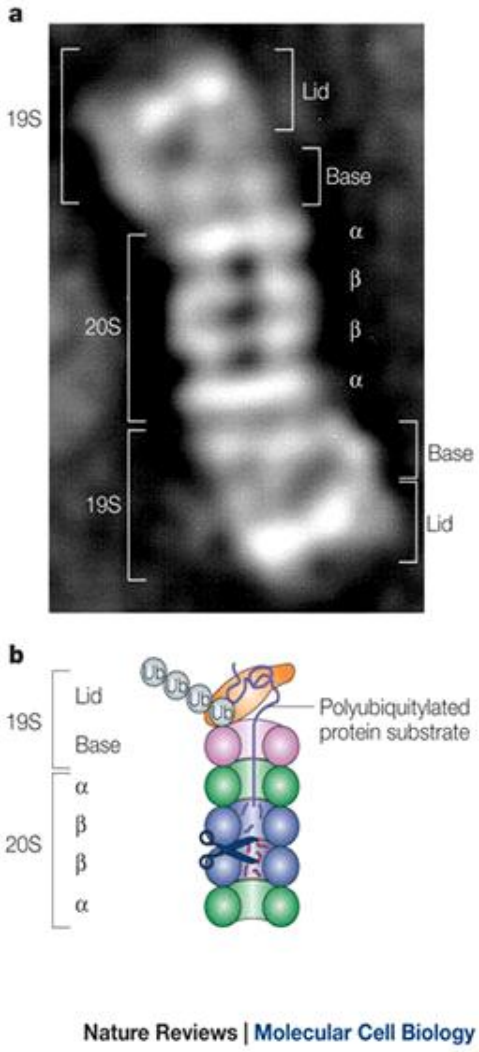

1.2.3. Electron-microscopy image and schematic representation of a 26S proteasome. (a) electron-microscopy image of ubiquitin *from Saccharomyces cerevisiae, (b)a schematic representation of the structure and function of the 26S proteasome. Ub, ubiquitin (Ciechanover 2005).*

1.2.2.1.2. Ubiquitin in autophagy

Besides proteasomal degradation, autophagy is one of the two cellular degradation pathways. The main catalytic component of the autophagic system is the lysosome, a single membrane organelle characterized by a very low pH and the presence of a number of endo- and exoproteases (Ciechanover 2005). The targets of autophagy are long lived proteins as well as complete organelles (Kraft, Peter et al. 2010). There are several different mechanisms by which autophagy can occur (Fig. 1.2.4.). The best characterized mechanisms in mammalian cells are macroautophagy, microautophagy, and chaperone-mediated autophagy (CMA) (Wong and Cuervo 2010). Macroautophagy is characterized by de novo formation of a double membrane vesicle, known as the autophagosome that subsequently fuses with the late endosome or lysosome. Microautophagy, much like macroautophagy, sequesters large regions of cytoplasm. However, in the case of microautophagy, the sequestration occurs directly via the lysosome (Wong and Cuervo 2010). Chaperone-mediated autophagy does not require vesicular transport but depends on the recognition of the KFERQ peptide motif within the substrate proteins by chaperones. The chaperone machinery, containing the constitutive form of heat shock protein 70 (Hsc70), heat shock protein 40 (Hsp40), heat shock protein 90 (Hsp90), the hsc70- interacting protein (hip), the Hsc70-Hsc90 organizing protein (hop) and Bcl2-associated athanogene 1 protein delivers the cargo protein to the lysosome where it interacts with lysosome-associated membrane protein type 2a (lamp2a). Subsequently the cargo is unfolded and pulled into the lysosome probably with the assistance of lysosomal hsp70 (Majeski and Dice 2004).

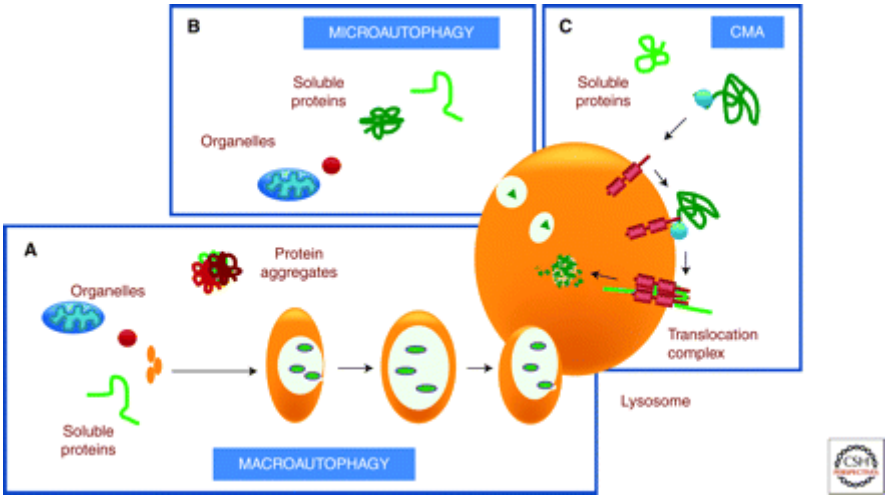

1.2.4. Different autophagic pathways*. Three different mechanisms by which cytosolic proteins can reach the lumen of the lysosome in the autophagic degradation pathway. (A) Macroautophagy, an entire region of the cytosol is sequestered into a double membrane vesicle that consequently fuses with lysosomes. (B) Microautophagy, the lysosomal membrane invaginates to trap regions of the cytosol forming single membrane vesicles. (C) Chaperone-mediated autophagy, cytosolic chaperones recognize a targeting motif in the substrate proteins leading to its delivery to the surface of the lysosome. The substrate protein subsequently binds to a lysosomal receptor that forms a translocation complex. The translocation of the target protein is mediated by the luminal chaperones (Wong and Cuervo 2010).*

For a long time autophagy was regarded as a nonselective process. In recent years it has been proposed that ubiquitination can provide selectivity to autophagy as well. It has been shown that organelles like mitochondria, ribosomes, and peroxisomes, cytoplasmic protein aggregates as well as certain intracellular bacteria can be removed from the cytoplasm by autophagy in a selective manner. This mechanism requires adaptor proteins that are able to bind both ubiquitin and LC3/GABARAP proteins on the lysosomal membrane, such as p62/sequestrosome1 and neighbor of BRCA1 gene (NBR1) (Kirkin, Lamark et al. 2009; Clague and Urbe 2010).

1.2.2.1.3. Ubiquitin in endosomal degradation

The lysosome is a final step in degradation of plasma membrane proteins such as membrane receptors and ion channels. Proteins residing at the plasma membrane are internalized by endocytosis after which they can either be recycled back to the membrane or degraded in the lysosome.

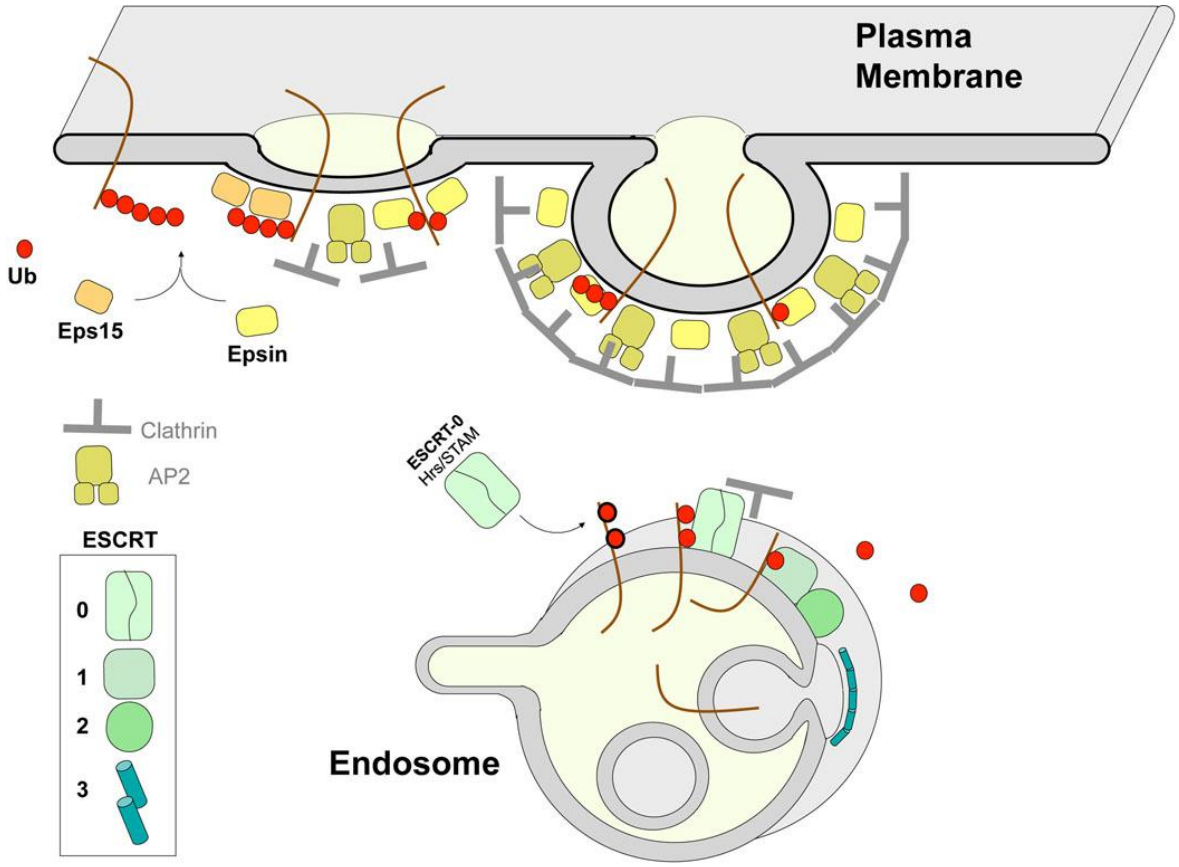

1.2.5. Ub-dependent endosomal trafficking

Eps15 and Epsin are early-acting clathrin associated proteins bind and concentrate ubiquitinated cargo in clathrin coated pits. Epsin and Eps15 both contain UIM (Ub-interaction motifs) that allow them to associate with Ub. Other Ub-binding proteins that have a similar function are not depicted. Ubiquitinated cargo is recognized by the ESCRT-0 subunits Hrs and STAM as well other Ub-binding ESCRT components to target ubiquitinated cargo into intralumenal vesicles of multivesicular bodies/late endosomes. Ub-binding domains are in addition found within ESCRT-I and ESCRT-II proteins that execute the deformation and scission of the membrane. This occurs in collaboration with the additional ESCRT-III polymer that constrict the neck of intralumenal vesicles (Piper and Lehner 2011).

Removal of proteins from the cell surface serves not only as a means for protein quality control but also as a mechanism to regulate signaling from certain receptors or transport of metabolites across the plasma membrane (Piper and Lehner 2011). Internalization of plasma membrane proteins is followed by sorting into intraluminal vesicles, either late

endosomes or multi-vesicular bodies (MVB). Here ubiquitin serves as a tag for internalization and sorting into the MVBs (Piper and Lehner 2011). Different ubiquitin signals from monoubiquitination to various polyubiquitin chains have been implicated in endocytosis, but the K63-linked polyubiquitin chain is emerging as the most common one. The best understood processes are the clathrin-mediated endocytosis of epidermal growth factor receptor (EGFR), class I major histocompatibility complex (MHC-I) and prolactin receptor. Epsin and Eps15 are two clathrin binding proteins that contain an ubiquitin interacting motif (UIM) (Fig. 1.2.5.). These proteins play important roles in the internalization of ubiquitinated cargo. It has been shown that Epsin plays a role in membrane bending and in recruiting additional adaptor proteins to clathrin coated pits. Furthermore ubiquitin plays a role in MVB sorting of the cargo through the interaction with ESCRT-0 complex that contains ubiquitin-binding domains (UBDs) in several components (Piper and Lehner 2011).

Interestingly, the $\alpha 5$ and $\beta 1$ integrin subunits and fibronectin have been shown to localize to multivesicular bodies/late endosomes in fibroblast. This occurs as a response to ubiquitination of the $\alpha 5$ subunit bound to fibronectin. Ubiquitination of the $\alpha 5$ subunit serves as a sorting signal for the endocytosed $\alpha 5\beta 1$ integrin and fibronectin to the multivesicular endosomes (MEVs) and is dependent on ubiquitin binding ability of ESCORT (Hurley and Emr 2006; Lobert, Brech et al. 2010). This process is required for the proper fibroblast migration (Lobert, Brech et al. 2010).

1.2.2.2. Role of ubiquitination in cell motility

In addition to the role of various E3 ligases and ubiquitination in regulation of cell proliferation, apoptosis, and development of neurodegenerative diseases, they also play a role in the regulation of cell motility. In recent years it has been demonstrated that various E3 ligases can regulate cell adhesion and migration on different levels by ubiquitinating specific substrates, such as adhesion molecules, regulators of actin polymerization, small GTPases, protein kinases, growth factor receptors and transcription factors (Huang 2010). One example for this is c-Cbl, a ubiquitously expressed E3 ligase family with three members in mammals (c-Cbl, c-Cbl-a, c-Cbl-b) (Keane, Rivero-Lezcano et al. 1995; Liu, DeYoung et al. 2003; Huang 2010). It has been demonstrated that c-Cbl can ubiquitinate the $\alpha 5$ integrin subunit leading to its degradation, which in turn results in reduced adhesion of osteoblasts on fibronectin (Kaabeche, Guenou et al. 2005). It has also shown

to influence integrin activation through ubiquitinating regulators of Rap1, thereby suppressing Rap1 activity (Kaabeche, Guenou et al. 2005). c-Cbl has been shown to negatively regulate actin polymerization, either by ubiquitination of mouse Disabled homologue 1 (mDab-1) or WAVE2 (Takenawa and Miki 2001; Suetsugu, Tezuka et al. 2004).

In recent years, two members of Nedd4 ubiquitin ligase family, Smad ubiquitin regulatory factor 1 and 2 (Smurf-1, Smurf-2), have been implicated in cell adhesion and migration (Huang 2010). An example of this is the Smurf-1-mediated ubiquitination and down regulation of RhoA in the lamellipodium (Wang, Zhang et al. 2003). In addition, Smurf-1 ubiquitinates and subsequently down regulates the talin head domain, leading to focal adhesion disassembly. This action of Smurf-1 on talin head is opposed by Cdk5 and through its ability to phosphorylation the talin head domain at Ser425 (Huang, Rajfur et al. 2009). Smurf-1 also ubiquitinates hPEM-2, a guanidine exchange factor for Cdc42, thus playing a role in the spatiotemporal regulation of Cdc42 during cell migration (Yamaguchi, Ohara et al. 2008).

In conclusion, ubiquitination and E3 ligases appear to be the new important regulators of actin polymerization, focal adhesion turnover and cell migration.

1.2.3. CHIP (STUB1)

C-terminal of Hsp70 interacting protein (CHIP) is an enzyme with E3/E4 ubiquitin ligase activity that is highly expressed in the nervous system and muscle tissue (Ballinger, Connell et al. 1999; Nyamsuren, Faggionato et al. 2007). It has two functional domains: the N-terminal tetratricopeptide domain (TPR) and the C-terminal U-box domain, which are highly conserved across species (Ballinger, Connell et al. 1999; Schulman and Chen 2005). The TPR domain mediates its interaction with chaperones such as hsp70 and hsp90, while the U box domain executes ubiquitin ligase activity (Schulman and Chen 2005). These two features allow CHIP to play an important role in protein quality control by integrating the UPS with the chaperone machinery. CHIP also regulates the cellular stress response by controlling the transcription of heat shock factor 1 (HSF-1) as well as down regulating the hsp70 by ubiquitination and proteasomal degradation after the stress stimulus has been removed (Min, Whaley et al. 2008).

1.2.3.1. CHIP and Hsp70/Hsp90 chaperone machinery in protein quality control

CHIP is a versatile E3 ligase with the ability to interact with various E2 ligases such as Ubc4, Ubc5, Ubc6 and Ubc13. Depending on the E2 ligase interaction, CHIP can form polyubiquitin chains of different linkage. For example, when interacting with UbcH5a, CHIP forms K48 polyubiquitin chains, while interaction with Ubc13/Uve1 leads to formation of K63 polyubiquitin chains (Zhang, Windheim et al. 2005). Additionally, K6 and K11 chain formation by CHIP has been reported (Kundrat and Regan 2010). This flexibility in chain formation enables CHIP to be involved in clearance of misfolded proteins not only by the ubiquitin proteasome system but also via ubiquitin-mediated selective autophagy (Kraft, Peter et al. 2010). CHIP links the molecular chaperones, such as Hsc70/Hsp70 and Hsp90 to the ubiquitin proteasome system thereby assuming a central role in cellular triage decisions (Fig. 1.2.8.). While Hsp70 is essential in protein quality control as it binds all misfolded proteins, Hsp90 binds so called client proteins that play central regulatory roles within the cell, such as protein kinases, transcription factors and receptors (Stankiewicz, Nikolay et al. 2010). Simultaneous binding of both Hsp70 and Hsp90 to HOP (Hsp70-Hsp90 organizing protein) allows the passage of client proteins from Hsp70 to Hsp90 followed by final folding and maturation (Kundrat and Regan 2010). Contrary to this, binding of CHIP to Hsp70 or Hsp90 is mutually exclusive. However, CHIP shows preference for ubiquitination of Hsp70-bound proteins. The misfolded proteins that cannot be refolded back to the native state spend more time in a complex with Hsp70 and are therefore more likely to be ubiquitinated by CHIP and subsequently degraded by proteasome (Stankiewicz, Nikolay et al. 2010). In addition, binding of the Hsp70 and Hsp90 to CHIP excludes their binding to HOP demonstrating mutual exclusion of cellular refolding and degradation pathways (Kundrat and Regan 2010; Stankiewicz, Nikolay et al. 2010). Under normal conditions proteins are found in a Hsp70-HOP-Hsp90 complex and the balance is shifted towards the folding process. However, upon inhibition of Hsp90 by geldanamycine or 17AAG, completion of the client protein folding is not possible. These unfolded proteins spend more time in a complex with Hsp70 and are consequently ubiquitinated by CHIP and degraded (Kundrat and Regan 2010).

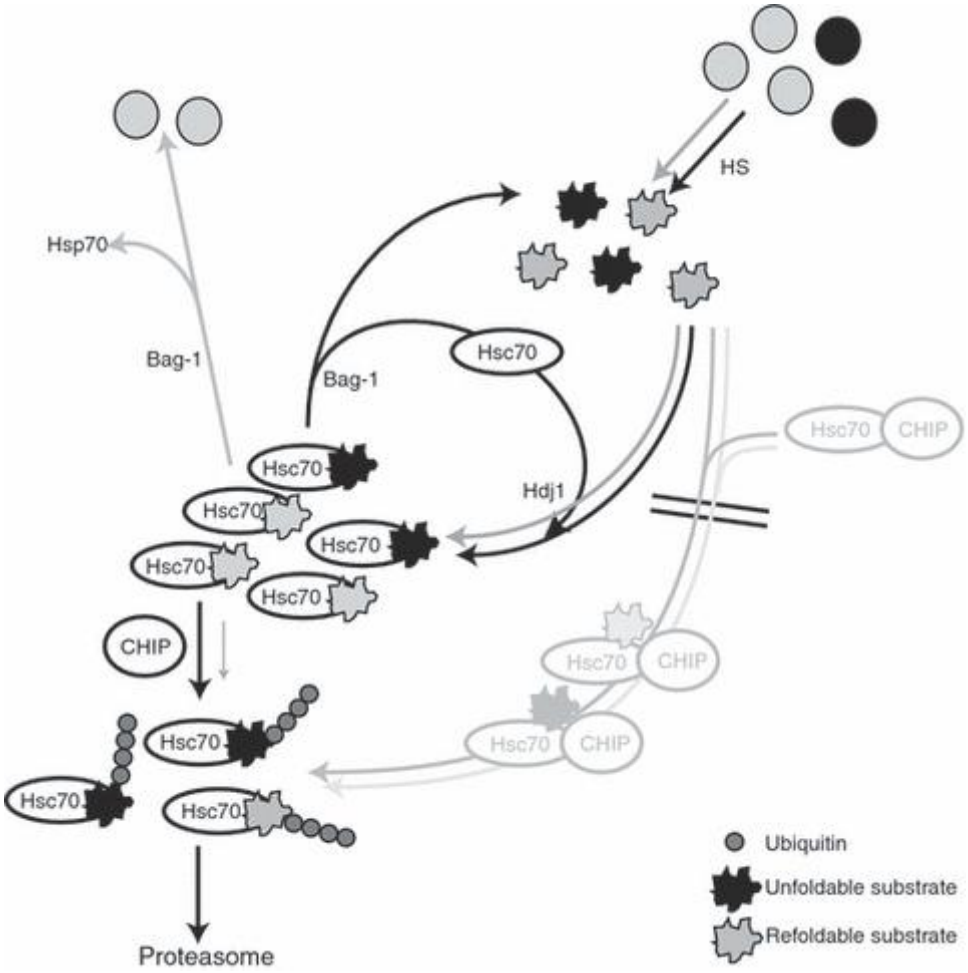

Figure 1.2.8. Role of CHIP in the triage decision. *Substrate proteins encountered by chaperones can be refolded (gray symbols and gray arrows) in only few cycles of chaperone binding, thus spending a short time in a Hsp70 chaperone-bound state. Protein substrates that cannot be effectively refolded (black symbols and black arrows) are repeatedly bound and released by the Hsp70 system (black arrows), and therefore spend a longer time in complex with the chaperones allowing efficient ubiquitination by CHIP (Stankiewicz, Nikolay et al. 2010).*

CHIP can also interact with various co-chaperones such as BAG1 and BAG3. In young cells the co-chaperone BAG1 is highly expressed promoting proteasomal degradation. With age the expression of co-chaperone BAG3 increases leading to more autophagic degradation (Fig. 1.2.9.). It seems that the ratio of BAG1 to BAG3 determinates the decision between the two degradation pathways and the ability of CHIP to interact with both co-chaperones allows it to act as a dual ubiquitin ligase targeting misfolded proteins to either autophagy or the proteasome (Kraft, Peter et al. 2010).

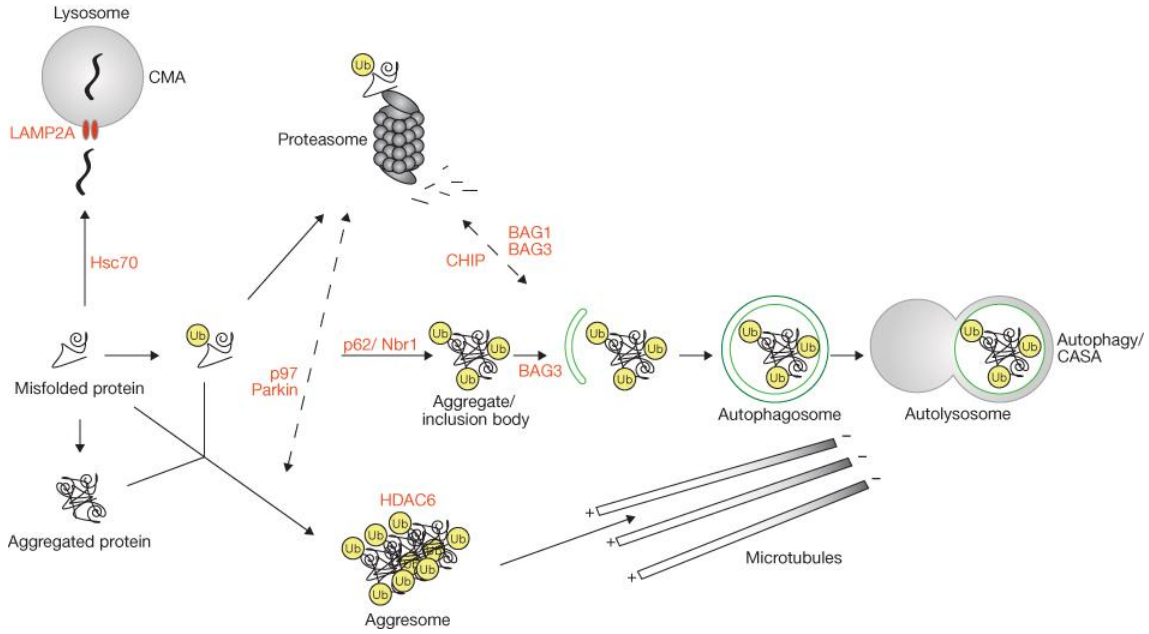

Figure 1.2.9. Various degradation pathways of misfolded proteins. *Depicted are three different pathways of misfolded protein degradation: 26S proteasomes, autophagy and chaperone-mediated autophagy (CMA). Misfolded proteins can be polyubiquitinated. This serves a recognition signal for proteasomal degradation. If misfolded proteins aggregate, they are targeted for autophagic clearance either by p62/NBR1-mediated autophagosomal engulfment or by aggresome formation coordinated by HDAC6. The decision between proteasomal and autophagic degradation is influenced by BAG1/BAG3 and CHIP, while p97 and parkin are involved in both proteasomal degradation and aggresome formation. It is still unclear how these different factors are coordinated and how the decision between different degradation pathways is made. Depicted in red are components involved during different steps of the degradation routes. Cross-talk between the different pathways is indicated by dashed arrows. Ub, ubiquitin (Kraft, Peter et al. 2010).*

1.2.3.2. Biological function of CHIP

Mice lacking CHIP expression are born in an expected Mendelian ratio, indicating that this protein is not essential for embryonic development. During the perinatal period CHIP-deficient mice show increased mortality up to 20% compared to wild type and heterozygous mice. The most interesting feature of those CHIP-deficient adult mice that fail to survive is the thymic atrophy that occurs due to hypocellularity and massive thymocyte apoptosis. However, the surviving CHIP-deficient mice do not display this phenotype (Dai, Zhang et al. 2003). Interestingly, these mice display accelerated ageing

with age-related changes affecting various organs and cell types leading to shortened life span (Min, Whaley et al. 2008). These mice also show an impaired response to physiological stress. The CHIP-deficient mice are unable to cope with a mild heat shock such as 42 ^{o}C administered for 10 min. While wild type mice normally survive thermal challenge, all knockout mice die during the heat exposure or in the recovery period, exhibiting lesions also common in humans suffering from a heat shock. These mice show characteristic stress response lesions such as edema, hyperemia and friability of the small intestine with blunting of the villi and thrombosis of subvillous arterioles. In addition, many different cell types show increased apoptosis in the gastrointestinal tract as well as in the spleen (Dai, Zhang et al. 2003). All this indicates that CHIP-mediated quality control mechanisms control cellular senescence and regulate longevity in mammals.

As a part of the system that regulates cellular proteostasis, CHIP plays a role in many neurodegenerative diseases that arise as a consequence of abnormal protein accumulation. CHIP is involved in regulation of aggregation of tau the protein responsible for Alzheimer´s disease. In addition, CHIP can cause both lysosomal and proteasomal degradation of α-synuclein thus playing a role in the progression of Parkinson´s disease. Furthermore, CHIP is involved in heat shock protein-mediated degradation of aggregated proteins such as huntingtin, ataxin and androgen receptor, making it part of the first line of defense in polyglutamine expansion diseases such as Huntington`s disease, several spinocerebellar ataxias and spinal and bulbar muscular atrophy (Dickey, Patterson et al. 2007). A wide range of substrates such as p53, ErbB2, estrogen receptor, myocardin illustrate CHIP´s involvement in different cellular physiological and pathophysiological processes from smooth muscle cell differentiation to breast cancer (Zhou, Fernandes et al. 2003; Tripathi, Ali et al. 2007; Patterson and Ronnebaum 2009; Xie, Fan et al. 2009).

2. Materials and Methods

2.1. Common chemicals

All chemicals used in this study, if not further specified, were purchased from the following companies: Carl Roth GmbH (Karlsruhe, Germany), Merck (Darmstadt, Germany), and Sigma Aldrich (Munich, Germany).

2.2. Animals

Mouse strains were maintained and bred in the animal facility of the Max Planck Institute of Biochemistry, Martinsried, Germany. The mice had free access to water and to standard rodent diet. The light cycle in the animal facility was set for 12 h. Mice of an age of 8 weeks were used for breeding. Mice were weaned and separated by sex and housed in different cages at an age of 3-4 weeks after birth. All weaned mice were marked with ear tags and clipped at the tail. DNA for genotyping was immediately isolated from the tails. All animals were treated according to the German Animal Protection Law.

2.2.1. Breeding scheme

CHIP+/- heterozygous mice were obtained from Cam Patterson from University of North Carolina at Chapel Hill School of Medicine, Department of Medicine, Chapel Hill, NC, USA. After the quarantine period the mice were transferred to a dirty animal facility where they were bred with 4-6 week old C57/BL6 females. The pregnant females from these breeding were used for an embryo transfer. In this way the animals were sanitized and introduced to the main animal facility.

2.3. Cell culture methods

2.3.1. Materials cell culture

5 ml Pipette: Corning, Costar Stripette, 4487
15 ml Pipette: Corning, Costar Stripette, 4488
25 ml Pipette: Corning, Costar Stripette, 4489

96-well: Corning, 35 3799
12-well: Corning, 35 3043
6-well: Corning, 35 3046
15 ml tube: Corning, 43 0791
50 ml tube: Falcon BlueMax, 35 2070
Cryogenic vial: Corning, 43 0489
100 mm dish: Falcon, 353003
140 mm dish: NUNC, 168381
DMEM High Glucose GlutaMAX: Invitrogen, 31966-021
Foetal bovine serum: Gibco, 10270-106
Trypsin: Trypsin / EDTA (10x), Gibco, 15400-054
P/S: Penicillin, Streptomycin (100x), PAA, P11-010
Fibronectin: bovine plasma fibronectin, Calbiochem, 341631
Phosphate Buffered Saline (PBS)

2.3.2. Isolation of mouse kidney fibroblasts

3 week old CHIP-/- and CHIP+/+ control mice were sacrificed and dissected as sterile as possible. The kidneys were collected in sterile PBS buffer. Kidneys were additionally rinsed in PBS and associated membranes were removed. The kidneys were dissected sagittally in 2 pieces each and rinsed again in PBS. Each kidney half was cut in small pieces and digested in 7 ml of 2 mg/ml Collagenase in DMEM + Pen/Strep for 30 min at 37°C with mixing every 10 min. After digestion the tissue was spinned down at 500 rpm for 5 min. After the removal of digestion medium the tissue was washed twice in DMEM+10%FCS+Pen/Strep to inactivate collagenase. The pellets were resuspended in DMEM+10%FCS+Pen/Strep and plated in 2 10 cm cell culture Petri dishes. The tissue was cultured for several days until the cells migrated out and attached to the dish. The cells were trypsinized and replated in order to remove any remaining tissue debris. Subsequently the cells were immortalized with SV40 virus and cloned. The cells were maintained in growth medium in a humidified atmosphere (5 % CO2, 95 % H2O).

Digestion medium

Collagenase type II 125 U/mg.....2 mg
Dissection medium.....1 ml
Collagenase type II, Worthington (Cat.No. LS 004196)

Growth medium

FBS .....10 ml

P/S.....1 ml

DMEM.....100 ml

2.3.3. Isolation of mouse embryonic fibroblasts

A CHIP+/- heterozygous timed mating was set up. The pregnant female was sacrificed and the E14 staged embryos were isolated as sterile as possible. The embryos were collected in sterile PBS buffer and additionally rinsed in PBS. The head and inner organs were removed and used for genotyping. The embryos were digested in trypsinization solution for 5 min. After digestion the tissue was spinned down at 500 rpm for 5 min. After the removal of the digestion medium the tissue was washed twice in DMEM+10 % FCS+Pen/Strep to inactivate the trypsin. The pellets were resuspended in DMEM+10 % FCS+Pen/Strep and plated in 6-well cell culture dishes. The tissue was cultured for several days until the cells migrated out and attached to the dish. The cells were trypsinized and replated in order to remove any remaining tissue debris. Subsequently the cells were immortalized with SV40 virus and cloned. The cells were maintained in growth medium in a humidified atmosphere (5 % CO2, 95 % H2O).

Digestion medium / Trypsinization solution

10x Trypsin /EDTA .....10 ml

PBS pH 7.4 .....90 ml

Growth medium

FBS .....10 ml

P/S.....1 ml

DMEM.....100 ml

2.3.4. Immortalization of mouse fibroblasts

Psi684 cells producing the SV40 virus were plated into a medium or large flask in a medium appropriate for the downstream application. When the cells reached 80-90% confluence the medium was changed. After the 10-12 h the medium was harvested and replaced. The harvested medium was spinned down at 900 rpm for 5 min and passed through a 0.22 µm filter in order to remove all cells from the viral supernatant. At this stage the viral supernatant was used fresh since the freezing down can cause the viral titer

to drop to 50 %, which reduces the efficiency of immortalization. The target cells were cultured in parallel and when they reached 50-60 % confluence the medium was removed and exchanged by the viral supernatant. For a 75 cm medium flask 7 ml of viral supernatant was used. After 1 h incubation period, 5 ml of fresh growth medium was added without removing the viral supernatant. The cells were kept in this medium over night after which the whole process was repeated once again. The next day the cloning was initiated by trypsinization and plating 200 cells on a 10 cm cell culture Petri dish.

2.3.4.1. Cell culture and trypsinization of immortalized mouse fibroblasts

Immortalized mouse fibroblasts were maintained in growth medium in a humidified atmosphere at 37 °C and 5 % CO2. In order to be passaged the cells were taken into suspension by trypsinization. The cells were washed in prewarmed PBS and detached from the substrate by incubation with trypsinization solution for approximately 2 min at 37°C. Detached cells were resuspended in growth medium.

Trypsinization solution

10x Trypsin /EDTA .....10 ml

PBS pH 7.4.....40 ml

2.3.4.2. Cryo-preservation of immortalized mouse fibroblasts

For long term storage frozen cultures were stored in liquid nitrogen tanks at -196 °C. The cells were trypsinized and resuspended in prewarmed growth medium. The cell suspension was centrifuged for 5 min at 900 rpm in order to remove trypsin. The cell pellet was resuspended in cooled freezing medium at an approximate concentration of $1x10^6$ cells/ml. The cell suspension was distributed in 1 ml aliquots in cryogenic vials and frozen on dry ice. The cells were stored at -80 °C for a short period of time after which they were transferred into liquid nitrogen at -196 °C for long term storage.

Freezing medium

FBS .....20 ml

DMSO.....10 ml

DMEM.....70 ml

2.3.4.3. Thawing of cryo-preserved fibroblasts

Frozen cells were placed in a water bath at 37 °C until the freezing medium had thawn. After this the cells were resuspended in prewarmed growth medium in approximately 10

fold volume of the initial cryoculture and centrifuged for 5 min at 900 rpm. The cell pellet was resuspended in growth medium and seeded in a flask of appropriate size. The cells were subsequently maintained in growth medium in a humidified atmosphere at 37 °C and 5 % CO2.

2.3.5. Establishment of ILK-Flag expressing stable cell lines

Primary fibroblasts were isolated and cultured as described previously. Single cell clones were obtained after which the *Ilk* gene was deleted by adenoviral expression of Cre-recombinase. ILK-/- fibroblast clones were retrovirally infected with Flag-tagged wild-type ILK or K341R pCLMFG constructs. Alternatively the CHIP-/- and CHIP+/+ kidney fibroblasts still expressing endogenous ILK were infected with the retrovirus expressing Flag tagged wild-type ILK. The fibroblasts stably expressing ILK-Flag or ILK-K341R were cultured in DMEM supplemented with 10% FCS.

2.3.5.1. Preparation of retroviruses

All retroviral preparations were done by Hildegard Reiter as previously described by Carsten Grashoff. Human embryonic kidney cells (HEK293T) were transiently transfected with pCLMFG construct packaging plasmids (encoding HIV *gag*, *pol* and *rev*) and a plasmid encoding the envelope of the vesicular stomatitis virus G by a calcium phosphate method in order to produce VSV-G pseudotyped retroviral vectors. The supernatant containing the VSV-G pseudotyped retrovirus was harvested, enriched by centrifugation and directly used for infection of ILK -/- , CHIP-/- or CHIP+/+ fibroblasts.

2.3.5.2. Calcium phosphate transfection of HEK293 cells

HEK 293 cells were expanded in growth medium at 37 °C and 10% CO2 in a humidified atmosphere. Cells were grown on 140 mm plates until 60 % confluence. Cells were incubated over night at 37 °C in 3 % CO_2 in 2.3 ml of transfection mixture. After this the medium was exchanged to growth medium. Cells were further cultured in growth medium at 3 7°C and 10 % CO_2.

2xBBS

BES pH 6.95.....4.26 g

NaCl.....6.54 g

Na2HPO4.....0,085 g

Filled up to 400ml with H2O

Transfection mix (for 1x 140mm dish)

DNA of pCLMFG..... 25 µg

DNA of packaging plasmid..... 25 µg

DNA of VSV-G env plasmid..... 12.5 µg

filled up to 1.16ml with sterile H2O, then addition of

$CaCl_2$ (2.5M) ..... 112 µl

vortexed, then addition of

2xBBS.....1.16 ml

inverted, incubate 10-15 min at room temperature

BES, Sigma (Cat.No. 9879)

2.3.5.3. Harvest of retroviral supernatant

The virus was harvested from HEK293 cells twice. The first harvest was done 24 h after initial transfection. The supernatant was collected and replaced by 16 ml growth medium after which the cells were incubated for additional 24 h at 37 °C in 10% CO2. The collected supernatant was filtered through a 0.45 µm filter. The filtrate was centrifuged at 50000x g for 2 h at 17 °C after which the pellets were resuspended in 50 µl HBSS, vortexed and stored at 4°C. The second harvest was performed 48 h after the initial transfection. The retroviral supernatant was collected and treated as the first harvest. For obtaining a higher concentration of the virus, pellets of the first and second harvest were combined, mixed with 2 ml of 20 % sucrose and centrifuged at 42000g for 2 h. Pellets were resuspended in 50-100 µl HBSS, mixed at room temperature for 45 min and pelleted by centrifugation. The supernatant was collected and stored at -80 °C.

Hanks' Balanced Salt Solution (HBSS), Gibco (Cat.No. 14175-046)

2.3.5.4. Infection of fibroblasts with VSV-G pseudotyped retroviral vectors

1.5-2x 10^6cells, approximately 50 % of confluence, were seeded on a 6-well plate and cultured over night in 1.5 ml of growth medium. The next day in the afternoon, 800 µl of growth medium containing 10-12 µl of the virus preparation was added onto the cells that were then incubated over night. After this the medium was changed to growth medium and the cells were grown until confluency. The cells were then expanded by trypsinization and replating onto 10 cm cell culture dishes. Finally, a subset of cells was frozen down for long term preservation and the remaining cells were used in experiments or further cloned into single cell clones.

2.3.6. Establishment of ILK-GFP expressing stable cell lines

Primary fibroblasts were isolated and cultured as described previously. Single cell clones were obtained after which the *Ilk* gene was deleted by adenoviral expression of Cre-recombinase. ILK-/- fibroblast clones were lentivirally infected with GFP-tagged wild-type ILK or K341R pHAGE-CMV-eGFP-W-mU6 constructs. All lentiviruses were produced and lentiviral transduction of fibroblasts was performed by Hildegard Reiter. The fibroblasts were expanded by culturing in DMEM supplemented with 10% FCS. The ILK-GFP, ILK-K341R GFP and ILK-/- GFP only expressing cells were sorted for the comparable high GFP expression using FACS Aria I cell sorter by Raphael Ruppert.

2.3.7. Establishment of clonal cell lines

In order to isolate single cell clones from a mixed population, cells were seeded in very low density of 200 cells/10 cm dishes and cultured in growth medium. After approximately 1 week single colonies were visible. The colonies were picked under sterile conditions with a 200 µl pipet. Cells were transferred into 200 µl pre-warmed 2x Trypsin/EDTA, incubated for 2 min at 37°C and resuspended in 2 ml of growth medium. Cells were cultured for approximately 1 week in 12-wells until confluent. The cells were then expanded to 6-well culture dishes by trypsinization and replating. Finally, a subset of cells were cryopreserved while the rest were expanded further and used in various assays.

2.3.8. 3D/ collagen gel migration assay

$1x10^6$ of cells were resuspended in 1 ml of growth medium. The cells were mixed with type I collagen in a 1:2 ratio, avoiding air bubble formation. The gels were loaded in self-made U-shaped invasion chambers consisting of objective slides, 18x18 mm cover slips, and paraffin. The gels were allowed to set at 37˚C for 30 min. DMEM supplemented with 10 % FCS and 1 mg/ml EGF as well as additional inhibitors, when required, were then added on top of the gel. The chambers were then sealed using paraffin and imaged using a Zeiss Axiovert 40C microscope (5X objective) equipped with a CCD camera (Prosilica, GC2450), heated stage (37 ˚C) and supplied with 4,7 % CO_2. Cell migration was tracked and quantified using the Chemotaxis and Migration plugin tool of ImageJ software. Statistical analyses on the data were performed using the GraphPad Prism software. Statistical significance was assessed by ANOVA followed by a Tucky post test.

Collagen gel

Collagen I…….750 µl

10XMEM...……..100 µl

$NaHCO_3$ pH 7.5…….……50 µl

Collagen 3mg/ml stock: PureCol, Advanced BioMatrix (Cat.No. 5005-B)

10XMEM, Invitrogen (Cat.No. 11430-030)

Object glass, Thermo Scientific (Cat.No. J1800AMNZ)

Cover Slips, Menzel Glaser (Cat.No. BB018018A1)

2.3.9. Biofunctionalized Micropatterned Substrates and 1D migration Assay

2,5 µm-line micropatterns were generated on PEG-coated cover slips using deep UV lithography (adapted from (Azioune, Storch et al. 2009)) by Dr. Julien Polleux and Zhu Min. Cells were seeded and grown on the micropatterns functionalized with fibronectin in 1% FCS supplemented DMEM. Live cell imaging was performed using a Zeiss microscope Axiovert 40C equipped with a CCD camera (Prosilica, GC2450). The stage was supplied with 4,7% CO_2 and heated at 37˚C. FireWire software (Molecular Devices, Downingtown, PA) was used for image acquisition as well as the microscope control. All images were obtained at +37°C and 5% CO_2 Cells were tracked manually using the Chemotaxis plug-in of ImageJ software.

2.4. Immunological methods

2.4.1. Materials immunological methods

Antibodies:
Primary antibodies used: anti-Ilk mouse (Transduction Laboratories), anti-ilk rabbit (Cell SignalingTechnology), anti-PINCH mouse (Transduction Laboratories), anti-parvin rabbit (Cell Signaling Technologies), anti-paxillin mouse (BD Biosciences), phalloidin Alexa546 (Invitrogen), anti-CHIP (Calbiochem).
Secondary antibodies used: Alexa488-, Alexa647- (Invitrogen) or Cy3- (Jackson Immuno Research Laboratories), anti-pFAK (Tyr397, Biosource), anti-FAK rabbit (Upstate), anti-GAPDH mouse (Calbiochem), anti-paxillin mouse (Transduction Laboratories), anti-

CHIP rabbit (Calbiochem), anti-FLAG M2 mouse HRP conjugated (Sigma) and goat anti-mouse HRP, and goat anti-rabbit HRP (Bio-Rad Laboratories).

2.4.2. Immunostaining of adherent cells

For cellular immunostaining, cells were grown on glass cover slides (Roth) coated with 5 µg/ml fibronectin or allowed to adhere and spread for 24 h. Cells were fixed in 4 % PFA, rinsed with PBS and permeabilized with 0.1 % Triton X-100. Nonspecific protein binding sites were saturated with 3 % bovine serum albumin (BSA) and 5 % goat serum in PBS, followed by incubation with primary antibodies over night at 4 ˚C or 1 h room temperature followed by incubation with secondary antibodies and DAPI (1:10 000 in PBS). The cover slides were washed and mounted on object glass slides with elvanol. The fluorescent images were collected by laser scanning confocal microscopy (DMIRE2; Leica) using Leica Confocal Software version 2.5 Build 1227 with ×100 oil objective.

Glass cover slides, Roth (Cat.No. P231.1)

Fixation solution

Paraformaldehyde (PFA) 4%

dissolved in PBS (pH 7.4), boiled for 1 min and cooled on ice

Permeabilization solution

Triton-X-100 ..... 0.1%

Dissolved in PBS (pH 7.4)

Blocking solution

bovine serum albumin (BSA) 3%

goat serum…….5%

Dissolved in PBS (pH 7.4)

Elvanol

Mowiol 4-88.....12 g

H2O.....30 ml

mixed for 10 min, incubated 2-3 h at RT, then addition of

0.2 M Tris-HCl pH 8.5.....60 ml

87 % glycerol.....30 ml

Mixed for 10min, and then kept at 4°C overnight, aliquoted and stored at -20°C

Mowiol, Roth (Cat.No.0713)

2.5. Biochemical methods

2.5.1. Materials biochemical methods

Centrifuge: Beckman Coulter, GS-15R

Ultracentrifuge (small): Beckman Coulter, TL-100 Ultracentrifuge

Ultracentrifuge rotor: Beckman Coulter, TL-100

Ultracentrifuge (large): Beckman Coulter, L8-60M

Ultracentrifuge rotor: Beckman Coulter, SW41

Protease inhibitor cocktail: complete Mini, EDTA-free, Roche, 12740900

2.5.2. Preparation of total protein lysates form adherent cells

Cells grown on polystyrene dishes at 70-80% of confluence were rinsed in ice cold PBS and suspended in lysis buffer. The cells were incubated for 10 min on ice to allow cell lysis to proceed after which the lysates were harvested with a cell scraper. Cell lysates were cleared by centrifugation at 15000xg for 5 min at 4°C. The protein concentration of the supernatant was determined using a bicinchoninic acid protein assay kit. After the protein concentrations were adjusted, lysates were reduced in the appropriate amount of 4x SDS sample buffer by incubating for 5 min at 95 °C and either frozen in -80°C or directly subjected to SDS-PAGE. After separation of polypeptides on SDS-PAGE they were transferred onto PVDF membranes and subjected to western blot analyses. Alternatively, the lysates were used for performing immunoprecipitation assays.

Cell lysis buffer

Tris/HCl pH 8.0.....50 mM

NaCl.....150 mM

Triton X-100 ..... 1 %

EDTA……..……...10 mM

protease inhibitor cocktail.....1 tablet/10ml

Phosphatase inhibitor I and II 100µl per 10ml of lysis buffer

4x SDS sample buffer

20 %SDS.....16 ml

1 M Tris pH 6.8.....8 ml

0.5 M EDTA.....0.32 ml

87 % glycerol.....16 ml

bromphenol blue ....0.001 %

before use, mercaptoethanol was added to a final concentration of 4 % and stored at RT

The following volumes of cell lysis buffer were used:

6-well plate ..... 250 µl

10 cm dish..... 0.5-1 ml

2.5.3. Determination of protein concentration-BCA protein assay

The BCA method is based on the reduction of Cu^{2+}- to Cu^{1+}-ions by proteins under alkaline conditions (Buiret-reaction). The detection of Cu^{1+}-ions is mediated by bicinchoninic acid, which is chelated by cuprous cations forming a complex with a strong absorbance at 562 nm. The assay was performed according to the instructions of the manufacturer.

BCA Protein Assay Kit, Pierce (Cat.No.23225)

2.5.4. Immunoprecipitation

Cell lysates were prepared as described above. For immunoprecipitation assays protein concentrations of 0.5-1.5 mg/ml in a volume of 0.5-1 ml were used. The beads were prepared by washing 3x in TBS with centrifugation for 5 min at 5000g between the steps. Usually 50-100 µl of the beads was used for incubation of 2 h with lysates. After the binding of the protein to the beads the beads were washed 2 times with lysis buffer and 2 times with PBS.

2.5.4.1. FLAG Immunoprecipitation

For immunoprecipitation of FLAG tagged proteins, cell lysates were incubated for 2 h at +4°C with anti-FLAG M2 affinity gel that had previously been washed 3 times with TBS to remove the methanol-containing storage buffer. 50 µl of the gel was applied to protein concentrations of 0.5-1.5 mg/ml in 0.5-1 ml of volume. After this the gel was washes 2 times with lysis buffer and 2 times with PBS to remove unspecifically bound material. Immunoprecipitated Flag tagged proteins were eluted by incubation with FLAG-peptide

for 30 min on ice. The gel was then centrifuged 5 minutes at 5000g and the supernatant was reduced by Laemmli sample buffer and boiled at 95°C for 5 min. The reduced samples were further subjected to SDS-PAGE or alternatively processed for mass spectrometry analysis.
Anti-FLAG M2 affinity gel, Sigma (Cat.No.A2220)
3xFLAG peptide, Sigma (Cat.No.F4799)

2.5.4.2. Mass Spectrometry

FLAG immunoprecipitation was performed as described above using lysates from fibroblasts stably expressing wt ILK-Flag and ILK-K341R. The parental ILK fl/fl fibroblasts were used as a negative control. In solution trypsin digestion was performed on immunoprecipitates followed by reversed-phase liquid chromatography (Proxeon Biosystems) coupled online to an LTQ-Orbitrap mass spectrometer (Thermo Fisher Scientific). Data were acquired with Xcalibur software and analyzed with MaxQuant software. The mass spectrometry analysis was performed by Dr. Tami Geiger.

Trypsin is a serine protease cleaving the peptide bonds in which the carbonyl group is contributed either by an Arg or Lys residue. After the digestion by trypsin ubiquitin modification leaves behind only a Gly-Gly dipeptide covalently attached to the target protein. However, other small protein modifiers such as SUMO leave the same Gly-Gly dipeptide and therefore cannot be distinguished from ubiquitin only by mass spectrometry.

2.5.4.3. In Vivo Ubiquitination Assay

In this assay covalent protein modifications are analyzed by performing an immunoprecipitation under reducing conditions. This allows disruption of noncovalent protein interactions as well as the inactivation of enzymes that catalyze removal of modifications. The immunoprecipitation can be performed by using an antibody against ubiquitin. This leads to precipitation of all ubiquitinated proteins allowing subsequent western blot analysis with antibodies against the target protein to confirm the ubiquitination. Alternatively, antibodies against target proteins can be used for immunoprecipitation followed by detection of ubiquitin with western blot.

Cells grown on polystyrene dishes at 70-80% confluence were rinsed with PBS. The PBS was subsequently removed and the cells were harvested from the dish by scraping and

collected in 1.5 ml eppendorf tubes. The cells were immediately resuspended in 100 µl of denaturing lysis buffer, mixed by vortexing and boiled for 5 min at 95˚C. Rapid denaturation is essential in order to inactivate very potent deubiquitinase enzymes. The lysates were then diluted 1:10 in non-denaturing lysis buffer followed by incubation on ice for 5 min. The non-denaturing buffer contains Triton-X 100 that allows the sequestration of SDS in micelles. This facilitates immunoprecipitation without interference of SDS with the antibody-antigen interaction. The Flag immunoprecipitation was subsequently carried out as described above.

Denaturing lysis buffer

Tris/HCl pH 7.4…….50 mM

SDS……..1 %

EDTA……...5 mM

Non-denaturing lysis buffer

Triton X-100……..……..1%

NaCl ……300 mM

Tris pH 7,4/HCl……...50 mM

EDTA…….…….5 mM

Both denaturing and non-denaturing buffers were supplemented with a complete protease inhibitor cocktail, 1tablet /10 ml of lysis buffer and 25 mM N-Ethymaleimid (NEM), an inhibitor of deubiqutinases, freshly before use.

2.5.4.4. GFP Immunoprecipitation

GFP immunoprecipitation was performed using the Miltenyi Biotec MultiMACS GFP Isolation Kit. Cells grown on polystyrene dishes at 70-80% of confluence were rinsed with ice cold PBS and harvested in lysis buffer provided by the manufacturer, collected in 1.5 ml eppendorf tubes and incubated for additional 20 min on ice. Cell lysates were cleared by centrifugation at 10000g for 10 min at 4 °C. The protein concentration of the supernatant was determined using a bicinchoninic acid protein assay kit. After protein concentrations were adjusted the lysates were used for immunoprecipitation assays. Typically concentrations of 0.5-1.5 mg/ml in 1 ml of lysis buffer volume were used. The lysates were incubated with 50 µl of magnetic anti-GFP beads for 30 min on ice with

occasional mixing. After this the lysates were loaded on the µ columns, placed into the µMACS separating magnet and allowed to flow through. The proteins bound to the beads were washed 2 times with 1:10 dilution of the lysis buffer in de-gassed TBS and 2 times with wash buffer II. The bound proteins were eluted and reduced with elution buffer preheated at 95˚C. The eluates were additionally incubated for 5 min at 95 ˚C after which they were subjected to SDS-PAGE.

GFP lysis buffer

Tris/HCl pH 8.0……..…..50 mM

Triton X-100…….…1 %

NaCl……150 mM

Wash buffer II

Tris/HCl pH 7.4…….…..20 mM

Elution buffer

Tris/HCl pH 6.8……..50 mM

DTT…….50 mM

EDTA……....1 mM

Bromphenol blue……...0,0005 %

Glycerol…….....10 %

2.5.5. One-dimensional SDS-polyacrylamide-gel electrophoresis (SDS-PAGE)

Protein lysates were typically precleared by centrifugation and reduced by boiling at 95˚C in the presence of sodium dodecyl sulphate (SDS). 2-Mercaptoethanol or dithiothreitol (DTT) was added to reduce disulfide bonds. In this assay proteins are separated electrophoretically. Separating and stacking gels that are differentially buffered are poured on top of each other in order to perform discontinuous gel electrophoresis. In the stacking gel proteins get concentrated at the stacking/separating gel interface. In the separating gel the proteins are separated according to molecular size in a denaturing gel (containing SDS). Here proteins were separated in the Mini gel format (7.3 mm x 8.3 mm x 1.5 mm) using the Mini Protean III System (BioRad). After polymerization of the polyacrylamide gel and assembly of the electrophoresis apparatus the gel running chamber was filled with SDS-PAGE running buffer. The protein samples were reduced in 4x SDS sample buffer and boiled for 5 min at 95 °C. Samples were loaded on the stacking gel. The electrophoresis was performed at 100V at room temperature.

Separating gel (10ml) 8 %.....10 %..... 12 % .....15 %

H2O..... 4.6 ml..... 4.0 ml .....3.3 ml ..... 2.3 ml

30 % ProtoGel..... 2.7 ,ml..... 3.3 ml .....4.0 ml ..... 5.9 ml

1.5 M Tris pH 8.8 ….. 2.5 ml..... 2.5 ml .....2.5 ml ..... 2.5 ml

10 % SDS..... 0.1 ml.....0.1 ml .....0.1 ml..... 0.1 ml

10 % APS..... 0.1 ml..... 0.1 ml .....0.1 ml..... 0.1 ml

TEMED..... 0.006 ml..... 0.006 ml .....0.006 ml .....0.006 ml

Stacking gel (5 ml)..... 5 %

H2O..... 3.4 ml

3 0% ProtoGel..... 0.83 ml

1 M Tris pH 6.8……..... 0.63 ml

10 % SDS..... 0.04 ml

10 % APS.....……...0.04 ml

TEMED..... 0.004 ml

10x SDS-PAGE running buffer (1l)

Glycine.....144 g

Tris-HCl.....30.3 g

SDS .....10 g

N,N,N',N'-Tetramethylethylenediamine (TEMED), Serva (Cat.No.35925)

ProtoGel (Ultra Pure), National Diagnostics (Cat.No.EC-890)

2.5.6. Western blotting and Immunoblotting

Western blotting is used to identify specific proteins by polyclonal or monoclonal antibodies. After the proteins are separated by SDS-PAGE they are electrically transferred onto an activated PVDF membrane. Subsequently, proteins bound to the surface of this membrane can be visualized by immunodetection reagents.

After separation of proteins by SDS-PAGE, the stacking gel was removed while the separating gel was placed in Western blotting transfer buffer. The PVDF membrane was activated by incubation in methanol and then washed in blotting buffer. Typically the semi-dry method of transfer was used in which a gel is placed on top of the PVDF membrane in between two layers of Whatman paper soaked with transfer buffer. Proteins were then electrically transferred 1.5 h with 100 mA at room temperature. After disassembly of the transfer sandwich, membranes were stained for 1 min with Ponceau S

solution and rinsed in H2O in order to visualize proteins bands on the membrane and to confirm the success of transfer. Membranes were subsequently washed in TBS-T and blocked for 1 h at room temperature in blocking buffer. Next, the primary antibody was incubated on the membrane either over night at 4 °C or for 1 h at room temperature (depending on the instructions of the antibody manufacturer or personal experience), membranes were washed 3 times 10 min with TBS-T and the appropriate secondary antibody was incubated with the membrane for 30 min at room temperature. After 6 washes for 10 min in TBS-T and an additional wash for 10 min in TBS only, membranes bound HRP was detected using a chemiluminescence-based detection kit.

Western Blotting transfer buffer (1l)

Tris-HCl.....6 g

Glycine.....28.8 g

Methanol.....200 ml

10x TBS (1000 ml)

Tris-HCl.....24.3 g

NaCl.....80 g

TBS-T (1000 ml)

Tween-20 .....1 ml

10x TBS.....100 ml in H2O

Blocking buffer

Skim milk powder ..... 5 % in TBS-T

Ponceau S solution, Sigma (Cat.No. P3504)

Chemiluminescence Reagent Plus, Western Lightning (Cat.No.NEL104)

2.5.7. In Vitro Ubiquitination Assay

For many known ubiquitin targets modification by ubiquitin (Ub) has been reconstituted *in vitro*. This assay typically involves incubation of recombinant target protein with recombinant or purified enzymes, Ub and ATP. Ub modification results in mobility shift of the target of approximately 8 kDa, and it can be detected by anti-Ub immunoblot. In vitro ubiquitination assay was performed by incubating recombinant ILK and CHIP with E1 (Calbiochem), UbcH5a (Sigma), 5 mM ATP, 2.5 mg/ml Ub (Sigma) in total of 20 µl of reaction buffer for 2-4 h at 30 °C. Reactions were stopped by adding Laemmli buffer, boiling at 95 ˚C and running the samples on a 4-12 % gradient gel Tris/HCl gel (BIORAD).

In vitro ubiquitination reaction:

ILK……....….0.36 µg

E1…….……..……1 µM

UbcH5a…….……..…1 µM

Hsp70….....1 µM

Hsp40…….….0.1 µM

CHIP…….……...…1-3 µM

Ub…….…….2.5 µg/µl

ATP…….……....100 mM

All the assays were performed in total of 20 µl of reaction volume.

In vitro ubiquitination reaction buffer

MOPS pH 7.2…….…...20 mM

KCl……...100 mM

MgC……..l25 mM

DTT……10 mM

PMSF……...…1 mM

E1 enzyme, Calbiochem (Cat.No.662070)

UbcH5a enzyme, Sigma (Cat.No. SRP6026)

Ubiquitin, Boston Biochem (Cat.No.U-100)

2.6. Molecular Biological methods

2.6.1. Materials Molecular Biological methods

Autoclave: KSG, KSG-112

Centrifuge: Eppendorf, 5417C

Centrifuge: Beckman Coulter, Avanti J-25

Centrifuge rotor: Beckman Coulter J 14 / J 25.50

Microwave: Daewoo, KOR 63D7

Thermocycler: Biometra T3

Thermomixer: Eppendorf 5350

2.6.2. Isopropanol extraction of tail DNA

For genotyping of mice, a small part of the mouse tail was amputated and digested with 500 µl DNA lysis buffer in an eppendorf tube over night. The next day the lysate was precleared by centrifugation 5 min 15000g at room temperature. 500µl Isopropanol (1:1) was added to the DNA solution and inverted several times until precipitated DNA flakes appeared in the solution. The DNA was centrifuged for 5 min at 15000xg. The supernatant was decanted and the DNA pellet was washed by 500 µl of 70% Ethanol. After washing, the DNA was centrifuged again for 5 min at 15000g. Pellets were air-dried for 1-2 min and subsequently resuspended in 250-300 µl H2O.

DNA lysis buffer

NaCl.....20 mM
Tris/HCl pH 7.6.....100 mM
EDTA .....5 mM
SDS ..... 0.2 %
proteinase K..... 100 µg/m

2.6.3. Bacteriological tools

Escherichia coli (E.coli) cultures were cultured in lysogeny broth (LB) rich medium. Media were prepared and autoclaved for 20 min at 120 °C. Antibiotics were added after the solutions were cooled below 50 °C. LB plates were poured into 100 mm Petri dishes and stored at 4°C.

LB medium

NaCl.....10 g
Trypton.....10 g
Yeast extract .....5 g
filled up to 1000 ml with H2O, autoclaved and stored at 4°C

LB plates

LB medium.....1000 ml
Agar-Agar.....15 g
autoclaved, poured into 100 mm Petri dishes, stored at 4 °C

Additives

Ampicillin..... 50 µg/ml

Kanamycin..... 25 µg/ml

Tetracycline ..... 12.5 µg/ml

2.6.3.1. Preparation of competent bacteria

An XL-1 blue *E.coli* bacterial culture was grown o/n in 10 ml LB +Tetracycline at 37 °C on constant shaking at 180 rpm. The next morning, 100 ml of LB+Tetracycline was inoculated with 2 ml overnight culture and grown until an optical density at 550 nm (OD550) of 0.5 was reached. The bacterial culture was placed on ice for 10 min and then centrifuged for 15 min at 4 °C with 1000g. The pellet was resuspended in 10 ml TSS and 2.9 ml glycerol (87%) was added. The bacterial suspension was distributed in 200 µl aliquots and immediately snap frozen in liquid nitrogen. Competent cells were stored at -80°C.

TSS (500ml)

polyethylenglycol .....50 g

Tryptone.....5 g

Yeast extract .....2.5 g

NaCl.....2.5 g

DMSO.....25 ml

1 M MgCl2 .....25 ml

Filtrated and stored at 4°C

2.6.3.2. Cryo-preservation of competent bacteria

The bacterial cultures were frozen by adding 250 µl glycerol (87 %) to 750 µl bacterial over night culture. Cryocultures were stored at -80 °C.

2.6.3.3. Transformation of competent bacteria

100 µl of competent bacteria were thawn on ice for 15 min. For simple retransformation of a plasmid, 1 µg of DNA was added and incubated on ice for 30 min. Alternatively, 1 µl of cloning reaction for newly cloned vectors was added to bacteria. Cells were then placed on 42 °C for 45 sec (heat shock) and subsequently placed on ice for 2 min. Bacteria were spread on LB plates with appropriate antibiotics. Plates were incubated

over night at 37 °C. Colonies appeared within 8-12 h depending on the transformed DNA construct.

2.6.3.4. Preparation of plasmid DNA from bacterial cultures

Bacterial colonies were inoculated in 5 ml LB medium containing appropriate antibiotics over night at 37 °C. 750 µl of this bacterial culture was frozen down as described above. 3 ml of bacterial culture was used for DNA isolation that was performed using the Qiagen Plasmid Mini Kit. This is a method based on an alkaline bacterial lysis, followed by binding of DNA to an anion-exchange resin under low salt and low pH conditions. Impurities such as proteins or RNA are removed by medium salt washing steps. DNA is eluted from the resin under neutral or alkaline pH conditions. Large amounts of DNA were prepared by the same method using larger volumes (ProOmega Midi Kit). DNA concentration was determined by photometric measurement at 260 nm. DNA was stored at -20°C.

Qiagen Plasmid Mini Kit, Qiagen (Cat.No. 12125)

PureYeald Midiprep Kit, ProOmega (Cat.No. A2492)

2.6.4. Recombinant protein purification

STUB-1 (CHIP) cDNA was subcloned in the pET-16b vector for the expression of a His tagged CHIP protein. *E.Coli* BL-21 strain was transformed as described above. The bacteria were grown in LB medium containing ampicillin. The 50 ml preculture was grown at 37˚C while shaking at 180 rpm over night. Next day a larger culture (3 l) was inoculated and grown until an optical density of 0.8 at 550 nm (OD550) was reached. At this point 0.5 mM Isopropyl β-D-1-thiogalactopyranoside **(**IPTG) was added to the culture in order to induce the synthesis of the recombinant protein. The bacterial culture was incubated over night at 37 ˚C while shaking at 180 rpm. Next day the bacteria were pelleted by centrifugation for 15 min at 6000g at 4 ˚C. After removal of the supernatant the bacterial pellet was resuspended in lysis buffer, 10 ml/3.9 g of bacterial pellet. The bacteria were lysed on ice for 30 min and sonicated on ice until the lysate had lost its viscosity. The lysates were precleared by centrifugation for 30 min at 20000g. NaCl was added into the supernatant to a final concentration of 150 mM and $MgCl_2$ to a final concentration of 2 mM.

A His pull down was performed to purify the His-tagged CHIP from the lysate. The Talon slurry was equilibrated in the His wash buffer containing 10 mM imidazole. 2 ml of the Talon slurry was then incubated with 20 ml of lysate for 20 min at room temperature while rocking. The Talon slurry with bound protein was washed 2 times in 20 ml of His wash buffer after which it was packed into a 2 ml disposable BioRad column. The elution was performed with 5 ml of His elution buffer while collecting 500 µl elution fractions. The protein concentration was determined by the BCA method. Fractions 1 and 2 had a protein concentration of 1.2 µg/µl while fraction 3 had 12 µg/µl of protein. The purity and the concentration of protein was also confirmed by SDS-PAGE followed by Coomassie staining. The fraction 3 as well as fractions 1 and 2 were pooled and dialyzed against 20 mM Tris pH 8.0, 150 mM NaCl. The dialysis was performed in 5 l volume of dialysis buffer for 2 h followed by and exchange of dialysis buffer and subsequent over night dialysis.

His wash buffer

Tris pH 8.0……... 20 mM

NaCl……...…….…150 mM

Imidazole…….….10 mM

His elution buffer

Tris pH 8.0…….…...20 mM

NaCl…….....….……..150 mM

Imidazole…….200 mM

Dialysis buffer

Tris/HCl pH 8.0……..……20 mM

NaCl…….150 mM

Isopropyl β-D-1-thiogalactopyranoside, Sigma (Cat.No. I6758)

TALON His Tag Purification resin, Clontech (Cat.No. 635501)

Disposable columns, BioRad (Cat.No. 731-1550)

2.6.5. Molecular cloning

In molecular biology restriction enzymes are commonly used to cleave DNA at specific sites. There are three subgroups of restriction enzymes. The type I restriction enzymes cut the DNA random far from their recognition sequence. They are complex multi-subunit enzymes. The type II enzymes cut the DNA within or close to the binding motif within the DNA molecule. They recognize and bind a specific DNA sequences. The type III restriction enzymes cleave the DNA outside of their recognition sequence and are complex molecules. The most widely used tool in molecular biological are type II restriction enzymes.

2.6.5.1. Digestion of DNA with restriction enzymes

All digestions were performed according to the manufacturer´s instructions. In general, reactions were performed using the following conditions and appropriate NEB buffer with or without BSA:

DNA digestion

DNA ..... 3-5 µg

NEB buffer …… ..... 3 µl

BSA(+/-)……..…..……....0.1 µl

Restriction enzyme.....5 U

filled up to 30 µl with H2O, incubated for 2 h at 37°C

All restriction enzymes were purchased from New England Biolabs (NEB).

2.6.5.2. Dephosphorylation of plasmid DNA

After the digestion of DNA with restriction enzymes reactive 5'-phosphate and a 3'-hydroxyl groups are generated. This leaves the possibility for self-ligation which can decrease the success of the cloning. In order to prevent this, the 5'-phosphate group was typically removed using shrimp alkaline phosphatase (SAP). Digestion enzymes were heat inactivated according to the manufacturer´s instructions. Subsequently the digestion reaction was incubated at high pH conditions for 30 min with SAP.

Dephosphorylation of DNA

DNA ..... 3-5 µg

SAP buffer ..... 3 µl

SAP.....5 U

In a total reaction volume of 30 µl filled in with H2O and incubated for 30 min at 37°C

2.6.5.3. Ligation of DNA fragments

In general the ligation of DNA occurs through the formation of a phosphodiester bond between a 3'-hydroxyl group and a 5'-phosphate group. In this study the DNA back bone was typically dephosphorylated after the digestion with restriction enzymes before proceeding to the ligation reaction. DNA inserts were generated by restriction enzymes or by PCR and subsequent restriction in order to create the ``sticky ends´´. The reactions were performed using 200 ng of total DNA. The ratios between the amounts of backbone and insert were typically 1:3, 2:5 or 1:5 depending on the sizes of the insert and the backbone DNA. In order to perform DNA ligation the following protocol was used.

DNA ligation

DNA backbone (vector) ..... 0.5-1 µl

DNA insert..... 5 µl

ATP (10mM).....1.5 µl

Fast link ligase buffer..... 1.5 µl

Fast link ligase..... 1 µl

In total reaction volume of 15 µl filled in with H2O and incubated for 45 min at room temperature. After this heat-inactivation was preformed for 10 min at 70°C. Typically 1 µl of the ligation reaction was used for transformation of bacteria as described above. Several colonies were picked and after DNA purification succesful cloning was confirmed by sequencing.

2.6.6. Polymerase chain reaction (PCR)

PCR is a method of enzymatic DNA amplification (Saiki et al. 1988). The reaction requires the presence of a DNA template as well as two primers. In addition, DNA polymerase and dNTPs are necessary to carry out the reaction. Typically *Taq* polymerase is used or alternatively a high fidelity polymerase. The amplification occurs in three different steps. The denaturation step requires a high temperature of 95 °C. The next step is annealing of the primers to the DNA template and it requires lower temperatures, usually 58-68 °C depending on the primer melting temperature. Finally the DNA synthesis occurs at typically at 72 °C but can also vary depending on the DNA polymerase used in the reaction.

2.6.6.1. PCR primers

All oligonucleotides were purchased from Metabion International, Martinsried, Germany. Oligonucleotides used for site directed mutagenesis were HPLC purified.

2.6.6.2. PCR reactions

Genotyping PCR reaction was performed using tail DNA and self-made recombinant *Taq* polymerase. The cloning PCR was performed using purified plasmid DNA or cDNA obtained by reverse transcription PCR from total cellular RNA and high fidelity polymerase such as PFU Ultra with an additional proof reading activity. Use of the different PCR buffers depended on the DNA polymerase in the reaction.

Genotyping PCR

DNA ……..... 1 µl
primer1 (10 pmol)..... 1 µl
primer2 (10 pmol)..... 1 µl
dNTP (10 mM)..... 1 µl
DMSO..... 0.5 µl
10x PCR buffer ..... 5 µl
Taq polymerase..... 0.5 µl
filled up to 50 µl with H2O, subjected to PCR

Different cloning PCR reactions and programs were used in order to generate various constructs used in this study. These will be discussed in chapters describing the cloning steps of particular construct in more detail.
The following PCR program was used to genotype the CHIP +/+ and -/- mice:

Genotyping PCR for CHIP +/+ and -/- mice

Step	Time (s)	Temp.(˚C)
1	300	95
2	30	95
3	30	65
4	60	72
5	30	95
6	30	55
7	60	72
8	600	72
9	∞	4

PCR's were performed as touch down from 65 -55 °C for 10 cycles by sequential reduction of the annealing temperature for -1°C per cycle (steps 2-4), followed by additional 35 cycles at 55 °C (steps 5-7).

2.6.7. Site directed mutagenesis

In vitro site-directed mutagenesis is a PCR-based method to generate mutations in DNA. The principle is based on two oligonucleotides carrying the desired mutation. The oligonucleotide primers are extended during temperature cycling by proof-reading DNA polymerase generating a mutant plasmid using the parental plasmid as a template. The parental plasmid that does not carry the mutation is digested with an endonuclease that only targets methylated DNA, typically DpnI. DNA from most of the *E. coli* strains is dam methylated so only the parental plasmid that has been purified from bacteria is susceptible to DpnI digestion. The newly synthesized plasmid generated in an in vitro PCR reaction is not susceptible to this digestion.

Site directed mutagenesis is a very powerfully tool in study of protein function since it allows for amino acids in the protein of interest exchanged inserted or deleted by means of mutation of expression plasmid DNA.

2.6.7.1. Design of mutagenesis primers

All oligonucleotides were ordered from Metabion with additional HPLC purification step to insure the exact sequence of the oligonucleotides. The oligonucleotides were designed according to following rules. The desired mutation was inserted approximately in the middle of the primer that was flanked by 10-15 bases of correct sequence on both sides. The melting temperature (Tm) of the primer was higher than 78°C so the length of the primer was adjusted accordingly. Primers can be longer than 45 base pairs with minimum of 40 % GC content. The Tm was calculated according to the following formula:
Tm= 81.5 + 0.41 (x %GC content) - 675/N - % mismatch
N is primer length in bases.

2.6.7.2. Mutagenesis

After the mutagenesis PCR was performed the reaction was subjected to digestion by adding 1µl of DpnI enzyme. This lead to the digestion of the parental DNA.

Mutagenesis PCR reaction

parental plasmid DNA.....100 ng
primer1.....125 ng
primer2.....125 ng
dNTPs (10mM) ..... 1 µl
10x reaction buffer ..... 5 µl
PfuUltra Polymerase..... 1 µl 2.5 U/µl
filled up to 50 µl with H2O, subjected to mutagenesis PCR program

Mutagenesis PCR

Step	Time (s)	Temp.(˚C)
1	30	95
2	30	95
3	60	55
4	300	68
5	∞	4

PCR was performed for 18 cycles.

The mutagenesis PCR reaction was subjected to digestion by adding 1 µl of Dpn I restriction enzyme (10 U/µl) and incubation for 1 h at 37 °C. The DpnI enzyme was heat inactivated by incubation at 80°C for 20 minutes. After this, 1 µl of this reaction was used for DNA transformation as described above.

2.6.8. Agarose gel electrophoresis

Agarose gel electrophoresis is a method used for separating, identifying or purifying DNA fragments. Typically the gels were prepared by dissolving a desired amount of agarose in 1xTAE buffer by boiling in a microwave for 3 minutes. Usually gels between 1 %-2 % were used, depending on the size of the DNA fragment analyzed. For 250 ml agarose solution 13 µl ethidium bromide was used in order to visualize DNA. The melted agarose was poured into casting platform. After allowing the gel to harden at room temperature it was placed into an electrophoresis chamber containing 1xTAE buffer. DNA was prepared by mixing with 6x loading buffer and loaded on the agarose gel. Electrophoresis was carried out at 150 V at room temperature. DNA bands were visualized under a UV light transilluminator at 366 nm.

TAE buffer (50x)

Tris-base .....242 g

EDTA .....37.2 g

glacial acetic acid.....57.1 ml

filled up to 1000ml with H2O

Agarose, Invitrogen (Cat.No. 15510-027)
Ethidiumbromid, Roth (Cat.No. 2218.1)

2.6.8.1. Extraction of DNA from agarose gels

DNA extraction from agarose gels was performed by using QIAEX Gel Extraction Kit (Qiagen) according to the manufacturer´s instructions.
QIAEX Gel Extraction Kit, Qiagen (Cat. No. 20021)

2.6.9. Expression vectors

All expression vectors in this study were generated by cloning using PCR, restriction enzymes or by performing site directed mutagenesis.

Additional ubiquitin and ubiquitin mutant expressing vectors were purchased from Addgene.

pRK5-HA-Ubiquitin-WT (Plasmid #17608)

pRK5-HA-Ubiquitin-K48 (Plasmid #17605)

pRK5-HA-Ubiquitin-K63 (Plasmid #17606)

2.6.9.1. RNA extraction and generation of cDNA

Mouse fibroblasts were plated and grown to the confluence of 70-80%. The lysis and extraction of RNA was performed using the RNAEasy Mini Kit according to the manufacturer´s instructions. RNA was stored at -80˚C.

Reverse transcription PCR was performed to obtain total cellular cDNA by using iScript Select cDNA Synthesis Kit according to the manufacturer´s instructions. The cDNA was stored at -20˚C and subsequently used for specific cDNA cloning such as cloning of the STUB1 (CHIP) cDNA.

RNAEasy Mini Kit (50), Qiagen (Cat.No. 74104)

iScript Select cDNA Synthesis Kit, BioRad (Cat.No.170-8890)

2.6.9.2. TOPO TA cloning

TOPO cloning system uses the DNA topoisomerase I that functions both as the endonuclease and polymerase. The topoisomerase is in this case bound by a covalent

bond to the 3´phosphate in the pentameric sequence 5´-(C/T)CCTT-3´of the vector backbone. The enzyme is therefore able to ligate any DNA sequence with the vector back bone. At the same time the enzyme releases itself from the backbone. In this study the TOPO cloning was performed at room temperature for 30 min, otherwise the reaction was preformed according to the manufacturer's instructions. This part of the work was carried out by a practical student Dennis Zimmermann.

TOPO cloning reaction

PCR producte……1 µl

TOPO……..1 µl

salt solution……1 µl

H2O……....…3 µl

CHIP cDNA was initially amplified from the total cellular cDNA generated by reverse transcription PCR from fibroblast RNA using following primers:

PCR primers

CHIP Fwd 5'CGCCATGAAGGGCAAGGAGGAAAAG3'

CHIP Rev 5'GGCCTCAATAGTCCTCTACCCAG3'

Subsequently the PCR product was cloned into the TOPO TA vector backbone as described above.

2.6.9.3. CHIP-WT-pEGFP-C1

CHIP was subcloned by excising the fragment using EcoRI enzyme and subsequently ligating it into the pEGFP-C1 vector. Digestion of CHIP-TOPO and pEGFP-C1 desired vector backbone was done for 2 h at 37°C. The vector backbone was additionally subjected to dephosphorylation for 30 min as described before. After the gel purification and extraction of linearized vector and insert of appropriate size form the agarose gel the ligation reaction was performed by using the Fast Link Ligation Kit as described above. In the reaction the ratio of insert to vector 3:1 (150 ng : 50 ng) was used.

2.6.9.4. CHIP-H260Q-pEGFP-C1

CHIP H260Q point mutation was generated by site directed mutagenesis as described above. The CHIP-WT-pEGFP-C1 was used as a template together with the following primers.

CHIP H260Q mut Fwd 5'GGACATTGAGGAGCAACTGCAGCGTGTGGGC3'

CHIP H260Q mut Rev 5'GCCCACACGCTGCAGTTGCTCCTCAATGTCC3'

2.6.9.5. CHIP-K30A-pEGFP-C1

CHIP K30A point mutation was generated by site directed mutagenesis as described above. The CHIP-WT-pEGFP-C1 was used as a template together with the following primers.

CHIP K30A mut Fwd5'CGAGTGCGCAAGAGCTCGCGGAGCAGGGAAACCGGC3'

CHIP K30A mut Rev 5'GCCGGTTTCCCTGCTCCGCGAGCTCTTGCGCACTCG3'

2.6.9.6. CHIP-Ubox-pEGFP-C1

The U-box domain of CHIP was subcloned by using CHIP Ubox EcoRI Fw and CHIP Ubox BamHI Rev primers. The CHIP-TOPO was used as a template and Herculase II high fidelity polymerase was used for amplification. The primers were designed so that they create EcoRI and BamHI restriction sites. After the PCR the reaction was ran on an agarose gel and PCR a product of the right size was extracted from the agarose gel as described above. Subsequently the extracted PCR product was subjected to digestion by these two enzymes allowing the formation of ``sticky ends´´ on the PCR product

PCR primers

CHIP Ubox EcoRI Fw 5´TGAATTCGAAGAAGCGCTGGAACAGTATCG3´

CHIP Ubox BamHI Rev 5´TGGATCCTCAATAGTCCTCTACCCAG3´

Cloning PCR reaction

CHIP-TOPO……1 µl (100µg)

CHIP U-box EcoRI Fw….……...1.25 µl

CHIP U-box BamHI Rev……1.25 µl

dNTPs……...…0.5 µl

5X buffer……10 µl

HerculaseII.……0. 5µl

The reaction was performed in total volume of 50 µl by adding the H_2O. Following PCR was performed:

Cloning PCR

Step	Time (s)	Temp.(˚C)
1	120	95
2	30	95
3	30	55
4	60	72
5	600	72
6	∞	4

Digestion of PCR product and 1 µl pEGFP-C1 desired vector backbone was done for 2 h at 37 °C. The vector backbone was additionally subjected to dephosphorylation for 30 min as described before. After gel purification and extraction of the linearized vector form the agarose gel, a ligation reaction was performed by using the Fast Link Ligation Kit as described above. In the reaction a ratio of insert to vector 3:1 (150 ng : 50 ng) was used.

2.6.9.7. CHIP-TPR-pEGFP-C1

TPR domain of STUB-1 was subcloned in pEGFP-C1 using CHIP TPR EcoRI Fw and CHIP TPR BamHI Rev primers and CHIP-WT-TOPO vector as a template. The high

fidelity polymerase Herculase II was used in the cloning PCR reaction. The primers were designed so that they create EcoRI and BamHI restriction sites. After PCR the reaction was ran on an agarose gel and a product of the right size was extracted from the agarose gel as described above. Subsequently the extracted PCR product was subjected to digestion by these two enzymes allowing the formation of ``sticky ends´´ on the PCR product.

PCR primers

CHIP TPR EcoRI Fw 5´GAATTCGCCCTTCGCCATGAAG3´

CHIP TPR BamHI Rev 5´TGGATCCTCAATCATCTTCATGACCCTCG3´

Cloning PCR reaction

CHIP-TOPO……1 µl (100 µg)

CHIP TPR EcoRI Fw……...1.25 µl

CHIP TPR BamHI Rev……1.25 µl

dNTPs……...…0.5 µl

5X buffer……10 µl

HerculaseII……0.5 µl

The reaction was performed in total volume of 50 µl by adding the H_2O. Following PCR was performed:

Cloning PCR

Step	Time (s)	Temp.(˚C)
1	120	95
2	30	95
3	30	55
4	60	72
5	600	72
6	∞	4

Digestion of PCR product and 1 µl pEGFP-C1 desired vector backbone was done for 2 h at 37°C. The vector backbone was additionally subjected to dephosphorylation for 30 min as described before. After gel purification and extraction of linearized vector form the agarose gel the ligation reaction was performed by using the Fast Link Ligation Kit as described above. In the reaction the ratio of insert to vector 3:1 (150 ng : 50 ng) was used.

2.6.9.8. CHIP-WT-pET-16b

CHIP-WT was subcloned to pET-16b backbone by using CHIP pET XhoI Fwd and CHIP U-box BamHI Rw primers and CHIP-WT-TOPO vector as a template. The Taq polymerase was used in the cloning PCR reaction. The primers were designed so that they create XhoI and BamHI restriction sites. After PCR the reaction was ran on an agarose gel and a product of the right size was extracted from the agarose gel as described above. Subsequently the extracted PCR product was subjected to digestion by these two enzymes allowing the formation of ``sticky ends´´ on the PCR product.

PCR primers

CHIP pET XhoI Fwd 5' CGCTCGAGTCCTTCGCCATGAAG3'

CHIP U-box BamHI Rw 5' TGGATCCTCAATAGTCCTCTACCCAG3'

Cloning PCR reaction

CHIP-TOPO……1 µl (100 µg)

CHIP pET XhoI Fwd ……...1.25 µl

CHIP U-box BamHI Rw ……...…1.25 µl

dNTPs……...…0.6 µl

5X buffer……..3 µl

$MgCl_2$……1.2 µl

Taq…….……...1 µl

The reaction was performed in total volume of 50 µl by adding the H_2O. Following PCR was performed:

Cloning PCR

Step	Time (s)	Temp.(˚C)
1	120	95
2	30	95
3	45	63
4	60	72
5	600	72
6	∞	4

The PCR product was first cloned back to the TOPO TA vector back bone. This step was necessary to create a XhoI digestion site. The new construct was termed CHIP pET XhoI TOPO. CHIP was than subcloned to a pET-16b backbone using XhoI and BamHI enzymes. Digestion of CHIP pET XhoI TOPO and pET-16b vector backbones was done for 2 h at 37 °C. The vector backbone was additionally subjected to dephosphorylation for 30 min as described before. After gel purification and extraction of the linearized vector and insert of appropriate size form the agarose gel, a ligation reaction was performed

using the Fast Link Ligation Kit as described above. The insert to vector ratios 3:1, 2:5 and 1:5 were used. After DNA purification from bacteria the cloning products were checked by EcoRV digestion. The positive clones were sent for sequencing with T7 forward primer and T7 terminator as reverse sequencing primer.

2.6.9.9. CHIP-H260Q-pET-16b

The same mutagenesis primers and protocol as for CHIP H260Q pEGFP-C1 was used to create H260Q mutation in the CHIP-H260R-pET-16b. The positive clones were confirmed by sequencing with T7 forward primer and T7 terminator as reverse sequencing primer.

2.6.9.10. ILK-K341R-3XFlag-pCLMFG

ILK K341R point mutation was generated by site directed mutagenesis as described above. The ILK-3XFlag-pCLMFG cloned by Carsten Grashoff was used as a template together with the following primers.

ILK K341R A1022G Fw

5´GAATCAGCATGGCTGATGTTAGGTTTTCTTTCCAGTGCCCTGGG3´

ILK K341R A1022G Rv

5´CCCAGGGCACTGGAAAGAAAACCTAACATCAGCCATGCTGATTC3´

The constructs were confirmed by sequencing as described above using following primers:

S_E fw 5´CATGCACTCAATAGCCGCAG3´

S_E rv 5´CTCCACATGTCTGCTGAGCG3´

2.6.9.11. ILK-K341R-3xFlag-pCMV-14

ILK K341R point mutation was generated by site directed mutagenesis as described above. The ILK-3XFlag-pCMV14 cloned by Carsten Grashoff was used as a template together with the following primers.

ILK K341R A1022G Fw

5´GAATCAGCATGGCTGATGTTAGGTTTTCTTTCCAGTGCCCTGGG3´

ILK K341R A1022G Rv

5´CCCAGGGCACTGGAAAGAAAACCTAACATCAGCCATGCTGATTC3´

The constructs were confirmed by sequencing as described above using following primers:

S_E fw 5´CATGCACTCAATAGCCGCAG3´

S_E rv 5´CTCCACATGTCTGCTGAGCG3´

2.6.9.12. ILK-K341R-pEGFP-C1

ILK K341R point mutation was generated by site directed mutagenesis as described above. The ILK-pEGFP-C1 cloned by Dr. Sara Wickström was used as a template together with the following primers.

ILK K341R A1022G Fw

5´GAATCAGCATGGCTGATGTTAGGTTTTCTTTCCAGTGCCCTGGG3´

ILK K341R A1022G Rv

5´CCCAGGGCACTGGAAAGAAAACCTAACATCAGCCATGCTGATTC3´

The constructs were confirmed by sequencing as described above using following primers:

S_E fw 5´CATGCACTCAATAGCCGCAG3´

S_E rv 5´CTCCACATGTCTGCTGAGCG3´

2.6.9.13. ILK -pHAGE2-CMV-eGFP-W-mU6

ILK was subcloned in pHAGE-CMV_eGFP-W-mU6, a gift from Dr. Marc Schmidt-Supprian, using ILK BsmBI Fwd and ILK NotI Rev primers and ILK-3XFlag-pCMV14 as a template. Herculase II high fidelity polymerase was used for amplification. The primers were designed so that they create BsmBI and NotI restriction sites. After the PCR the reaction was ran on an agarose gel and PCR a product of the right size was extracted

from the agarose gel as described above. Subsequently the extracted PCR product was subjected to digestion by these two enzymes allowing the formation of ``sticky ends´´ on the PCR product

PCR primers

ILK BsmBI Fwd 5´ ATCGTCTCACTGACATGGACGACATTTTCAC 3´

ILK NotI Rev 5´ ATGCGGCCGCCTTGTCCTGCAT 3´

Cloning PCR reaction

CHIP-TOPO……1 µl (100µg)

ILK BsmBI Fwd ….…….……...1.25 µl

ILK NotI Rev ……..…1.25 µl

dNTPs……....…0.5 µl

5X buffer……10 µl

HerculaseII……0. 5µl

The reaction was performed in total volume of 50 µl by adding the H_2O. Following PCR was performed:

Cloning PCR

Step	Time (s)	Temp.(˚C)
1	120	95
2	30	95
3	30	55
4	120	72
5	600	72
6	∞	4

Digestion of PCR product and 1 µl pHAGE-CMV-eGFP-W-mU6 desired vector backbone was done for 2 h at 37 °C. The vector backbone was additionally subjected to dephosphorylation for 30 min as described before. After gel purification and extraction of the linearized vector form the agarose gel, a ligation reaction was performed by using the Fast Link Ligation Kit as described above. In the reaction a ratio of insert to vector 3:1 (150 ng : 50 ng) was used.

2.6.9.14. ILK-K341R-pHAGE2-CMV-eGFP-W-mU6

ILK K341R point mutation was generated by site directed mutagenesis as described above. The ILK -pHAGE2-CMV-eGFP-W-mU6 was used as a template together with the following primers.

ILK K341R A1022G Fw

5´GAATCAGCATGGCTGATGTTAGGTTTTCTTTCCAGTGCCCTGGG3´

ILK K341R A1022G Rv

5´CCCAGGGCACTGGAAAGAAAACCTAACATCAGCCATGCTGATTC3´

The constructs were confirmed by sequencing as described above using following primers:

S_E fw 5´CATGCACTCAATAGCCGCAG3´

S_E rv 5´CTCCACATGTCTGCTGAGCG3´

2.7. Microscopy

2.7.1. Confocal microscopy

Confocal images were collected by using a confocal microscope (Leica DMIRE2) with 100x oil objectives at RT. Leica Confocal Software (version 2.5 Build 1227) was used for image acquisition and evaluation.

2.7.2. Live-cell microscopy

Live cells were recorded using a Zeiss Axiovert 40C microscope equipped with a CCD camera (Prosilica, GC2450). The stage was supplied with 4,7% CO_2 and heated at 37˚C. FireWire software (Molecular Devices, Downingtown, PA) was used for image acquisition as well as the microscope control.

2.7.3. Fluorescence recovery after photobleaching (FRAP) in 1D

Fluorescence recovery after the photobleaching is an optical technique used for quantifying the diffusiveness of proteins in the cell membrane or cytoplasm (Carman 2012). Shortly, a defined region is photo-bleached and the movement of unbleached molecules from the surrounding environment is monitored over time (Fig. 2.1.). The movement of the molecules observed is defined by two major components: diffusion and interaction with other molecules. There are two important parameters that can be calculated by this method the diffusion coefficient and the mobile fraction of the molecule (M_f). Diffusion coefficient is the rate by which molecules move in and out of the monitored region and mobile fraction is the percentage of the molecules that undergo detectable movement (Carman 2012).

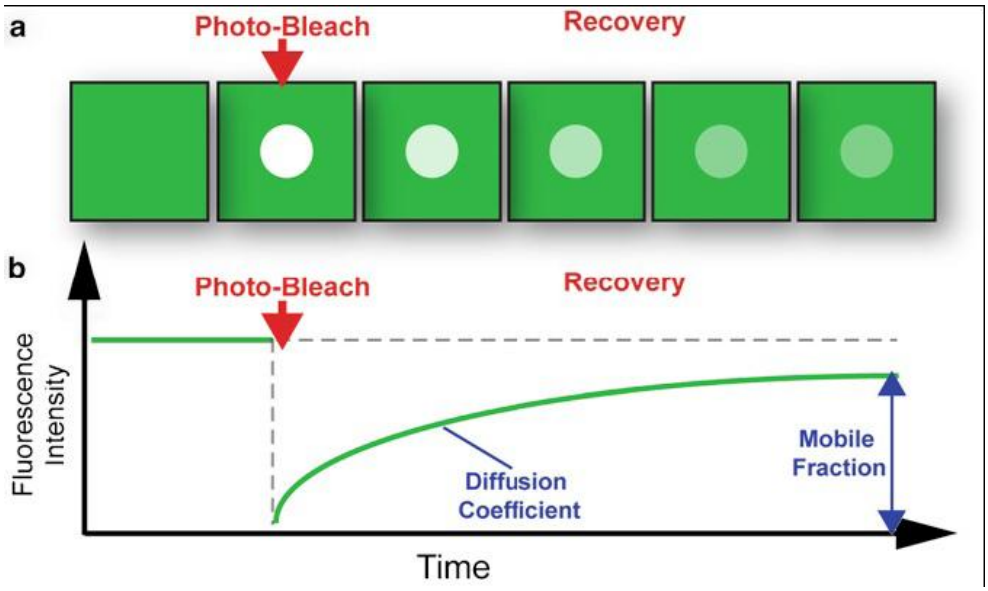

Figure 2.1. Fluorescence recovery after photobleaching (FRAP). *(a) Graphic representation of fluorescent area of the cell (green) and bleached region (white) and the recovery of the florescence over time. (b) Typical intensity profile measured by FRAP. The saturation point of the curve (plateau) allows the calculation of the mobile fraction of the fluorescent molecule. Diffusion coefficient is calculated from the recovery curve* (Carman 2012) .

In this particular setup cells were seeded and allowed to spread for 90 min on glass-bottom dishes with 2,5 µm-line micropatterns functionalized with fibronectin. Bleaching was performed with a 405 nm laser for 3x100 ns. Images were captured with an Axiovert 200 (Zeiss) microscope, a CSU10 spinning-disc confocal scanhead (Yokogawa), and a Cascade II EMCCD camera (Photometrics), with a 100× oil objective. Images were collected at 37°C, 5% CO_2. Acquisition was controlled by Metamorph Software (Molecular Devices). Images were collected before, directly after and during recovery of bleaching with a rate of 1 frame/2 s in the first minute and 1 frame/20 s for the additional 39 min. Recovery after bleaching was calculated as described previously (Tagawa, Mezzacasa et al. 2005). Briefly, fluorescent intensity (I) was measured from the three independent unbleached areas as well as the bleached area before bleaching ($=I_{[0]}$) and during recovery ($=I_{[t]}$). Relative fluorescent intensity (RI) was then calculated according to the following equation $RI=(I_{total[0]}/I_{bleached[0]}) \times (I_{bleached[t]}/I_{total[t]})$. Unspecific bleaching during image acquisition is corrected in this equation. All measured intensities were first divided by the average intensity of the three background areas before their use in the RI equation. This allowed the additional correction for the background intensity fluctuation. The sampled data was analyzed by nonlinear regression fitting. The fitted curves allowed the extraction of the important parameters such as half time ($\tau_{1/2}$) and mobile and immobile fraction of the protein (M_f, I_f)

2.8. Statistical Analysis

Statistical analyses were performed using GraphPad Prism software (GraphPad, version 5.0). Statistical significance was determined by the Mann-Whitney U-test, with the exception of Figs. 3.2.5. and 3.2.6., where analysis of variance (Two-way ANOVA) in combination with a post-hoc Bonferrony test was used, and Figs. 3.2.3., where analysis of variance (one-way ANOVA) followed by Tuckey´s posttest was usedand 3.2.4. where a paired t-test was used. Normal distribution of data was confirmed with the Kolomogorov-Smirnov test (alpha=0.05).

3. Results

3.1. ILK is posttranslationally modified by ubiquitin

ILK is a central scaffolding element of β1 and β3 integrin containing focal adhesions (Hannigan, Leung-Hagesteijn et al. 1996). Taken that ILK regulates many cellular functions such as cell spreading, migration and proliferation (Sakai, Li et al. 2003) this study sought to investigate the mechanisms of ILK turnover and its effect on cellular behavior. As ubiquitination is one of the most common posttranslational modifications involved in regulation of a wide range of cellular processes like protein degradation, DNA repair, transcription, signal transduction, endocytosis and sorting (Welchman, Gordon et al. 2005), modification of ILK by ubiquitin was investigated. To this end, denaturing immunoprecipitation assays were performed followed by mass spectrometry using a cell line stably expressing ILK-Flag. This cell line was generated from ILK fl/fl fibroblasts that were isolated from the adult kidney of ILK fl-fl mice. The floxed ILK allele was deleted by infecting the cells with adenoviral Cre to yield ILK -/- cells. ILK-Flag cells were then generated as a rescue cell line re-expressing a Flag-tagged ILK by stabile integrating pCLMFG retrovirus in ILK-/- fibroblasts as described in the Materials and Methods section. The parental ILK fl/fl cell line, expressing ILK but lacking the Flag tag, was used as a negative control in the immunoprecipitation assays. The principle of this assay is to denature the protein lysate abolishing all protein-protein interactions but retaining covalent modifications. In addition, enzymes that might remove these modifications are inactivated by denaturation as well. Subsequently an immunoprecipitation reaction is performed to isolate the protein of interest, after which the posttranslational modifications such as ubiquitination can be identified using western blot or mass spectrometry analysis.

Taken that deubiqutinases are potent enzymes, all buffers used in the in vivo ubiquitination assay were supplemented with 25 mM N-Ethymaleimid (NEM), a deubiquitinase inhibitor, in order to prevent loss of this covalent modification during the course of the assay. Lysis of the adherent cells was performed in a denaturing buffer containing 1 % SDS and immediately boiled at 95 ˚C for 5 min for additional inhibition of deubiquitinase enzymes and denaturation of protein complexes. The lysates were

diluted in a 1:10 ratio in non-denaturing buffer containing Triton-X 100, leading to the sequestration of SDS in micelles. This allowed the immunoprecipitation assay to be performed without SDS negatively affecting the antibody-antigen interaction. Anti-FLAG M2 affinity gel from Sigma was used to perform the ILK-Flag immunoprecipitation. In this system a FLAG M2 antibody is covalently attached to agarose resin. Bound proteins are subsequently eluted using a competitive elution with excess of Flag peptide, circumventing the uncoupling of high amounts of IgGs. This is crucial, as ILK has similar molecular weight as the IgG heavy chain and it is difficult to resolve them in a SDS polyacrylamide gel, which can make consequent analysis of ILK immunoprecipitates difficult. Immunoprecipitates were resolved with SDS-PAGE after which silver stain was performed revealing a putative ILK band at approximately 50 kDa size as well as additional bands of higher molecular weights (Fig.3.1.1.). The indicated bands were analyzed by mass spectrometry, revealing that also the higher molecular weight bands contained ILK. This suggested that ILK is posttranslationally modified, leading to an increase in molecular weight.

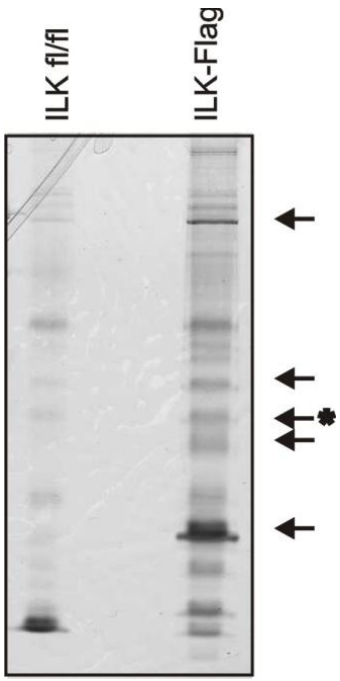

Figure 3.1.1. *Silver staining from immunoprecipitates of ILK-FLAG expressing fibroblasts. ILK fl/fl cells were used as a negative control. Arrows indicate bands analyzed by mass spectrometry. ILK and ubiquitin was identified from all bands analyzed. Gly-gly modification of K341 on ILK was detected in the band marked with an asterisk.*

In addition, a glycine-glycine (Gly-Gly) modification on lysine 341 of ILK was identified (Fig 3.1.1, band marked by asterisk). Analysis by mass spectrometry requires the digestion of proteins into smaller peptides by trypsin. Trypsin is an endopeptidase able to cleave only the peptide bonds in which the carbonyl group is contributed either by an Arg or Lys residue. Although the ubiquitin is covalently attached to a target protein it is also cleaved into small peptides by trypsin leaving behind only a Gly-Gly dipeptide. However, other small protein modifiers such as SUMO leave the same signature mark therefore cannot be distinguished from ubiquitin only by mass spectrometry. Therefore this result demonstrated that ILK is modified posttranslationally and that this modification could be attachment of ubiquitins or ubiquitin-like molecules

To confirm the result from mass spectrometry analysis and to determine if the posttranslational modification detected is ubiquitination, an in vivo ubiquitination assay was performed, followed by western blot analysis. This assay is based on the denaturing immunoprecipitation method described above. For this, CHO cells were transfected with ILK-Flag (ILK-3xFlag-pCMV14) and HA-ubiquitin, whereas the control cells were transfected by either HA-ubiquitin only or ILK-Flag only.

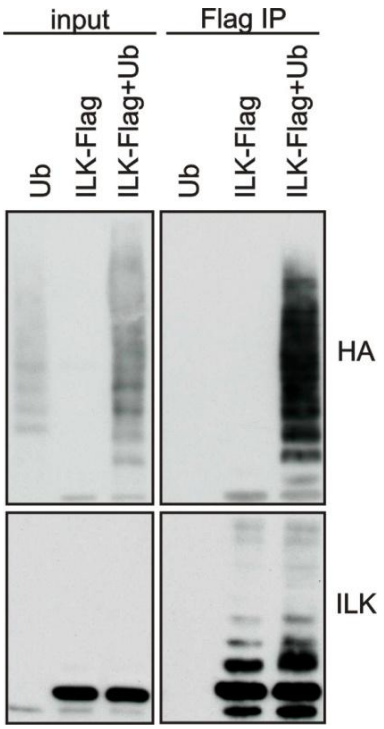

Figure 3.1.2.*Western blot analysis of Flag immunoprecipitates from CHO cells expressing HA-tagged ubiquitin, ILK-Flag or both. Ubiquitination of ILK is detected by both HA and ILK antibody.*

Immunoprecipitation was performed as described above. After the elution with Flag peptide immunoprecipitates were analyzed by western blot. The immunoblot with HA antibody revealed a typical ladder band pattern derived from polyubiquitin chains of different length covalently attached to the target protein (Fig.3.1.2.). As the control transfected only with HA-ubiquitin gave no signal, one can conclude that the ubiquitination pattern arises from the specific modification of ILK. The immunoblot with ILK antibody revealed a ladder pattern of ILK-Flag both with and without HA-ubiquitin expression. This demonstrated that ILK can be ubiquitinated by endogenous ubiquitin and that this can be enhanced by over-expression of HA-ubiquitin.

The ubiquitin molecule contains 7 lysine residues that can serve as ubiquitination sites for formation of polyubiquitin chains. Cells use various ubiquitin linkage patterns to differentially control signaling pathways (Behrends and Harper 2011). The most common polyubiquitin chains are the K48- K63-linked chains (Hochstrasser 2009; Behrends and Harper 2011). In order to determine the type of polyubiquitin chain attached to ILK, an in vivo ubiquitination assay was performed using ILK-Flag fibroblasts transiently transfected with wild type (wt) ubiquitin HA (pRK5-HA-Ubiquitin-Wt, Addgene), or alternatively with ubiquitin mutants containing a single lysine, either only K48 or only K63 (pRK5-HA-Ubiquitin-K48, pRK5-HA-Ubiquitin-K63). ILK fl/fl cells and ILK-Flag cells mock transfected with the empty vector were used as controls for the immunoprecipitation and transient transfection, respectively. The ubiquitin constructs were expressed for 24 h, after which an in vivo ubiquitination assay was performed as described above. The immunoprecipitates eluted with Flag peptide were resolved by SDS-PAGE and subsequently analyzed by western blot. Immunoblotting with antibodies against HA and Flag epitopes were then performed, detecting either ubiquitin or ILK, respectively.

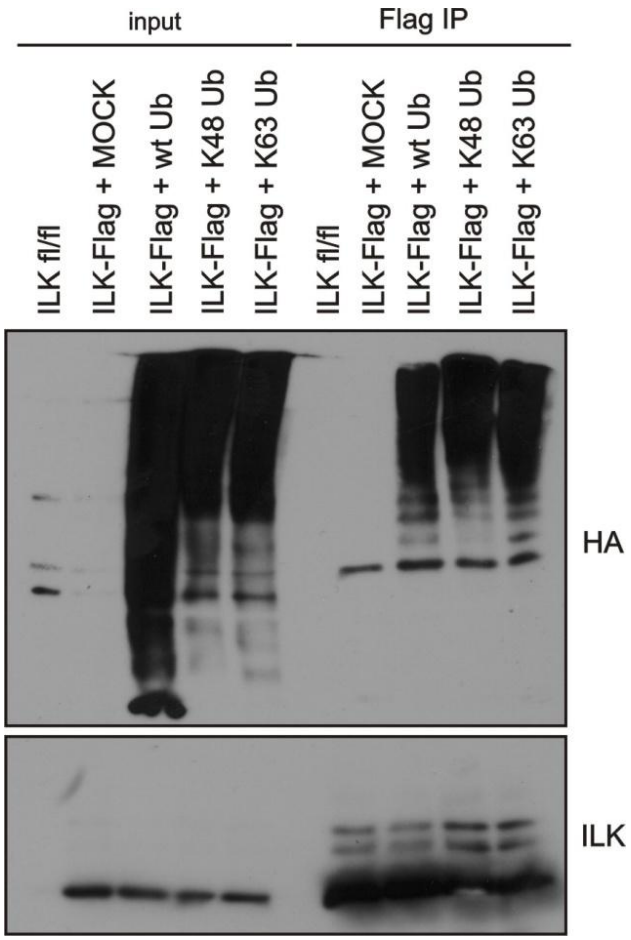

Figure 3.1.3. *Western blot analysis of Flag immunoprecipitates from ILK -/- fibroblasts expressing ILK-Flag and HA-tagged ubiquitin or ubiquitin mutants containing a single lysine K48 or K63. Both K48- and K63-linked ubiquitin chains are detected.*

The analysis of the Flag immunoblot revealed the typical ladder pattern of ILK bands indicative of posttranslational modifications (Fig3.1.3.). In addition, the HA immunoblot confirmed that this modification is indeed ubiquitination. Furthermore there was no significant difference in ILK ubiquitination between K48 and K63 HA-ubiquitin expressing cells leading to the conclusion that ILK is modified by both K48- and K63-linked polyubiquitin chains.

The mass spectrometry analysis had shown that the lysine K341 on ILK is ubiquitinated. In order to verify this and to assess whether this ubiquitin is indispensible for ubiquitination of ILK, fibroblasts expressing a mutant ILK containing a lysine 341 to arginine mutation were subjected to in vivo ubiquitination assays. By performing a site directed mutagenesis PCR using wt ILK-Flag as a template, lysine 341 was mutated to arginine as described in the Materials and Methods section. This amino acid change

abolished the possibility of a covalent isopeptide linkage of the ubiquitin C terminus to the ε-amino group of this lysine in the substrate (Kerscher, Felberbaum et al. 2006), but maintained the charge of the amino acid.

In vivo ubiquitination assays were subsequently performed with ILK-/- fibroblasts transiently transfected with either ILK-Flag or ILK-K341R-Flag constructs. The parental ILK fl/fl cell line was used as a negative control. The immunoprecipitates eluted by Flag peptide were resolved by SDS-PAGE and analyzed by immunoblotting. Analysis of immunoblots using either an anti-ubiquitin antibody or an anti-Flag antibody showed absence of a ubiquitination ladder pattern in ILK-K341R-Flag expressing fibroblasts compared to the ILK-Flag expressing fibroblasts. This suggested that the K341 is a major ubiquitination site in ILK. In addition, both immunoprecipitates contained similar levels of ubiquitin confirming that overall ubiquitination in both cell types was unchanged (Fig.3.1.4.).

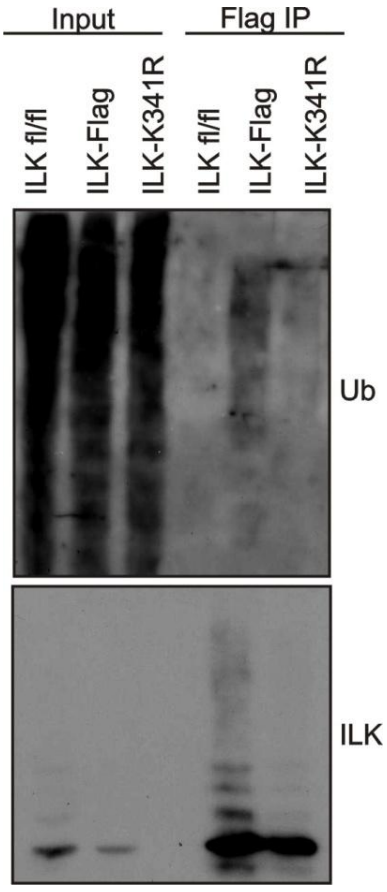

Figure 3.1.4. *Western blot analysis of Flag immunoprecipitates from ILK -/- fibroblasts expressing ILK-Flag or ILK-K341R. Ubiquitin and ILK-Flag immunoblots show major difference in detected ubiquitination.*

3.2. K341R mutation leads to migration defects in fibroblasts

Absence of ILK leads to a severe migration defect in fibroblast (Sakai, Li et al. 2003) It was therefore of interest to investigate if the ubiquitination of ILK a K341 is relevant in this process. To investigate the influence of ubiquitination of ILK on migration, stable cell lines expressing ILK-GFP and ILK-K341R-GFP were generated by lentiviral transduction and subsequent FACS sorting for GFP expressing cells. The ILK-GFP, ILK-K341R GFP and GFP only expressing ILK-/- control cells were sorted for comparable expression levels of GFP. Immunofluorescence staining for paxillin and actin could confirm that both ILK-GFP and ILK-K341R GFP localize to focal adhesions and rescue actin organization defect of ILK -/- cells (Fig. 3.2.1.).

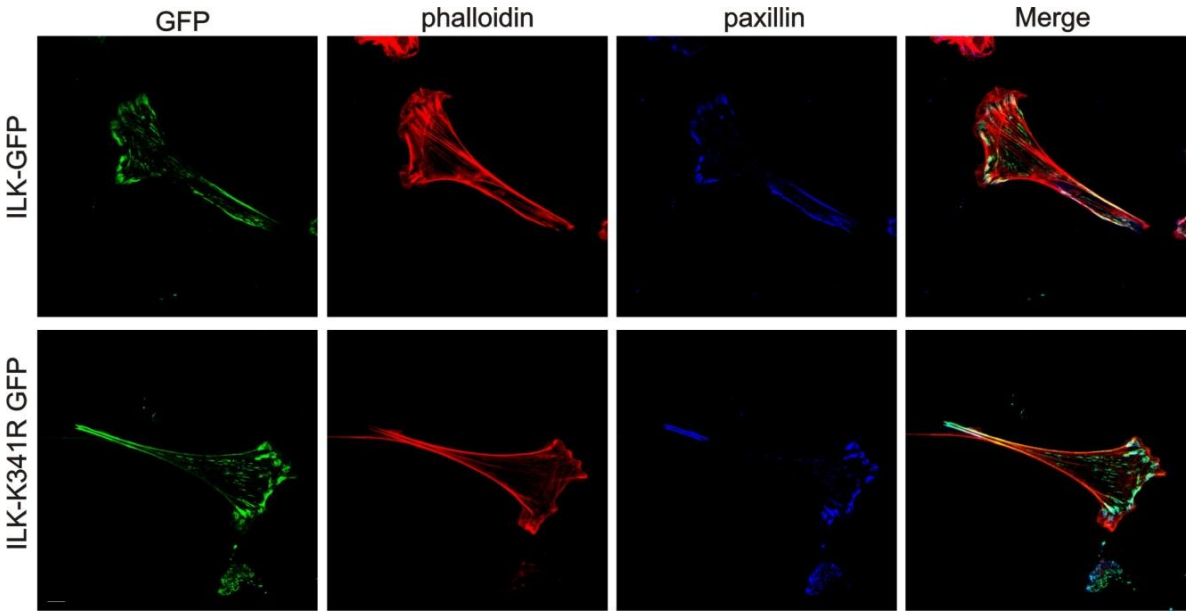

Figure 3.2.1. *Immunofluorescence analysis of fibroblasts expressing either ILK-GFP or ILK-K341R GFP. Paxillin staining was used to confirm the localization of ILK to FAs. Phalloidin staining shows no difference in actin cytoskeleton between two cell lines.*

The ability of ILK-GFP, ILK-K341R GFP as well as GFP ILK-/- fibroblasts to migrate within a 3-dimensional (3D) collagen matrix was analyzed by embedding the fibroblasts in collagen gels as previously described (Lammermann, Bader et al. 2008). The gels were casted in self-made chambers and allowed to settle for 30 min at 37 ˚C and 4.5 % CO_2. The migration process was imaged as described in Materials and Methods by Zeiss Axiovert 40C microscope equipped with a CCD camera (Prosilica, GC2450) and a heated stage (37˚C) supplied with 4,7 % CO_2. Image acquisition was performed using FireWire

software (Molecular Devices, Downingtown, PA). Migrating cells were subsequently tracked using the Chemotaxis and Migration tool of ImageJ software (Fig.3.2.2.).

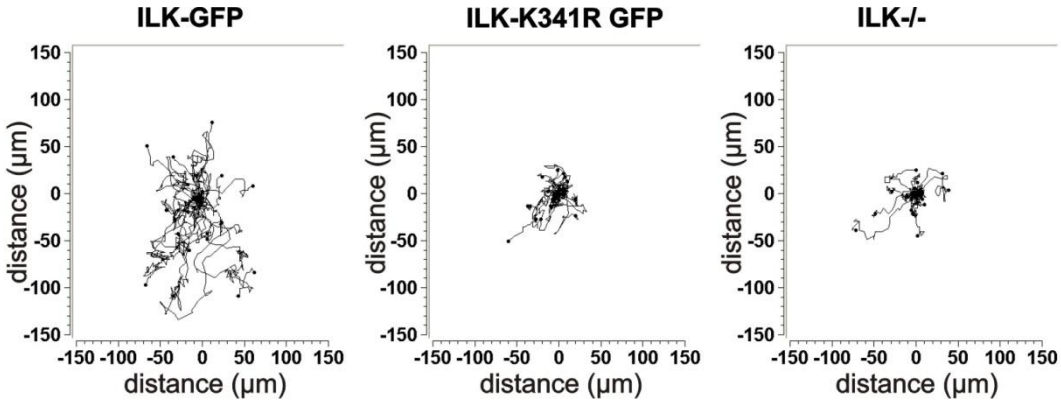

Figure 3.2.2. *Representative plots of migration tracks demonstrating reduced migration of ILK-K341R GFP and ILK-/- control fibroblast expressing only GFP compared to ILK-GFP cells.*

The migration distance and velocity was quantified from the live cell imaging data using ImageJ software (Fig.3.2.3.). The statistical significance was analyzed using the GraphPad Prism software by performing an ANOVA test followed by a Tucky post-hoc test. The quantifications demonstrate that the migration velocity and distance of ILK-K341R fibroblasts was significantly decreased compared to ILK-GFP control. The migration velocity and distance of ILK-K341R fibroblasts were comparable to ILK-/- cells. This led to the conclusion that mutation of K341 impairs fibroblast migration.

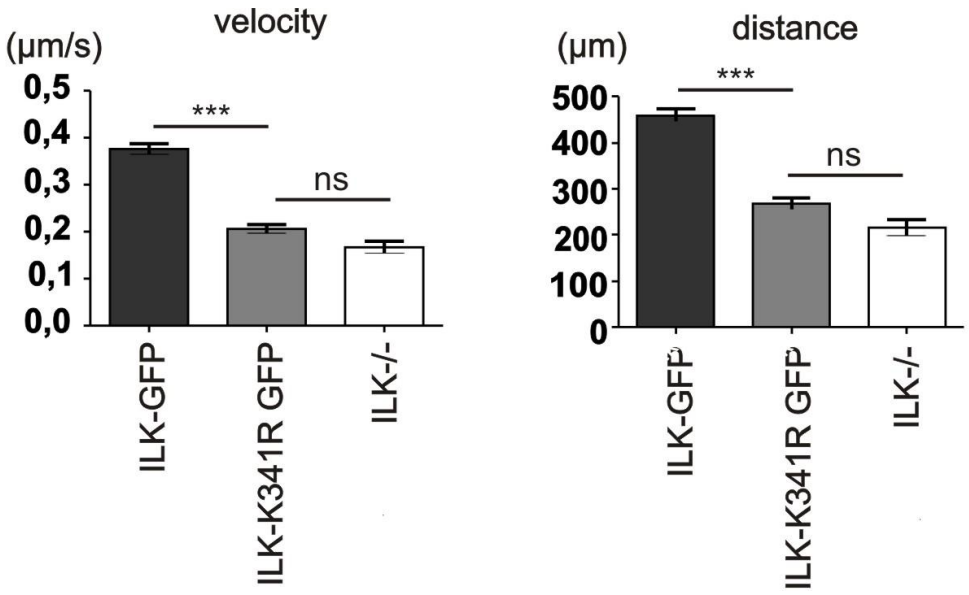

Figure 3.2.3. *Quantitative representation of velocity and distance differences between ILK-GFP, ILK-K341R GFP and ILK-/- cells. The ANOVA followed by Tuckey´s post test was performed. Data is expressed as mean ± SEM. n=6; ***p<0.0001; ns=not significant.*

3.2.1. K341R mutation leads to the reduced mobile fraction of ILK protein measured by FRAP

To further clarify potential mechanism of impaired migration of ILK-K341R expressing fibroblasts, the turnover of ILK-GFP and ILK-K314R-GFP protein in FAs was analyzed. For this, florescence recovery after photo bleaching (FRAP) was used. Usually, the cells investigated by this approach are seeded on a 2-dimentional (2D) glass bottom cell culture dishes. However, in this study it was observed that ILK-K341R-GFP cells display a defect in migration within 3D collagen matrix. As performing FRAP analysis in a 3D collagen matrix would be technically difficult, a 1D approach was used. This was chosen as it has been reported by Doyle et al. that 1D topography mimics migration phenotypes observed in fibrillar 3D cell-derived matrices (Doyle, Wang et al. 2009). Firstly, behavior of ILK-GFP and ILK-K341R GFP fibroblasts on 1D micropatterns was investigated to confirm similar migratory behavior as in 3D collagen matrix. To this end cells were seeded on micropatterned 2,5 µm lines functionalized by fibronectin. The cells were kept in 1% FCS containing DMEM to prohibit serun-derived fibronectin from attaching to the coverslip. The migration of the cells was observed and recorded by a Zeiss Axiovert 40C microscope equipped with a CCD camera (Prosilica, GC2450) and heated stage (37˚C)

supplied with 4,7% CO_2, as described in Materials and Methods. Quantification of cell migration on 1D fibronectin-coated micropatterns was the performed, and this assay could recapitulate the migration defect observed in 3D (Fig. 3.2.4.).

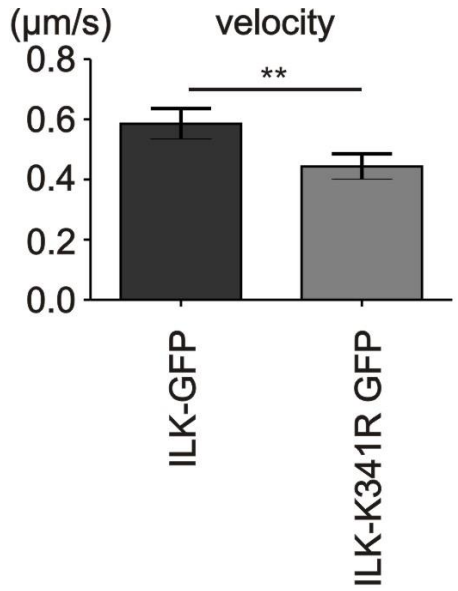

Figure 3.2.4. *Quantitative representation of velocity and distance differences between ILK-GFP, ILK-K341R GFP. The paired T-tests were performed. Data is expressed as mean ± SEM. n=3; **p=0.009*

The FRAP analysis of the ILK turnover in FAs was performed by seeding cells on fibronectin-functionalized micropatterned lines of 2.5 µm width in DMEM supplemented by 1% FCS. The cells were allowed to attach and spread for 90 min before starting the analysis. As this assay was performed in a 1D environment it was termed 1D FRAP analysis. Imaging was performed using an Axiovert 200 (Zeiss) microscope, a CSU10 spinning-disc confocal scanhead (Yokogawa), and a Cascade II EMCCD camera (Photometrics), with a 100× oil objective. Images were collected at 37°C, 5% CO_2, and controlled by Metamorph Software (Molecular Devices). Bleaching was performed with a 405 nm laser for 3x100 ns. Images were collected before, directly after and during recovery from bleaching with a rate of 1 frame/2 s for the first minute after bleaching and 1 frame/20 s for additional 39 min. Recovery after bleaching was calculated as described previously (Tagawa, Mezzacasa et al. 2005) according to the equation $RI=(I_{total[0]}/I_{bleached[0]}) \times (I_{bleached[t]}/I_{total[t]})$ that allows the correction for unspecific bleaching of the cells during the course of imaging. The fluorescent intensity (I) was measured from

three separate unbleached control regions as well as the bleached area before bleaching (=$I_{[0]}$) and during recovery (=$I_{[t]}$) by use of Metamorph Software. Average intensity per area was used. All measured intensities were first divided by the average intensity of the three background areas before their use in the RI equation. This allowed the additional correction for background intensity fluctuation that can occur during imaging. The observation was made that overall dynamics of the FA turnover is changed in 1D comparing to 2D as seen by prolonged halftime when compared to previous studies of FA protein dynamics. The reported recovery rates of FA proteins are in the range of few minutes and depend on the proximity of the observed protein either to integrin (slower recovery) or actin (faster recovery) (Wehrle-Haller 2007; Lele, Thodeti et al. 2008; Wolfenson, Lubelski et al. 2009). Nonlinear regression analysis of the results gave the best fit for the sampled data. This allowed the calculation of the recovery rate and mobile and immobile fractions (M_f, I_f) of the protein. Comparison of these parameters for wt ILK and K341R ILK protein showed no difference in the overall recovery rates but interestingly a difference in the M_f and I_f of the proteins. The results showed that K341R mutant ILK has a reduced M_f (M_f=0,483) in FAs compared to the wt ILK protein (M_f=0,735) (Fig. 3.2.5.).

A

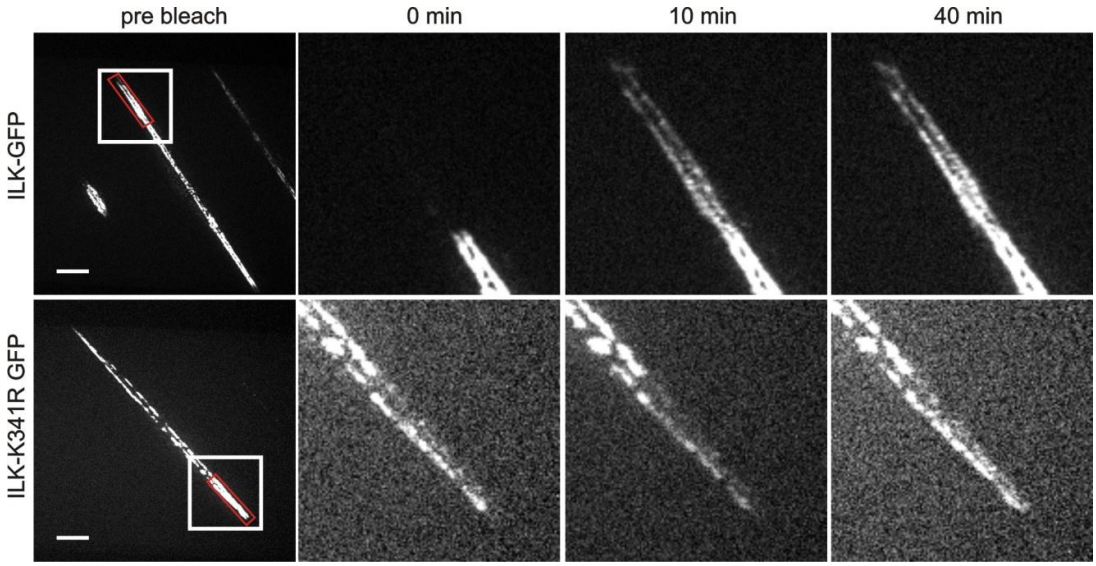

B

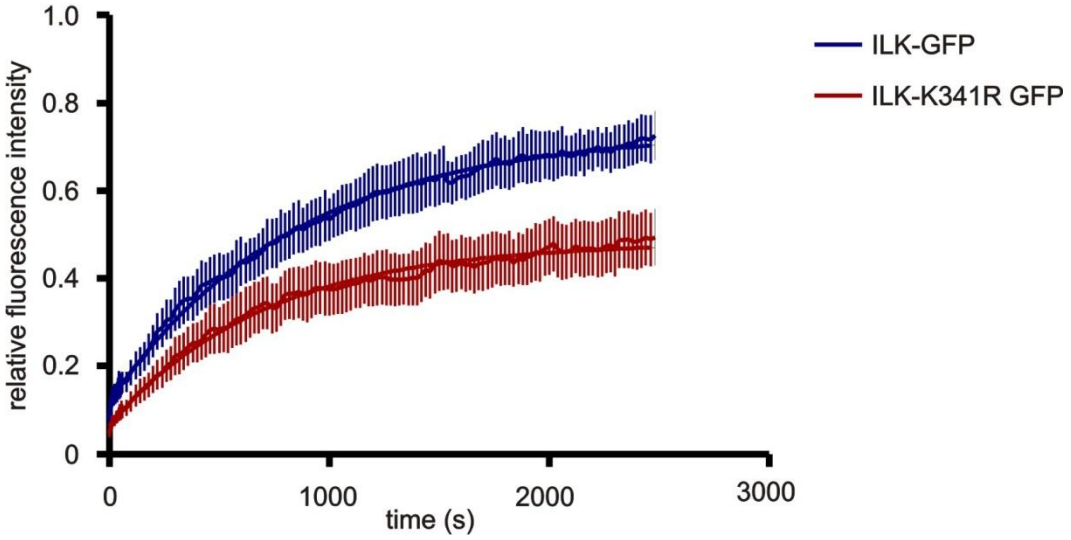

Figure 3.2.5. *FRAP analysis of ILK-GFP and ILK-K341R GFP. (A) Stills showing morphology of fibroblasts and FAs on 1D micropattern at different points of the FRAP analysis. (B)The recovery curves calculated form recorded data. The solid smooth lines represent the best fit curves of a nonlinear regression analysis. The ANOVA with Bonferrony-post test was performed. Data is expressed as mean ± SEM. n=9; ***p<0.0001*

3.2.2. K341R mutation leads to disturbed clathrin mediated internalization of ILK protein in FAs

It has been demonstrated that integrin and ILK recycling within the myotendinous junction of D.melanogaster depends on clathrin-mediated endocytosis and the Rab5 GTPase (Yuan, Fairchild et al. 2010). In order to address whether the altered turnover of K341R ILK observed in the FRAP analysis was due to altered endocytosis. Additional FRAP asssays were performed in the presence of the Chlorpromazine (CPZ), a inhibitor of clathrin-mediated endocytosis. The analysis was performed as described above, after which data was fitted using nonlinear regression and the M_f of ILK in cells treated with CPZ was calculated. The comparison of the results showed that M_f of K341R mutant ILK (M_f=0,552) was unchanged in CPZ treated cells as compared to untreated cells (M_f=0,483). However, the M_f of wt ILK was drastically reduced in CPZ treated cells (M_f=0,481) compared to the untreated cells (M_f=0,735). The results also showed that there was no significant difference between M_f of wt ILK protein in CPZ-treated cells compared to the K341R mutant ILK protein in untreated cells. This led to the conclusion that ubiquitination of ILK at K341 might be important for the clathrin-mediated endocytosis of the ILK protein.

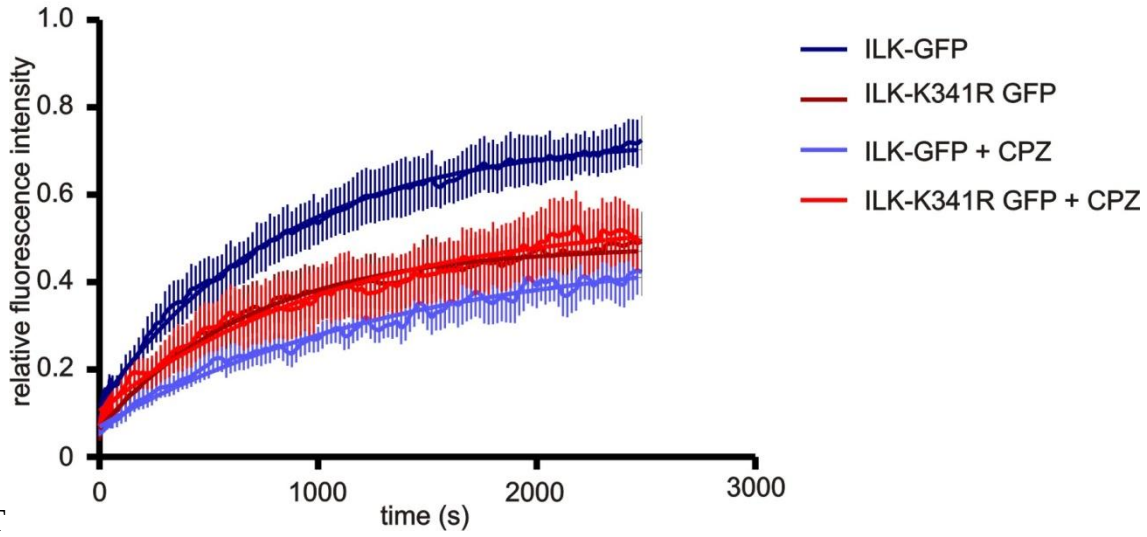

T

Figure 3.2.6. *FRAP analysis of ILK-GFP and ILK-K341R GFP in presence of CPZ. The recovery curves calculated form recorded data. The solid smooth lines represent the best fit curves of a nonlinear regression analysis. The ANOVA with Bonferrony-post test was performed. Data is expressed as mean ± SEM. n=7; ***p<0.0001*

The initial in vivo ubiquitination assays showing reduced ubiquitination of ILK in the K341R mutant was performed in ILK -/- cells that were transiently transfected with wt or K341R ILK. However, the migration and FRAP assays were preformed in stable cell lines where the expression levels of wt and mutant ILK were accurately adjusted. Therefore additional in vivo ubiquitination assays wete performed using a stable cell line generated by transduction of a pCLMFG retrovirus expressing either wt ILK-Flag or ILK-K341R-Flag. Using these stable cell lines as well as the parental ILK fl/fl cell line as a negative control, an in vivo ubiquitination assay was performed.

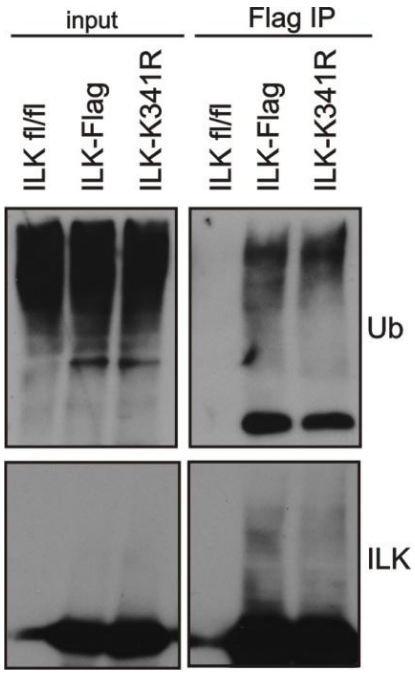

Figure 3.2.7. *Western blot analysis of Flag immunoprecipitates from ILK -/- fibroblasts expressing ILK-Flag or ILK-K341R. Ubiquitin and ILK-Flag immunoblot show no major difference in detected ubiquitination.*

The immunoprecipitates eluted by Flag peptide were resolved by SDS-PAGE and analyzed by immunoblotting. Analysis of immunoblots using either an anti-ubiquitin antibody or an anti-Flag antibody unfortunately showed that the ubiquitination ladder pattern is unaffected by the K341R mutation. In addition, both immunoprecipitates contained similar levels of ubiquitin (Fig.3.1.4.). This allowed the conclusion that ubiquitination of the ILK-K341R-Flag mutant is comparable to wt ILK-Flag, implying that the K341 is dispensable for ubiquitination of ILK in stable cell lines. This finding opposes the previous experiments in this study performed using transient transfection. However, this finding is in line with numerous previous studies showing that lysine

residues are usually dispensable for ubiquitination and that ubiquitin chains can be assembled on various lysine residues within target proteins (Kundrat and Regan 2010).

3.3. ILK interacts with the E3 ligase CHIP

After confirming that ILK is modified by ubiquitination, further studies on the role of this posttranslational modification were performed. First, an experiment to identify novel interacting partners that might be involved in the ubiquitination of ILK was carried out. To this end co-immunoprecipitation experiments using the Flag affinity tag were performed. These experiments were performed using ILK-Flag cells that were compared to ILK fl/fl cells as a negative control and K341R-Flag cells to assess whether K341 is involved in specific protein-protein interactions. After in-solution tyrosine digestion the co-immunoprecipitates were analyzed by mass spectrometry. The immunoprecipitates were performed in biological triplicates and quantitative analysis of the precipitates was performed using a label-free method based on spectral comparison (Lee, Kwon et al. 2011). As shown in Fig.3.3.1. the mass spectrometry analyses identified known major interacting partners of ILK such as PINCH-1, α and β parvin as well as RSU-1, confirming the validity of this assay. No specific binding partners involving K341 were identified. Interestingly, however, the analyses revealed significant binding to a chaperone complex consisting of Hsp70, Hsp90, Dnaja1 and Dnaja2, Bag2, as well as the E3 ligase CHIP (C terminus of Hsp70 interacting protein or Stub 1). CHIP is an E3 ligase involved in protein quality control. It contains a tetratricopeptide (TRP) motif important for the interaction with Hsp70 and Hsp90 and a U-box domain with ubiquitin ligase activity (Murata, Chiba et al. 2003). Through its interaction with molecular chaperones CHIP is involved in the decision of whether the misfolded proteins enter degradation or refolding pathway (McDonough and Patterson 2003).

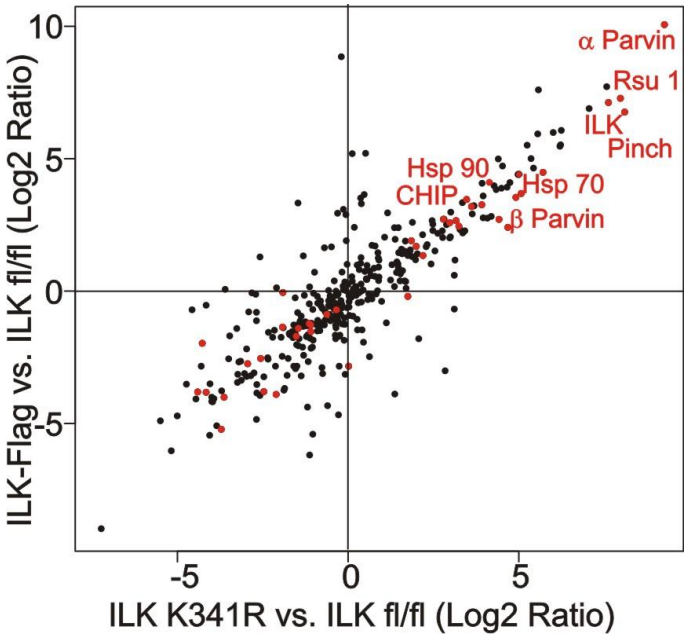

Figure 3.3.1. *Quantification of peptides co-precipitated with ILK-Flag. High ILK-Flag to ILK fl/fl ratio indicates specific binding. Identified components of the IPP complex and the novel interaction partners CHIP, Hsp90 and Hsp70 are highlighted in red.*

To further confirm the interaction between ILK and CHIP, Flag co-immunoprecipitation assays was carried out in wt ILK-Flag cells, using both ILK-/- and ILK fl/fl cells as negative controls. After the Flag peptide elution the immunoprecipitates were resolved with SDS-PAGE and analyzed by western blot.

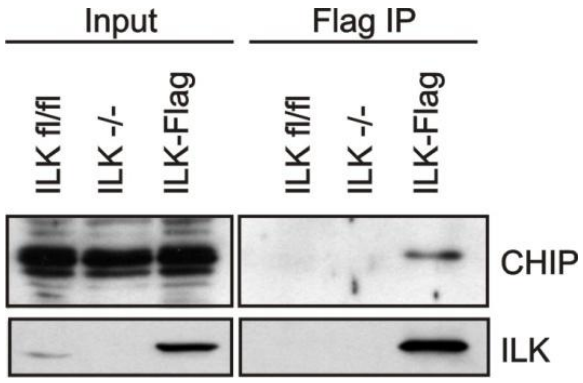

Figure 3.3.2. *Flag pull-down from ILK -/- fibroblasts expressing ILK-FLAG. CHIP is detected in the ILK immunoprecipitate.*

Immunoblotting using an anti-ILK antibody confirmed the success of the IP. In addition immunoblotting using an anti-CHIP antibody showed that endogenous CHIP co-

precipitated with ILK-FLAG (Fig.3.3.2.). This corroborated our previous mass spectrometry result showing that CHIP is a novel interaction partner of ILK.

In order to characterize the interaction of ILK and CHIP in more detail, mapping of the interacting region within CHIP was carried out. To this end CHIP cDNA was cloned from fibroblast RNA using reverse transcription and subsequently subcloned into the pEGFP-C1 vector allowing a N-terminal EGFP-CHIP fusion protein to be expressed. CHIP was cloned from mouse fibroblast cDNA generated from total RNA by PCR using CHIP-specific primers. Next, CHIP cDNA was cloned into the TOPO vector from which it was consequently subcloned into the pEGFP-C1 backbone using restriction enzymes. The TPR and Ubox domains of CHIP were cloned into EGFP-C1 vector by performing PCR with specific primers followed by restriction enzyme cloning. There are two point mutations of CHIP that have been reported to be relevant for its function. Mutation of lysine 30 to alanine (K30A) abolishes the interaction of CHIP with its major interacting partner hsp70, whereas the mutation of histidine 260 to glutamine (H260Q) abolishes the E3 ligase activity (Dai, Zhang et al. 2003; Murata, Chiba et al. 2003; Zhou, Fernandes et al. 2003; Zhang, Windheim et al. 2005). These two mutants of CHIP were cloned by performing site directed mutagenesis using the CHIP-WT-pEGFP-C1 as a template.

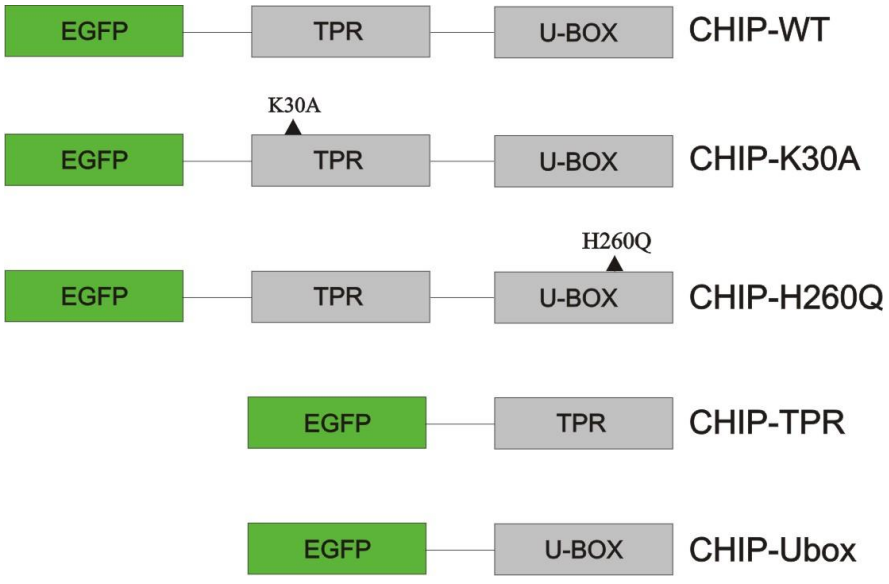

Figure 3.3.3. *Schematic illustration of various EGFP-CHIP constructs.*

All EGFP-CHIP constructs (Fig. 3.3.3.) were transiently transfected into the ILK fl/fl cell line. After allowing the fusion proteins to be expressed for the 24 h, the cells were lysed and subjected to co-immunoprecipitation analysis. Here the µMACS GFP Isolation Kit

from Milteyi Biotec containing a GFP antibody covalently coupled to magnetic MicroBeads was used. This allows efficient immunoprecipitation without interference of the IgG heavy chain. The immunoprecipitates were resolved on an SDS-PAGE and analyzed by western blot. The immunoblotting was done using anti-ILK and anti-CHIP antibodies. The analysis revealed a strong ILK band in the immunoprecipitates from cells expressing the Ubox of CHIP (Fig. 3.3.4.). This indicated that ILK interacts with the Ubox domain of CHIP. Interestingly more ILK was co-precipitated with CHIP-Ubox than CHIP-WT. This can be explained by the asymmetric structure of the CHIP dimer in which only one of the Ubox domains is available for the interactions, while the other is masked by the TPR domain (Schulman and Chen 2005). Furthermore, the H260Q mutation did not affect the interaction of CHIP with ILK, indicating that the catalytic activity of CHIP is not a requirement for this interaction. Interestingly, although ILK did not co-precipitate with the TPR domain, the K30A point mutation that was generated in the TPR domain of full length CHIP abrogated ILK binding. This is probably due to the loss of interaction of CHIP with hsp70, indicating that hsp70 might stabilize the interaction between ILK and CHIP (Pratt, Morishima et al. 2010).

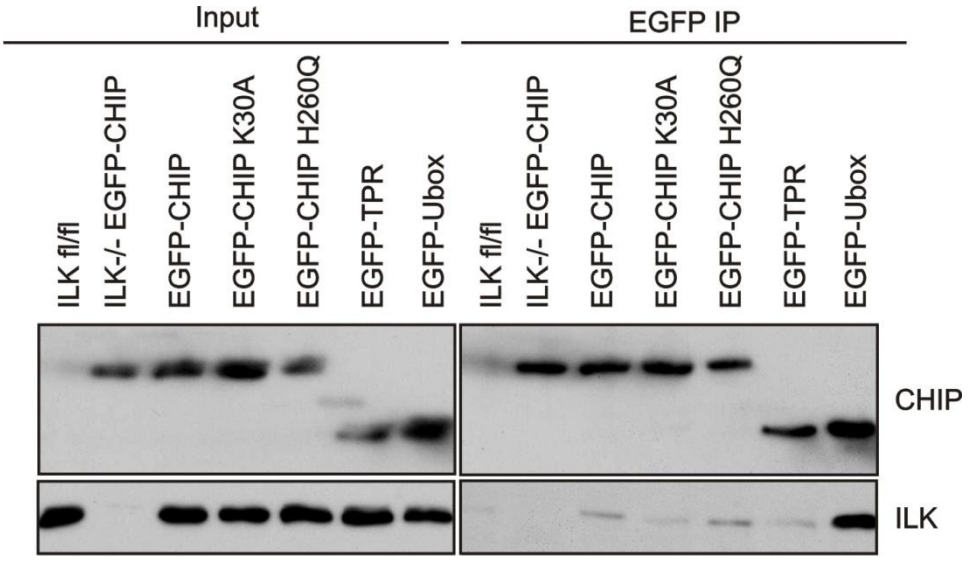

Figure 3.3.4. *GFP-pull down from fibroblasts expressing EGFP-CHIP or mutants. ILK is detected in immunoprecipitates of full length EGFP-CHIP and EGFP-Ubox. K30A mutation of CHIP abrogates ILK binding.*

To investigate whether the interaction between ILK and CHIP is direct, an in vitro binding assay was carried out using recombinant proteins. To this end CHIP-WT was subcloned into the pET-16b backbone vector allowing bacterial expression of His-tagged

CHIP-WT protein. BL21 E.coli strain was transformed with CHIP-WT-pET-16b construct and after IPTG induction bacterial cells were lysed and His-CHIP was purified using HisPur Cobalt NTA resin from Thermo Scientific. The success of induction and purity of the recombinant protein was confirmed by running the samples on an SDS-PAGE and performing a Coomassie staining (Fig.3.3.5.). The purification of recombinant CHIP-WT protein was successful, giving a yield of 12 µg/µl, as measured by BCA assay.

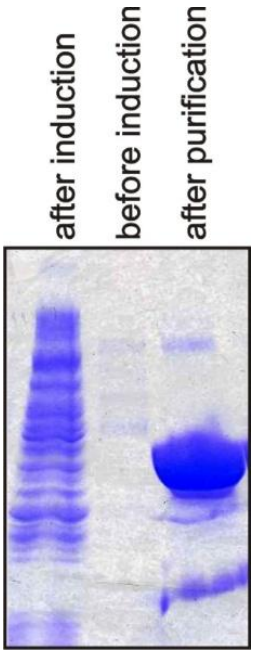

Figure 3.3.5. *Coomassie stained SDS polyacrylamide gel showing the bacterial lysate before and after the induction of CHIP-His expression by 1mM IPTG as well as the purified protein.*

Next, 5 µg of recombinant His-CHIP-WT and recombinant ILK-Myc/DDK (expressed in HEK293 cells, purchased from OriGene) were incubated in His pull down buffer containing 20 mM imidazole for blocking unspecific binding to the resin. After incubation at 25 ˚C for 2 h in an end-over shaker, the cobalt NTA resin was added and incubation was carried out for an additional 2 h. ILK without CHIP-WT protein was used as a control. After elution of the resin with 200 mM imidazole, the eluate was resolved by SDS-PAGE and analyzed by western blot. Immunoblotting with an anti-CHIP antibody revealed a strong band corresponding to CHIP in the reaction containing both CHIP and ILK, but no CHIP staining was detectable in the ILK only control reaction (Fig.3.3.6.). This indicated that that the pull down was successful and specific for His-tagged CHIP. The immunoblot with an anti-ILK antibody showed a band corresponding to ILK in the

reaction containing both ILK and CHIP, but no band was visible in the ILK only control pull down. This indicated that there is a direct interaction between ILK and CHIP. However, the levels of ILK pulled down in this reaction were relatively low, implicating that the presence of additional proteins could strengthen this interaction, as already seen in the GFP pull down experiment (Fig. 3.3.4.).

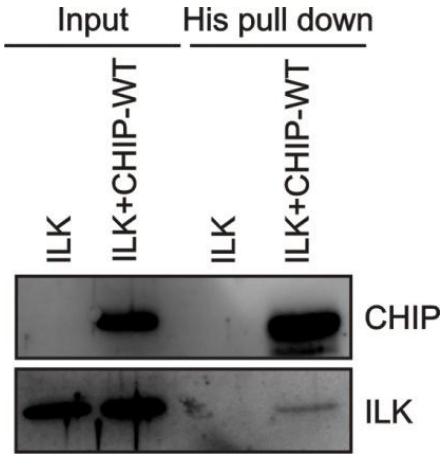

Figure 3.3.6. *Western blot of a His pull down with recombinant His-tagged CHIP and GST-tagged ILK. ILK co-precipitates with CHIP.*

3.4. ILK and CHIP partially co-localize in mature focal adhesions

To visualize the cellular compartment in which the ILK-CHIP interaction might take place, immunofluorescence stainings of ILK and CHIP in adherent ILK fl/fl and ILK-/- fibroblasts were carried out. Cells were seeded on glass coverslips and allowed to adhere and spread over night. Next, cells were fixed in 100 % methanol and subsequently blocked with 3% BSA/5% goat serum in PBS. ILK and CHIP were detected with primary antibodies and fluorescent secondary antibodies diluted in 1 % BSA as described in Materials and Methods. The stainings were visualized by confocal microscopy. CHIP was found to localize in the cytoplasm into fiber-like structures as well as into focal adhesions, where it co-localized with ILK. The localization of CHIP to focal adhesions was independent of ILK since a similar staining of CHIP was observed in ILK-/- cells. (Fig.3.4.1.).

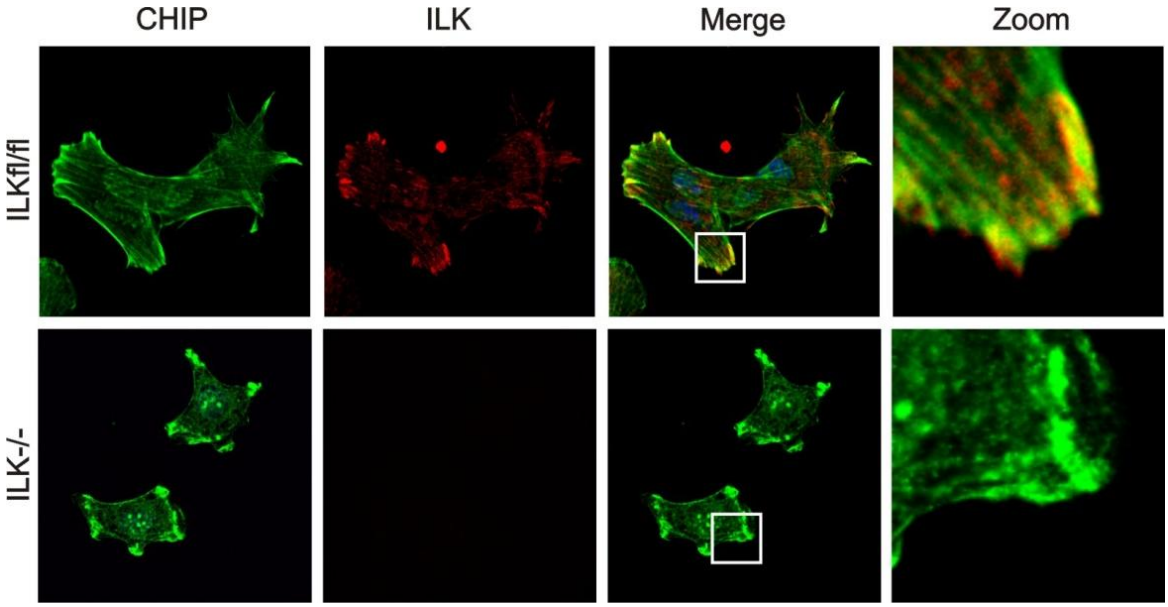

Figure 3.4.1. *Immunofluorescence analysis of endogenous CHIP and ILK in ILK fl/fl and ILK-/- fibroblasts. Note co-localization in focal adhesions. CHIP localizes to focal adhesion also in the absence of ILK.*

To confirm the correct localization of EGFP-CHIP-WT fusion protein that had been used in the immunoprecipitation as well as to provide additional evidence for the localization of CHIP, immunofluorescence analysis of ILK fl/fl fibroblast expressing EGFP-CHIP-WT was carried out. To this end adherent ILK fl/fl fibroblast seeded on glass cover slips were transiently transfected with EGFP-CHIP-WT using the Lipofectamine 2000 transfection reagent. After 24 h of protein expression cells were fixed in 4 % PFA. Immunostaining of endogenous ILK was subsequently carried out as described above. ILK staining and EGFP-CHIP-WT were visualized by confocal microscopy (Fig.3.4.2). Localization of EGFP-CHIP fusion protein to fiber-like cytoplasmic structures and accumulation in focal adhesions, closely resembling the localization of endogenous CHIP, could be observed. This demonstrated that over-expressed EGFP-CHIP-WT protein localizes properly in the cell and supported our observation that CHIP localizes to focal adhesions as well as fiber-like structures resembling actin stress fibers in the cytoplasm.

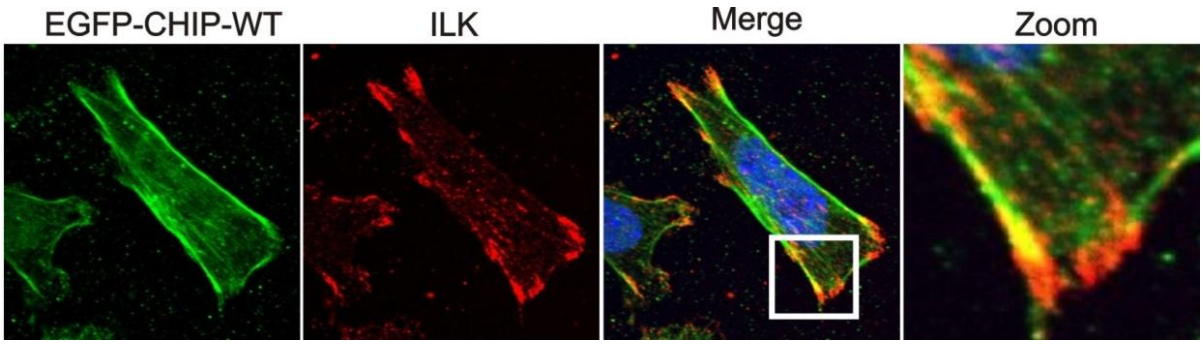

Figure 3.4.2. *Immunofluorescence analysis of transiently transfected EGFP-CHIP-WT and endogenous ILK in ILK fl/fl fibroblasts. Note co-localization in focal adhesions.*

In order to determine whether the localization of CHIP depends on the actin cytoskeleton and to assess the kinetics of CHIP localization to focal adhesions, ILK fl/fl cells were subjected to immunofluorescence analysis during the time course of cell spreading (Fig. 3.4.3.). Cells were seeded on glass cover slips coated with 5 µl/ml fibronectin and allowed to adhere and spread. Cells were fixed at time points corresponding to the various stages of cell spreading. Cells were then immunostained using phalloidin to visualize polymerized F-actin as well as antibodies against the focal adhesion protein paxillin and CHIP. Inspection by confocal microscopy revealed that CHIP co-localized with actin stress fibers during both early and late stages of cell spreading. Co-localization of CHIP with paxillin was observed when actin stress fibers were already visible. This suggested that actin polymerization might drive the localization of CHIP.

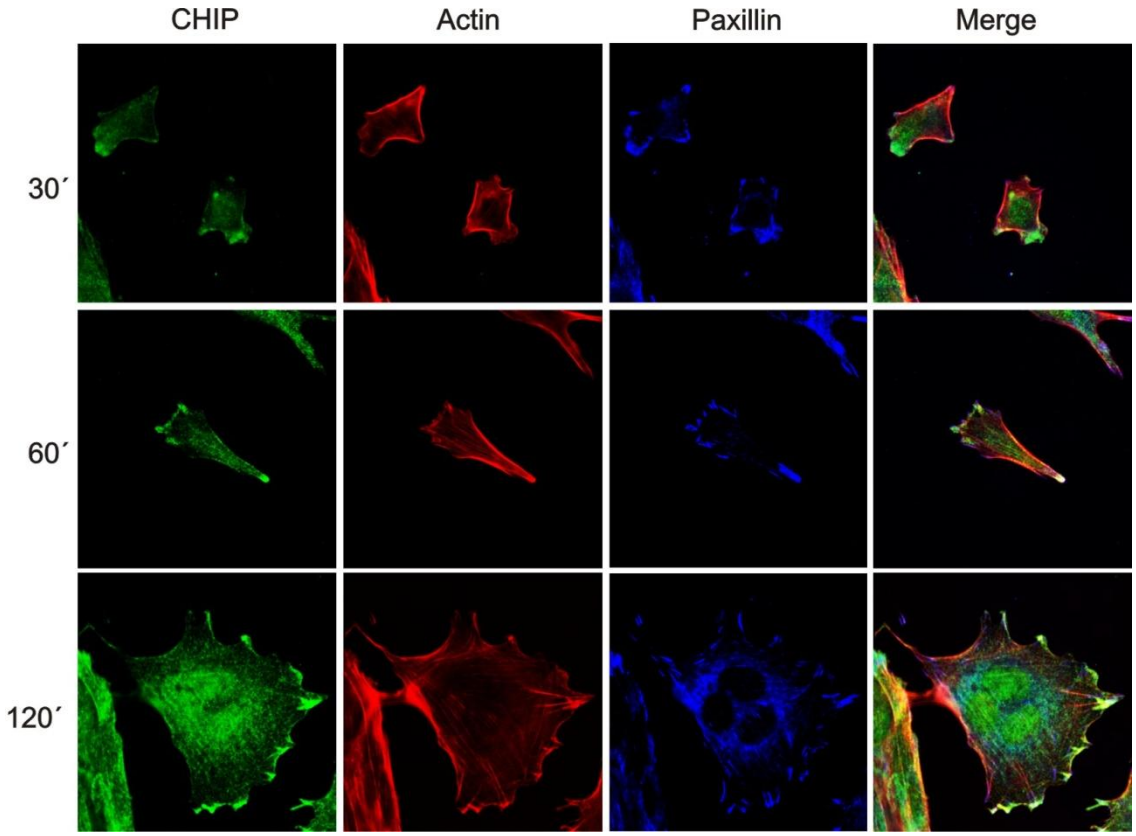

Figure 3.4.3. *Immunofluorescence analysis of endogenous CHIP, paxillin, and actin in ILK fl/fl fibroblasts during cell spreading. CHIP localizes to focal adhesions during late stages of cell spreading.*

To address this potential interaction of CHIP with polymerized actin, actin co-sedimentation assays were performed essentially as described previously (Riedl, Crevenna et al. 2008). In this assay 3 mM of recombinant His-tagged CHIP was incubated with increasing concentrations of polymerized actin. Actin was allowed to polymerize by incubating it in high salt buffer. The reactions were pelleted by ultracentrifugation at 60 000g. The supernatant and pellet were separated and resolved by SDS-PAGE. Coomassie blue staining of the gel revealed co- sedimentation of CHIP with actin. The co-sedimentation correlated with the amount of polymerized actin, indicative of a specific interaction. This demonstrated the interaction of CHIP and polymerized actin.

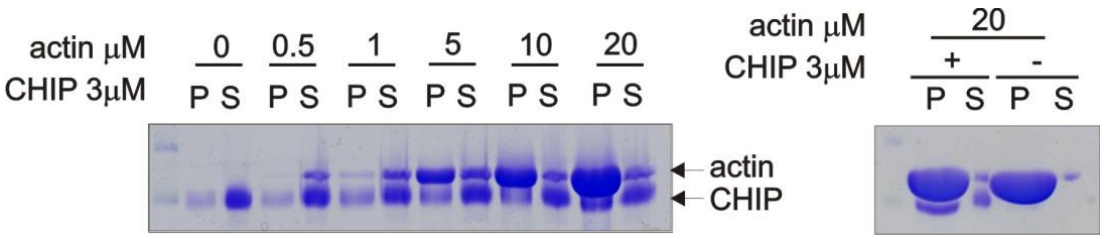

Figure 3.4.4. *Coomassie staining of an actin co-sedimentation assay. Recombinant CHIP co-sediments with polymerized actin.*

3.5. CHIP ubiquitinates ILK

The results so far had shown that CHIP both interacts and co-localizes with ILK. In order to address whether CHIP is capable of ubiquitinating ILK through its E3 ligase activity, an in vitro ubiquitination assay with recombinant CHIP-WT and ILK was performed essentially as previously described (Arndt, Daniel et al. 2005). Recombinant ubiquitin, E1 ubiquitin activating enzyme, and UbcH5a E2 ubiquitin conjugating enzyme were all purchased from Boston Biolabs. In addition, the reactions were supplemented with recombinant hsp40 and hsp70 proteins that were gifts from Dr.Jörg Höhfeld. ILK-Flag fusion protein was purified from CHO cells that were transiently transfected with ILK-p3XFlag CMV14. After 24 h of protein expression a large-scale Flag immunoprecipitation was performed. The immunoprecipitates were extensively washed in order to remove any co-immunoprecipitates before the elution by Flag peptide. The protein yield was 0.12µg/µl as measured by BCA assay. Expressing the protein in a mammalian system has the advantage that posttranslational modifications that might be important for protein-protein interaction will be present. This will not be the case for proteins expressed in E.coli.

A series of ubiquitination reactions with constant concentrations of ILK, Ub, E1, E2 as well as Hsp40/Hsp70 but increasing concentrations of CHIP was carried out (Fig.3.5.1.).

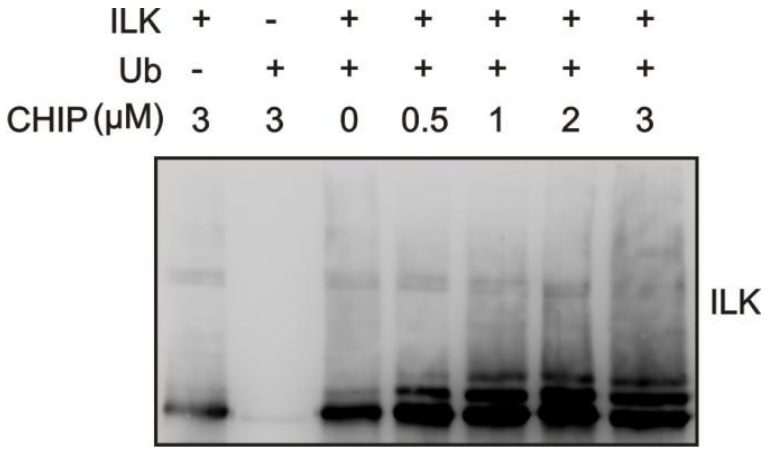

Figure 3.5.1. *Western blot analysis of an in vitro ubiquitination assay. CHIP ubiquitinates ILK in a dose-dependent manner.*

The reactions were carried out at 37 ˚C for 2 h after which they were terminated by heat inactivation at 95 ˚C in Laemmli buffer. Reactions were resolved by a 4-15% gradient SDS-PAGE and analyzed by western blot. The immunoblot for ILK revealed a typical ladder pattern. The intensity of the high molecular weight bands correlated with the concentration of CHIP indicating an increase in the efficiency of the reaction with increasing amounts of CHIP in the reaction. This shows that the reaction is specific. It should be noted that some background ubiquitination was observed also in the absence of CHIP. This probably arises from minor impurities of the ILK protein preparation since the same impurity was also observed in the reaction lacking ubiquitin.

The specificity of the reaction was further confirmed by performing and in vitro ubiquitination assay comparing CHIP-WT and the CHIP-H260Q mutant that does not E3 ligase activity (Fig.3.5.2.). Furthermore, to exclude that the ubiquitination arises from impurities of the ILK-Flag preparation, this in vitro ubiquitination assay was carried out with a commercially available recombinant ILK-Myc/DDK expressed in HEK293 (purchased from OriGene). The recombinant CHIP-H260Q mutant was generated by performing site directed mutagenesis using a CHIP-WT-pET16b vector as a template. The His-tagged mutant protein was then expressed and purified as described earlier for the CHIP-WT protein. In vitro ubiquitination reactions were performed with a constant concentration of all recombinant proteins including ILK, CHIP-WT, CHIP-H260Q, ubiquitin, E1, E2 and Hsp40/Hsp70.

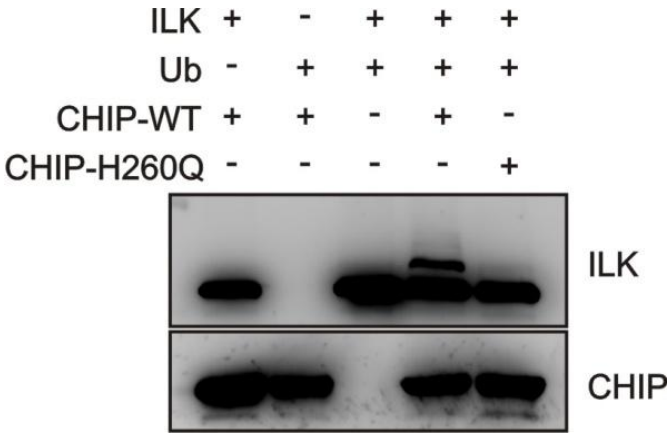

Figure 3.5.2. *Western blot of an in vitro ubiquitination assay. CHIP-WT but not the ligase-dead H260Q-CHIP mutant ubiquitinates ILK.*

The reactions were incubated at 37 ˚C for 2 h, terminated by heat inactivation at 95˚C in Laemmli buffer and subsequently resolved by 4-15% gradient SDS-PAGE and analyzed by western blot. Immunoblot for CHIP revealed an equal intensity of both CHIP-WT and CHIP-H260Q confirming equal concentration of CHIP-WT and CHIP-H260Q in the reactions. Immunoblot for ILK showed a ladder pattern typical for ubiquitination only in the CHIP-WT sample indicating absence of ubiquitination in the reaction containing the E3 ligase dead CHIP mutant (CHIP H260Q).

Since in vitro ubiquitination assays can give rise to unspecific ubiquitination reactions due to the high concentrations of enzymes, and in order to assess whether CHIP is capable of ubiquitinating ILK also in vivo, an in vivo ubiquitination assay was performed using CHO cells transiently transfected with ILK-3XFlag-pCMV14, Ub-HA-pcDNA3.1, CHIP-WT-pEGFP-C1 or CHIP-H260Q-pEGFP-C1 mutant (Fig.3.5.3.). After expressing the proteins for 24 h cells were lysed using the denaturating protocol followed by Flag immunoprecipitation. Immunoprecipitates were resolved using SDS-PAGE and analyzed by western blot. CHO cells transfected with CHIP-WT and ubiquitin-HA; ILK-Flag; ILK-Flag and ubiquitin-HA or ILK-Flag and CHIP-WT without ubiquitin were used as controls. Band intensities of CHIP-WT and CHIP-H260Q in the input lanes were equal in indicating equal expression of CHIP-WT and CHIP-H260Q protein. Immunoblotting with antibodies against ILK and against ubiquitin revealed a stronger ladder pattern in the immunoprecipitates of cells transfected with CHIP-WT compared to cells transfected with CHIP-H260Q. This indicated that increased expression of CHIP-WT leads to a strong increase in ILK ubiquitination, whereas over-expression of CHIP-H260Q mutant

does not enhance the basal level of ILK ubiquitination. Taken together these experiments demonstrate that CHIP is capable of ubiquitinating ILK both in vitro and in vivo.

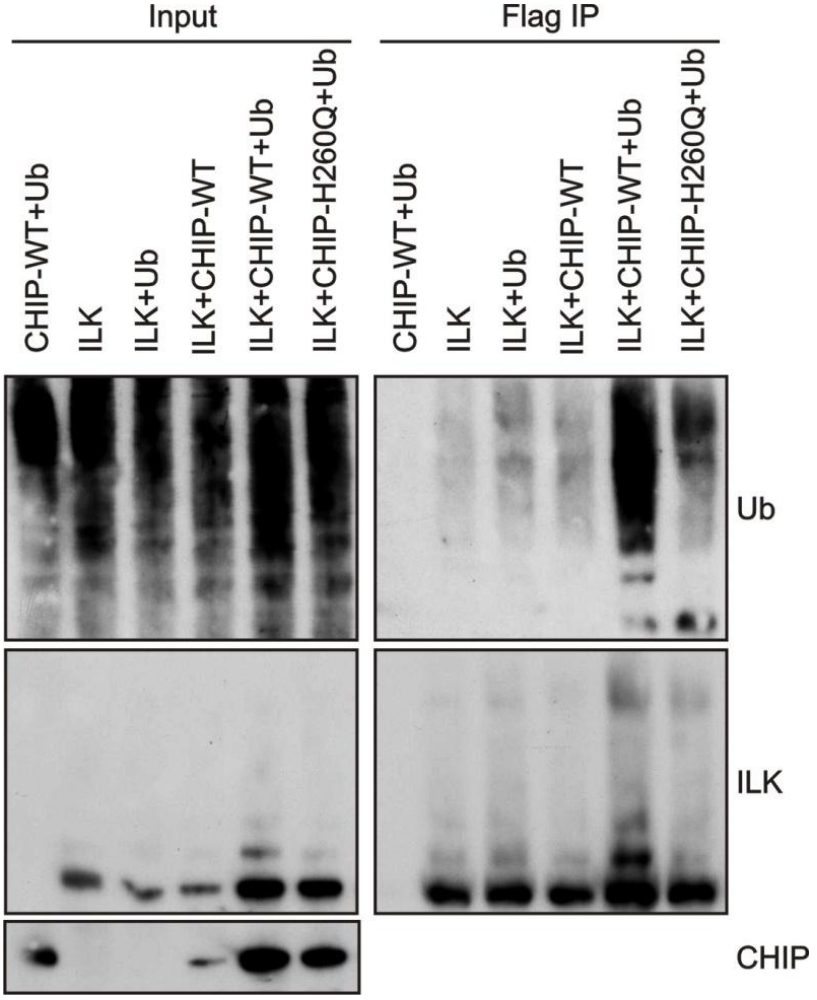

Figure 3.5.3. *Western blot analysis of Flag immunoprecipitates from CHO cells expressing ILK-Flag, CHIP, CHIP-H260Q and ubiquitin-HA. Expression of CHIP but not ligase-dead mutant enhances ubiquitination of ILK.*

3.6. ILK is degraded both by proteasome and lysosome

A major consequence of ubiquitination, particularly through K48-linked chains, is proteasomal degradation of the target protein (Ciechanover 1994). As this study could demonstrate that ILK is modified by K48-linked polyubiquitin chains, further investigation of the consequences of ILK ubiquitination in fibroblasts was carried out. To this end ILK fl/fl fibroblast were treated with the proteasomal inhibitor MG132 or the DMSO solvent as control. After 6 h of treatment cells were lysed and analyzed by

western blot (Fig.3.6.1.). Immunoblotting with antibodies against ubiquitin was used as a positive control to confirm that the inhibition was successful, as this should lead to an accumulation of ubiquitinated proteins. This was found to be the case as the intensity of the ubiquitin signal in the inhibitor treated cells was significantly stronger compared to control. ILK levels were not found to be increased in response to inhibitor treatment. Actin was used as a loading control, demonstrating equal loading of the two samples. The result could either indicate that ILK is not degraded by proteasome, or that its half-life is significantly longer than 6 h. In addition, this experiment suggested that ILK might be degraded by the lysosome as blocking the proteasome has been shown to increase lysosomal degradation (Chen and Yin 2011). In agreement with this, ILK levels were found to be slightly decreased upon MG132 treatment (Fig.3.6.1.).

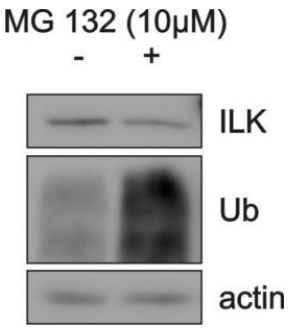

Figure 3.6.1. *Inhibition of proteasome with MG132 results in decrease in ILK levels. Ubiquitin is used as a positive control for MG132 treatment and actin as loading control.*

In recent years it has been shown that ubiquitination does not only lead only to proteasomal degradation of target proteins but it can also act as a target signal for lysosomal degradation (Wong and Cuervo 2010). In particular, long-lived cytosolic proteins are often degraded via the lysosomal pathway (Wong and Cuervo 2010), and this can be induced by activation of autophagy by starvation or rapamycin (Klionsky, Abeliovich et al. 2008). In order to determine the half-life of the ILK protein and its degradation kinetics under starvation, ILK fl/fl fibroblasts were treated with cycloxeximide (CHX), an inhibitor of protein synthesis that acts by blocking translational elongation (Fig. 3.6.2.). In parallel, the cells were treated with CHX in serum-free medium to induce autophagy through starvation. Control cells were treated with DMSO. The cells were then lysed at different time points and analyzed by western blot. The immunoblot for ILK showed a moderate decrease in ILK levels after 12 h of treatment with CHX and after 24 h of treatment ILK levels were found significantly reduced.

Starvation was observed to enhance this effect. β-catenin immunoblot was used as a positive control for the success of CHX treatment and immunoblot for GAPDH was used as a loading control. This indicated that ILK is a long lived protein with a half-life of approximately 12-24 h, and that starvation, possibly by activation of autophagy, reduces this half-life.

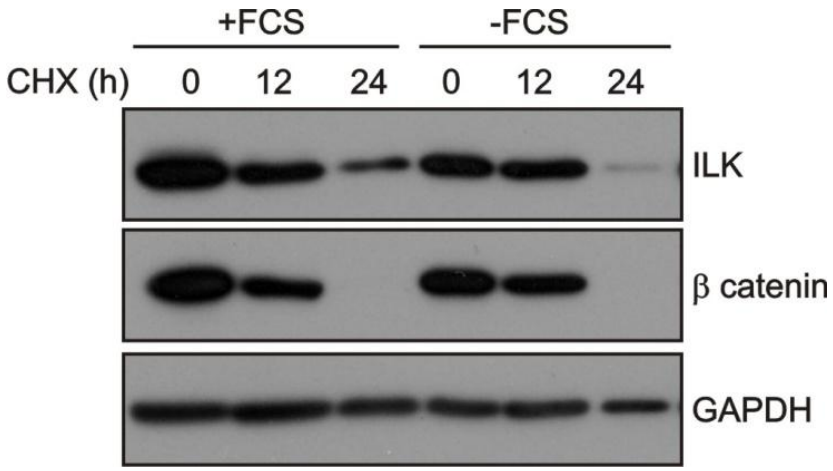

Figure 3.6.2. *Western blot of fibroblasts treated with cycloheximide (CHX) to block protein synthesis for time points indicated. Majority of ILK is degraded in 24 h. Serum starvation enhances degradation. β-catenin was used as a positive control for CHX treatment, and GAPDH as loading control.*

As ILK was found to have a relatively long half-life, we decided to combine inhibition of protein synthesis with inhibition of degradation to clarify whether ILK is degraded by the proteasome or by the lysosome. ILK fl/fl fibroblasts were treated with CHX for 12 h in order to block protein synthesis in combination with the proteasomal inhibitor MG132, the lysosomal inhibitor bafilomycin, the lysosomal activator rapamycin, or the vehicle DMSO (Fig.3.6.3.). After 12 h of incubation cells were lysed and analyzed by western blot. Immunoblot with antibodies against LC3, a marker for lysosome activation showed significantly stronger staining in the bafilomycin treated cells, indicating that lysosomal degradation was successfully blocked resulting in LC3 accumulation. The LC3 staining was reduced in rapamycin treated cells indicating that lysosomal degradation was induced, resulting in LC3 degradation. The immunoblot for ILK revealed a significant increase in ILK staining in bafilomycin treated cells compared to the DMSO control. In addition, bafilomycin could partially restore ILK levels in CHX treated cells, indicating that ILK can be degraded by the lysosome. However, also the MG132 treatment could

restore ILK levels in CHX-treated cells. Interestingly, MG132 blocked ILK degradation in CHX-treated cells more efficiently than bafilomycin. GAPDH immunostaining was used as a loading control. This indicated that ILK can be regulated both by proteasomal and lysosomal degradation pathways and suggested that majority of ILK is degraded via the proteasome.

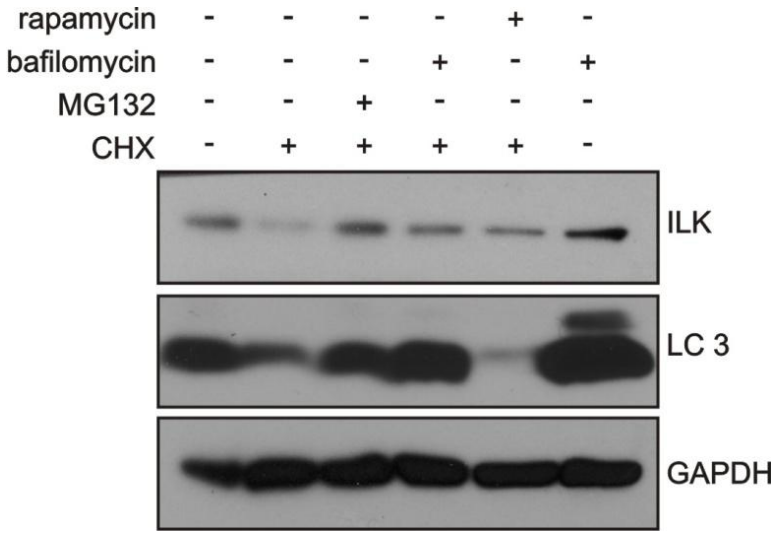

Figure 3.6.3. *Western blot of fibroblasts treated with cycloheximide (CHX) to stop protein synthesis for time points indicated. Inhibition of proteasome with MG132 retards ILK degradation as well as inhibition of lysosome with bafilomycin. Induction of autophagy by rapamycin has no major effect. LC3 is a positive control for inhibition of lysosome and induction of autophagy. GAPDH is used as loading control.*

3.7. ILK is rapidly degraded by CHIP in the absence of Hsp90

ILK has been shown to be a Hsp90 client protein in HT1800, COS-7 and NL-17 cells (Aoyagi, Fujita et al. 2005). As Hsp90 was identified in our interaction screen and it has been shown to act in co-operation with CHIP, it was of interest to test whether ILK is a Hsp90 client also in mouse fibroblasts. ILK fl/fl cells were therefore treated with 17AAG, an inhibitor of Hsp90 (Fig.3.7.1.). The control cells were treated with the vehicle DMSO. Cells were lysed after 12 h and 24 h of treatment and analyzed by western blot.

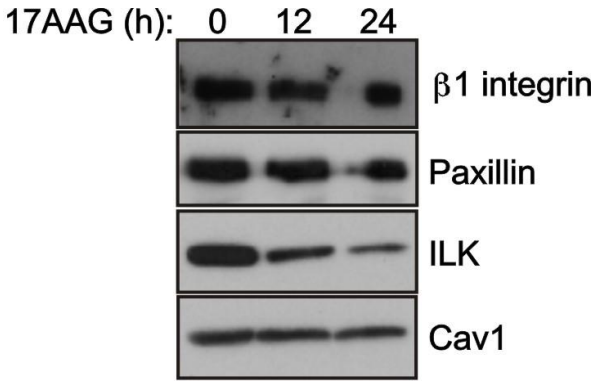

Figure 3.7.1. *Western blot of fibroblasts treated with 17AAG to inhibit Hsp90 for time points indicated. Inhibition of Hsp90 with 17AAG leads to rapid degradation of ILK. Caveolin-1 was used as a loading control. β1 and paxillin were used as negative controls for the inhibitor treatment. Assay performed by Dr. Sara A. Wickström.*

Immunoblotting with antibodies against ILK revealed a significant decrease in ILK staining already after 12 h and a more pronounced effect after 24 h indicating that ILK protein levels were reduced. The immunoblots for the focal adhesion proteins paxillin and β1 integrin showed no change in staining intensity, indicating that the effect is specific for ILK and not a general phenomenon for focal adhesion proteins. Caveolin-1 was used as a loading control.

Based on this result we hypothesized that Hsp90 is a chaperone for ILK, and inhibition of chaperone activity leads to degradation of ILK. As previous experiments implicated that ILK can be degraded by both proteasomal and lysosomal pathway, it was of importance to analyze which of these pathways is involved in ILK degradation upon Hsp90 inhibition. Inhibiting the degradation pathway should in this case maintain ILK levels also in the presence of the Hsp90 inhibitor. To test this, ILK fl/fl fibroblasts were treated with 2.5 μM 17AAG to inhibit Hsp90 and to induce ILK degradation in combination with either the proteasomal inhibitor MG132 or the lysosomal inhibitor bafilomycin (Fig.3.7.2.). Control cells were treated with DMSO or 17AAG alone. After 12 h of treatment cells were lysed and analyzed by western blot. The immunoblot for ILK revealed a decrease in ILK staining in samples treated with 17AAG as well as in samples treated with a combination of 17AAG and bafilomycin. However, in samples treated with a combination of MG132 and 17AAG, ILK staining was significantly stronger. This indicated that inhibition of Hsp90 leads to the degradation of ILK through the proteasome, whereas the lysosomal degradation pathway is not involved.

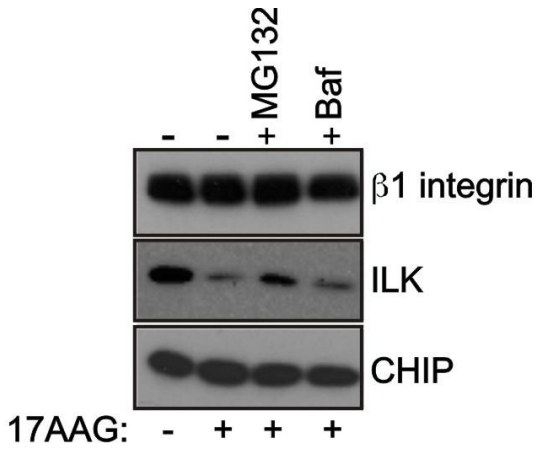

Figure 3.7.2. *Western blot of fibroblasts treated with 17AAG to inhibit Hsp90 in combination with MG132 or bafilomycin. Inhibition of the proteasome with MG132 rescues ILK from degradation induced by 17AAG treatment. β1 integrin was used as negative control for the inhibitor treatment. Assay performed by Dr. Sara A. Wickström.*

β1 integrin was used as a negative control for the inhibtion treatment. Immunoblot for CHIP demonstrated that CHIP protein levels remained constant in all samples, excluding that variation in ILK levels could be a result of altered levels of CHIP.

CHIP interacts with Hsp90 and Hsp70, and the complex is involved in the triage decision of protein refolding versus degradation (Pratt, Morishima et al. 2010). Therefore it was of importance to address whether the degradation of ILK that occurs when Hsp90 is inhibited by 17AAG involves CHIP. To this end, CHIP+/+ fibroblasts and two independent CHIP-/- cell lines were treated with 17AAG after which ILK levels were analyzed by western blot (Fig.3.7.3.). Two concentrations of the inhibitor, 1 and 5 µM, were used. Control cells were treated with the vehicle DMSO.

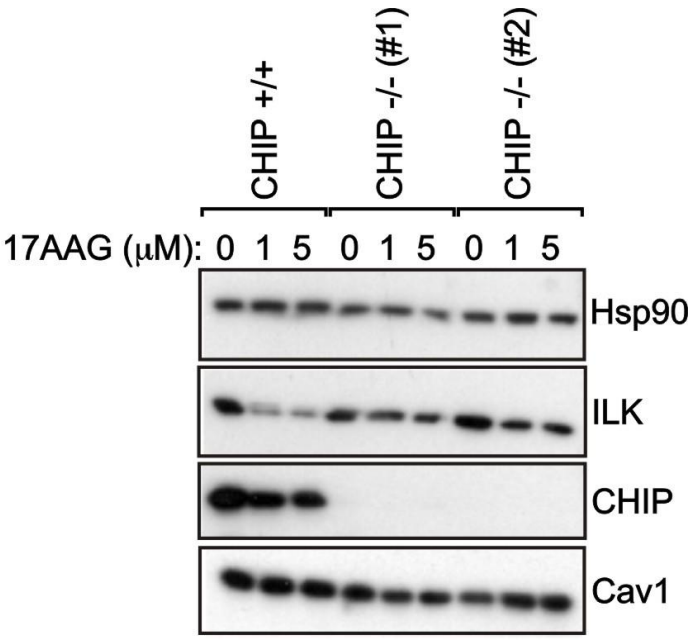

Figure 3.7.3. *Western blot of CHIP +/+ and CHIP -/- fibroblasts treated with different concentrations of 17AAG to inhibit Hsp90. Inhibition of Hsp90 with 17AAG leads to rapid degradation of ILK in CHIP +/+ cells. This effect was attenuated in the CHIP-/- fibroblasts. CHIP was used to confirm the absence of the protein in CHIP-/- cells and caveolin-1 was used as a loading control. Assay performed by Dr. Sara A. Wickström.*

The immunoblot for ILK revealed a significant decrease in ILK staining in 17AAG-treated CHIP +/+ cells, whereas only a modest decrease was observed in both independent CHIP-/- cell lines. This indicates that CHIP is involved in the degradation of ILK when Hsp90 is inhibited. The CHIP immunoblot confirmed the absence of CHIP protein in CHIP-/- cells. Caveolin-1 was used as a loading control.

To confirm the results from the mass spectrometry analyses that Hsp90 interacts with ILK and to assess whether the inhibition of Hsp90 activity leads to increased interaction of ILK with the E3 ligase CHIP, immunoprecipitation experiments in the presence of 17AAG were performed. ILK-Flag cells were treated with 17AAG and lysed after 0, 30, 60 and 120 min of treatment. These brief time points were selected to avoid degradation of ILK during the course of the experiment. The lysates were subsequently subjected to immunoprecipitation using the Flag affinity resin as described previously (Fig.3.7.4.). The immunoprecipitates were eluted by Flag peptide and analyzed by western blot. The immunoblot for Hsp90 confirmed the interaction between Hsp90 and ILK and showed that this interaction gradually decreases upon inhibition of Hsp90 activity. The

immunoblot with antibodies against CHIP revealed increased CHIP staining in immunoprecipitates of 17AAG-treated cells, indicating that the interaction between ILK and CHIP increases upon inhibition of Hsp90. Interestingly the α–parvin immunoblot showed decreased staining in of α–parvin in the immunoprecipitates of the inhibitor-treated cells, indicating that ILK might be released from the IPP complex, or that the complex might be destabilized. The immunoblot for ILK-FLAG was used as a control for the succes of the immunoprecipitation.

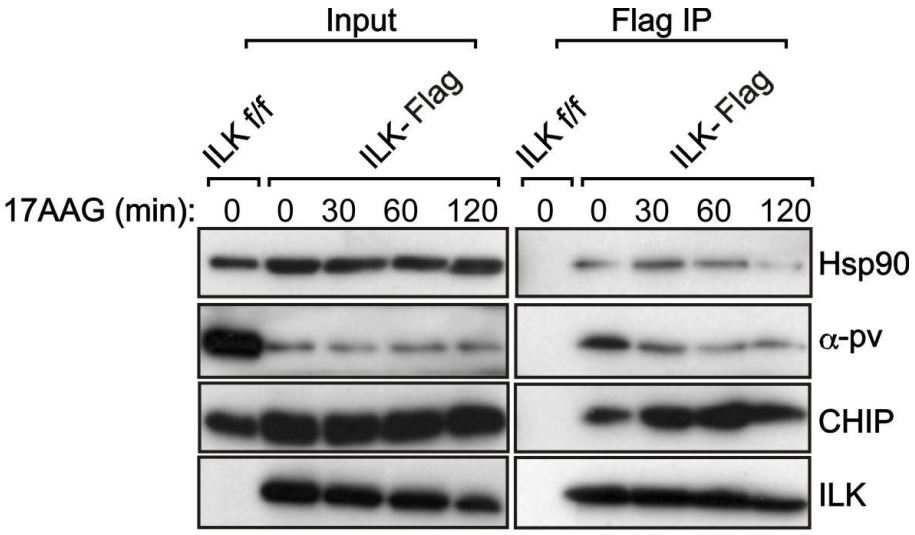

Figure 3.7.4. *Western blot of Flag immunoprecipitation of fibroblasts treated with 17AAG to inhibit Hsp90 for time points indicated. Inhibition of Hsp90 with 17AAG leads to increased interaction between ILK and CHIP and a decreased interaction between ILK and α-parvin. Assay performed by Dr. Sara A. Wickström.*

The 17AAG inhibitor studies in this chapter were performed by Dr. Sara A. Wickström.

3.8. Functional consequences of ILK-Hsp90 interaction

I*n vitro* studies conducted on fibroblasts, chondrocytes and keratinocytes have demonstrated the role of ILK in cell spreading, focal adhesion formation and migration (Grashoff, Aszodi et al. 2003; Sakai, Li et al. 2003; Lorenz, Grashoff et al. 2007). In order to analyze potential functional consequences of the interaction of ILK with Hsp90 and subsequent stabilization of ILK protein levels, the ability of fibroblasts to migrate within a 3-dimensional (3D) collagen matrix was analyzed. Fibroblasts were embedded in collagen gels in the presence or absence of the Hsp90 inhibitor 17AAG. The gels were

casted in self-made chambers and allowed to settle for 30 min at 37 ˚C and 4.5 % CO_2. The migration process was imaged by Zeiss Axiovert 40C microscope equipped with a CCD camera (Prosilica, GC2450) and a heated stage (37˚C) supplied with 4,7 % CO_2. Image acquisition was performed using FireWire software (Molecular Devices, Downingtown, PA). Migrating cells were subsequently tracked using the Chemotaxis and Migration tool of ImageJ software (Fig.3.8.1.).

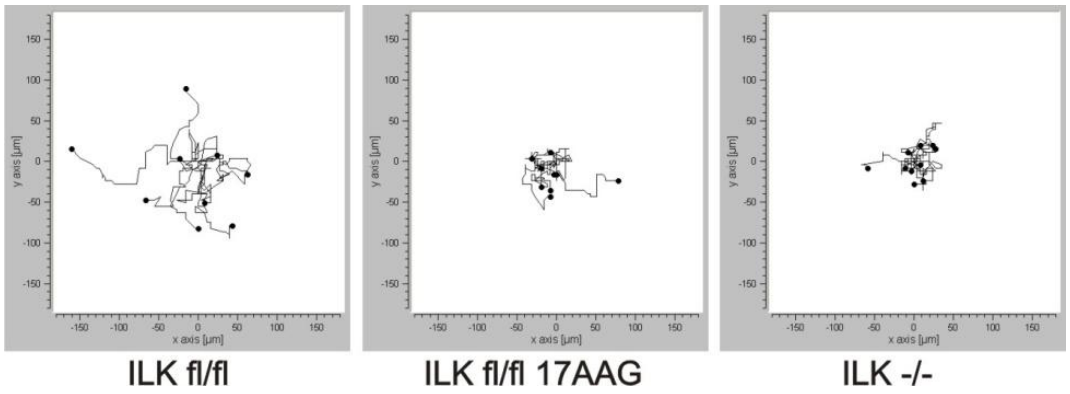

Figure 3.8.1. *Representative plots of migration tracks demonstrating reduced migration of ILK fl/fl fibroblasts treated with 17AAG or untreated ILK-/- fibroblasts compared to untreated ILK fl/fl cells.*

The migration distance and velocity was quantified from the live cell imaging data using ImageJ software (Fig.3.8.2.). The statistical significance was analyzed using the GraphPad Prism software by performing an ANOVA test followed by a Tucky post-hoc test. The quantifications demonstrate that the migration velocity and distance of ILK fl/fl fibroblasts treated with 17AAG inhibitor was significantly decreased compared to non-treated ILK fl/fl control. The migration velocity and distance of ILK fl/fl fibroblasts treated with 17AAG were comparable to ILK-/- cells. This led to the conclusion that inhibition of Hsp90, which induces degradation of ILK, also impairs fibroblast migration.

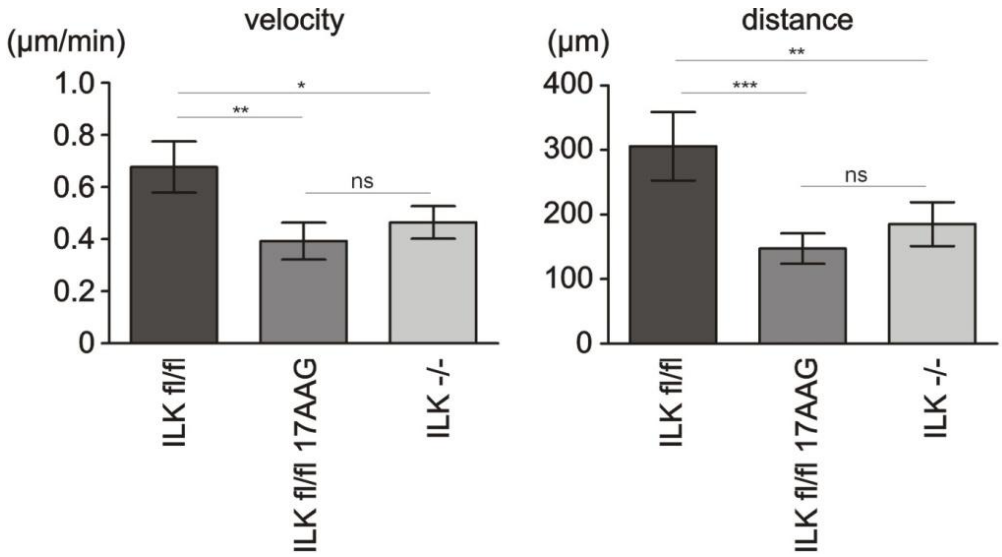

Figure 3.8.2. *Quantitative representation of velocity and distance differences between ILK fl/fl cells treated with 17AAG and untreated ILK-/- and ILK fl/fl fibroblasts. One way ANOVA test followed by Tucky´s post test was performed for statistical analysis. Data is expressed as mean ± SEM. n=5; *p<0.005, **p=0.0037(velocity) and 0.0010(distance), ***p=0.0004; ns=not significant.*

4. Discussion

Cell migration is a central process during development as well as during regenerative processes such as wound healing in adult organisms. Cell movement is achieved by coordinated assembly and disassembly of focal adhesions that couple to the actin cytoskeleton to generate the force and cell shape changes required for locomotion. To understand the detailed molecular mechanisms underlying focal adhesion dynamics, it is critical to study the regulation of individual focal adhesion proteins. As ILK is a major scaffold protein downstream of β1 integrins, alterations in levels of its function are likely to affect focal adhesions on a more global level. Therefore it was of interest to investigate how ILK might be regulated on the molecular level. The results of this study demonstrate that ILK is polyubiquitinated via K48- and K63-linked ubiquitin chains. The ubiquitin chains can be attached on K341 on ILK, but this lysine is dispensable for ubiquitination of ILK. ILK is further shown to interact with the chaperone-E3 ligase complex consisting of Hsp90, Hsp70 and CHIP. Hsp90 activity is required to stabilize ILK, and inhibition of Hsp90 activity leads to increased interactions between ILK and CHIP. CHIP is capable of ubiquitinating ILK, leading to its proteasomal degradation.

4.1. ILK is posttranslationally modified by ubiquitin

4.1.1. ILK is ubiquitinated at lysine 341

Ubiquitination is one of the most abundant posttranslational modifications of the proteome. It targets proteins to proteasomal and lysosomal degradation, but can also regulate the subcellular localization and recycling of target protein. This study sought to unravel the molecular mechanisms by which ILK is regulated by identification of posttranslational modifications on ILK and subsequent investigation of their functional significance. To this end mass spectrometry analysis of ILK immunoprecipitates was performed. The results showed that ILK is modified by a glycine-glycine dipeptide side chain on lysine 341. It is likely that other modified sites remained undetected as the peptides identified in the mass spectrometer depend on the presence of trypsin cleavage sites within the protein, therefore generating a bias towards certain peptides. The glycine-glycine modifications that remain covalently attached to the target protein after trypsin digestion are not specific for ubiquitin but can also be the consequence of modification by

other small proteins. Although abundant amounts of ubiquitin peptides were also detected in the mass spectrometry analysis, supporting the notion that ILK is ubiquitinated, further investigation of the nature of this modification by western blot analysis of the immunoprecipitates was carried out. In vivo ubiquitination assays performed in CHO cells expressing HA-ubiquitin together with ILK-Flag could confirm that ILK is indeed ubiquitinated in vivo. This does not, however, exclude that ILK could also be modified by other small proteins or molecules, and identification of additional posttranslational modifications of ILK might be important to fully understand how this protein is regulated. The results from the mass spectrometry analysis showed that lysine 341 contains an ubiquitin modification. To investigate the potential functional relevance of this lysine as a ubiquitination site, a point mutation in ILK cDNA leading to the exchange of the lysine 341 to arginine was introduced. This particular amino acid was chosen because it keeps the positive charge of the lysine residue while abolishing the possibility of ubiquitin attachment. Initial experiments performed by transient transfection showed a reduction, but not complete absence, of ILK ubiquitination in mutants where lysine 341 was replaced by an arginine. This lead to the initial conclusion that K341 is a major ubiquitination site on ILK, but that other ubiquitination sites most likely exist.

4.1.2. ILK is modified by both K48 and K63 polyubiquitin chain

Ubiquitin can assemble into various polyubiquitin chains depending on the recipient lysine in the ubiquitin molecule. Taken that there are seven lysine residues in ubiquitin molecule (K6, K11, K27, K29, K31, K48, K63), there are seven different possibilities for chain formation. In addition, polyubiquitin chains can be assembled in a linear fashion by N-terminal conjugation or in a branching manner by alternating the acceptor lysine residue in ubiquitin. This gives the wide variety of different possibilities for polyubiquitin chain formation (Ikeda and Dikic 2008). Various chains serve as different signals and lead to different outcomes for the target protein (Ikeda, Crosetto et al. 2010). Therefore it was important to identify the type of chain(s) assembled on ILK. To this end in vivo ubiquitination assays were performed using HA-tagged ubiquitin mutants that can only assemble K48- or K63-linked chains, allowing unequivocal identification of the type of chain assembled. Our results could demonstrate that ILK is modified by both K48 and K63 polyubiquitin chains. K48-linked chains target proteins to degradation, whereas K63-linked chains often regulate protein function or localization. Therefore this result suggests

that ubiquitination of ILK might have several functional outcomes, depending on the type of chain assembled.

4.2. Fibroblasts carrying a K341R mutation in ILK display reduced migration

As a central scaffold linking integrin to actin cytoskeleton, ILK is important for migration of fibroblasts as well as several other cell types (Grashoff, Aszodi et al. 2003; Sakai, Li et al. 2003). Therefore, in order to elucidate the potential role of ubiquitination at K341 in processes regulated by ILK, migration assays were performed. These assays were performed in a 3D environment as this provides more physiological and in vivo relevant mode of cell migration compared to 2D (Rhee 2009; Harunaga and Yamada 2011). In addition a 1D environment was used as a simplified model for 3D topology (Doyle, Kutys et al. 2012). Both of these assays demonstrated a reduction in migration of ILK-K341R expressing fibroblasts as measured by velocity and distance compared to the ILK-wt expressing cells. This led to the initial conclusion that the ubiquitination of ILK at this particular lysine, or other potential functions of this lysine is important for fibroblast migration

4.2.1. Fibroblasts carrying a K341R mutation show altered turnover of ILK in FAs

This study employed new approach to investigate the turnover of proteins in FAs in a1D environment that can be used as a simplified model for cell behavior in 3D environment. In agreement with previous reports showing increased stability of FAs in 1D and 3D compared to a 2D environment ,this study could demonstrate a slow overall turnover rate of ILK protein in FAs of cells seeded in 1D fibronectin functionalized micropatterned lines (Doyle, Wang et al. 2009; Doyle, Kutys et al. 2012). Furthermore, this suggested that ubiquitination of ILK at K341 might be important for the stability of ILK in FAs. The mutation of lysine 341 to arginine that abolished the ubiquitination of ILK at this site led to the significant decrease in the mobile fraction (M_f) and a concomitant increase in the immobile fraction (I_f) of ILK. As the migration of cells depends on the tight regulation of FA turnover, the increased stability of the mutant ILK might explain the reduced migration of the fibroblast expressing mutated ILK. Further studies are necessary to investigate of the précised role of this lysine in the function of ILK. Furthermore the

overall turnover of FAs should be examined to determine if K341R mutation influences the global rates of FA turnover.

In addition, this study could show K341 of ILK might be necessary for clathrin-mediated endocytosis. This is in agreement with studies performed on the myotendinous junction of D.melanogaster showing that integrins and ILK are endocytosed in clathrin and Rab5 dependant manner and that this is important for the remodeling of the myotendinous junction and muscle function. One could speculate that ILK is regulated in a similar manned in mammals. It has been already demonstrated that mammalian muscles express high levels of ILK and that ILK is important for the maintenance of the murine myotendinous junction (Wang, Chang et al. 2008). Additional studies are required to determine K341 and the ubiquitination of ILK are involved in the maintenance of myotendinous junction in mammals.

4.2.2. Lysine 431 is dispensable for ILK ubiquitination

Using a retroviral construct a stable cell lines expressing either wt ILK-Flag or the K341R-Flag mutant were generated. The in vivo ubiquitination assay failed to show any difference in the ubiquitination pattern of wt and mutant ILK, indicating that lysine 341 is dispensable for ILK ubiquitination. This was not surprising as it is has been shown that ubiquitination is rarely specific for a particular lysine. Because of this known lack of specificity we decided not to attempt to identify additional lysines that might act as ubiquitin acceptors on ILK.

This result is in stark contrast to the data obtained by transient transfection of the cells. It is possible that the variation in expression levels between wt and mutant ILK in the transient transfection experiments might explain the observed differences in the ubiquitination levels of the two proteins. Precise control of protein levels is not possible in transient transfection experiments. It is also possible that the unphysiological overexpression of ILK protein that is often a consequence of transient transfection led to the saturation of ILK in FAs and subsequent accumulation of excess ILK in the cytoplasm, leading to abnormal patterns of ubiquitination. Unfortunately this issue remains unresolved thereby fundamentally questioning the interpretation of the migration, turnover and endocytosis data shown in this study. It might be possible that ubiquitination of ILK at this particular lysine provides a docking site for a potential adaptor for endocytosis, regardless of compensatory ubiquitination at other lysine sites. However, we

can also not fully exclude that the observed defects in migration and turnover in cells expressing the K341R mutant ILK could be cell culture artifacts. It should, however, be noted that two independent pairs of cell lines were generated, one pair expressing Flag-tagged mutant and wt ILK, and one pair expressing GFP-tagged mutant and wt ILK. In addition, both mixed populations and single cell clones were analyzed, and the defects were consistently observed. However, as no change in ubiquitination between wt and K341R ILK was observed, and no interaction partners that would fail to bind K341R mutant ILK were detected, it was beyond the scope of this study to resolve this controversy.

4.3. CHIP is a novel interacting partner of ILK

To further characterize this posttranslational modification we were prompted to identify the E3 ligase responsible for it. Therefore a mass spectrometry screen was performed where immunoprecipitates from wt ILK-Flag cells were compared to the ILK fl/fl negative control in order to identify specific binders as well as to immunoprecipitates from K341R-Flag cells in order to identify partners that would interact with lysine 341. This analysis was successful as all major known binding partners of ILK such as Pinch-1, α-parvin, β-parvin and RSU-1 were identified. There was, however, no significant difference in the interactome of wt versus K341R mutant ILK. Importantly the screen revealed significant binding of ILK to a chaperone complex consisting of Hsp70 and Hsp90. In addition, we could identify the E3 ligase CHIP as a major interaction. This was the only E3 ligase that was identified as a statistically significant interactor in this screen. The fact that it acts in co-operation with Hsp90 and Hsp70, also detected in the screen, further increased the probability that this hit was specific. Therefore further investigation of the ILK-CHIP interaction was carried out. As the detection of CHIP in the co-immunoprecipitate from ILK-Flag cells also by western blotting was possible, conclusion could be made that CHIP is a new interacting partner of ILK.

4.3.1. Characterization of ILK-CHIP interaction

In order to characterize this novel interaction in more detail the domains of CHIP mediating the interaction were investigated. To this end different truncation mutants of CHIP containing either the Ubox or the TPR domain as well as two full-length point mutants abolishing the interaction with Hsp70 (CHIP-K30A) or the ubiquitin ligase

function of CHIP (CHIP-H260Q) were cloned. The co-immunoprecipitation of ILK in cells expressing the various CHIP constructs showed that ILK binds very strongly to the Ubox domain and that this interaction is even stronger that the interaction with full-length CHIP. This can be explained by structural studies of CHIP showing that it is an asymmetrical dimer (Schulman and Chen 2005). The structure of CHIP reveals that only one of the Ubox domains is exposed at the protein surface while the other one is buried underneath the TPR domain. Therefore, the functional CHIP dimer has two TPR domains but only one Ubox domain exposed at the surface (Schulman and Chen 2005). The deletion of the TPR domain and expression of Ubox domain only gives rise to additional binding sites that are absent in the full length CHIP dimer. Furthermore, the reduction of ILK binding to the CHIP-K30A mutant was observed. As this mutation abolishes the interaction of CHIP with Hsp70 it is likely that the interaction of CHIP and ILK is stabilized by Hsp70. This further implies that the CHIP-ILK interaction is indeed part of a larger complex involving molecular chaperones.

In vitro binding experiments with recombinant additionally showed that the interaction between ILK and CHIP is direct. The binding under our experimental conditions was, however, relatively weak. Therefore it does not exclude the possibility that Hsp70 could strengthen the interaction. The role of Hsp70 in this interaction should be addressed in more detail in future studies.

4.4. CHIP and ILK co-localize in mature focal adhesions

This study could demonstrate the partial co-localization of endogenous CHIP and ILK proteins in focal adhesions. The localization of CHIP to focal adhesions was, however, not dependent on ILK, as CHIP was found in adhesions also in ILK -/- cells. In addition to partially localizing to adhesions, CHIP was found to co-localize with actin stress fibers. This pattern of localization differs from previous studies where CHIP has been shown to have a diffuse cytoplasmic staining pattern (Dai, Zhang et al. 2003). These differences could arise from different cell fixation methods as well as different antibodies used in the stainings. Importantly, this study could demonstrate that the CHIP-GFP fusion protein also localizes to adhesions and stress fibers, providing additional support that CHIP indeed localizes to these structures. Interestingly, CHIP localization was found to be independent of ILK. This led to the hypothesis that CHIP could localize to adhesions and stress fibers by interacting directly with polymerized actin. This hypothesis was

confirmed by using co-sedimentation assays with recombinant CHIP and polymerized actin. This provides a putative mechanism for the localization of CHIP.

The process of adhesion maturation from nascent adhesions to focal complexes and focal adhesions as well as fibrillar adhesions depends on actin polymerization (Vicente-Manzanares and Horwitz 2011). Therefore co-localization of CHIP and ILK was investigated to determine the dependency of this co-localization on the maturation status of matrix adhesions and on stress fiber formation. Immunofluorescence analyses of CHIP during the various stages of cell spreading confirmed that CHIP localizes to mature focal adhesions. Taken together the conclusion could be made that ILK and CHIP co-localize only in mature focal adhesions that this co-localization depends on actin stress fiber formation. This data fits to the observation of others that CHIP is part of the chaperone machinery for cytoskeletal proteins such as myosin and filamin (Nyamsuren, Faggionato et al. 2007; Arndt, Dick et al. 2010).

4.5. CHIP is an E3 ligase ubiquitinating ILK

CHIP is a E3 ubiquitin ligase involved in ubiquitination of a wide range of proteins (Dickey, Patterson et al. 2007). As CHIP was the only E3 ligase present in the ILK interactome, it was a likely candidate for the E3 ligase responsible for ubiquitinating ILK. This study demonstrated that CHIP ubiquitinates ILK in vitro in a dose dependant manner. In addition, it could be observed that in vitro ubiquitination of ILK occurs only in presence of wt CHIP and not CHIP-H260Q ligase dead mutant. These observations lead to the conclusion that ILK can be ubiquitinated by CHIP in vitro. However, the in vitro ubiquitination studies have to be taken with some caution as they involve high concentrations of recombinant proteins and thus can give false positive results. Therefore it was necessary to address this question in an in vivo experiment as well. Despite a wide range of substrates, in most cases CHIP has been shown to be redundant and the ubiquitination is often compensated by other E3 ligases (Morishima, Wang et al. 2008; Taipale, Jarosz et al. 2010). Therefore, to avoid potential redundancy, overexpression studies were performed to address whether CHIP is capable of ubiquitinating ILK in vivo. Overexpression of CHIP in CHO cells led to a robust increase in ILK ubiquitination, whereas the ligase dead mutant did not display this effect. Taken together these results allow the conclusion that ILK is an in vivo target of CHIP ubiquitination.

4.6. ILK is degraded by both proteasome and lysosome

K48-linked polyubiquitin chains target proteins for proteasomal degradation (Adhikari and Chen 2009), while the K63-linked polyubiquitin chain has been implicated in selective autophagy (Kirkin, Lamark et al. 2009; Clague and Urbe 2010). CHIP can catalyze the formation of several different polyubiquitin chains, depending on the E2 ligase interaction. For example, when interacting with UbcH5a CHIP forms K48-linked polyubiquitin chains, while interaction with Ubc13/Uve1 leads to formation of K63-linked polyubiquitin chains (Zhang, Windheim et al. 2005). This study revealed that ILK can contain both K48- and K63-linked polyubiquitin chains. Therefore the obvious question was which degradation pathway regulates ILK. There are several lines of evidence that suggest that ILK can be degraded both via the proteasome and via the lysosome. First, treatment of cells with MG132, a proteasomal inhibitor, lead to a reduction of ILK levels, which was contrary to the expected increase in ILK levels if ILK would have been targeted exclusively to the proteasome. The ubiquitin-proteasome system and the autophagy-lysosome system are synergistic, cooperative and complementary systems working to maintain cellular homeostasis (Chen and Yin 2011). It has been demonstrated that autophagy can be activated by proteasomal inhibition (Ding, Ni et al. 2007). Therefore it is possible that the reduction of the ILK protein levels after the proteasomal inhibition is due to the activation of autophagy-lysosome system. Second, it was observed that starvation of cells leads to faster turnover of ILK protein. As starvation has been shown to activate autophagy, it supports the conclusion that ILK is degraded by the autophagy-lysosome system. Third, however, blocking the proteasome in the presence of CHX that inhibits protein synthesis inhibited the degradation of ILK more efficiently than blocking the lysosome. Taken together the conclusion could be made that ILK can be degraded by both machineries and the pathway used might depend on the cellular context and the type of ubiquitin chain.

Components of the IPP complex depend on the integrity of the complex for their stability. For example, in the absence of ILK, PINCH and parvin are degraded by the proteasome (ref). It would therefore be of interest to analyze whether this proteasomal degradation involves CHIP-mediated ubiquitination.

4.7. Hsp90 interaction protects ILK from CHIP ubiquitination

CHIP is involved in the triage decision between refolding and degradation of misfolded proteins. This mechanism includes the interaction of CHIP with the chaperones Hsp70 and Hsp90. Therefore, it was investigated whether ILK degradation is regulated by its interaction with Hsp90 and Hsp70, as these proteins were also detected in the interactome screen. Treatment of cells with the Hsp90 inhibitor 17AAG led to an almost complete depletion of ILK protein. Therefore, the conclusion could be made that ILK is Hsp90 client protein in mouse fibroblasts. This is in line with the literature demonstrating ILK interaction with Hsp90 protein in HEK 293T, human fibrosarcoma HT1080 and COS-7 cells (Aoyagi, Fujita et al. 2005). Here it would be interesting to note that may of the Hsp90 clients are kinases such as v-Src (Wayne, Mishra et al. 2011). It is possible that kinase-like domain of ILK, although lacking the structural flexibility essential for kinase activity (Fukuda, Gupta et al. 2009) allows the interaction with Hsp90 as a client protein. Interestingly, the depletion of ILK in response to Hsp90 inhibition was comparable to the effect of blocking protein synthesis by CHX treatment, suggesting that the entire cellular pool of ILK might require Hsp90 for its stability.

4.7.1. Hsp90 inhibition leads to the proteasomal degradation of ILK

As ILK degradation induced by Hsp90 inhibition could be successfully rescued by proteasomal inhibitor MG132 but not by the lysosomal inhibitor bafilomycin, the conclusion could be made that inhibition of Hsp90 leads to proteasomal and not lysosomal degradation of ILK. In addition, the ILK protein levels could be partially rescued by deletion of CHIP as demonstrated by Hsp90 inhibition in CHIP-/- cells. This suggests that Hsp90 promotes folding of ILK and thereby protects it from ubiquitination by CHIP and subsequent proteasomal degradation. This hypothesis is further supported by co-immunoprecipitation experiments in 17AAG-treated cells. The interaction between ILK and CHIP is increased upon inhibition of Hsp90. Interestingly, the interaction of ILK with its key binding partner α-parvin is reduced, implying that Hsp90 might promote the formation of the IPP complex, or alternatively stabilize it after it has formed. In fact, Hsp90 has been shown to stabilize several multiprotein complexes, for example by folding and thereby stabilizing a core component of a protein complex (Taipale, Jarosz et

al. 2010). Whether Hsp90 indeed has this function for the IPP complex as well, remains a task for future studies.

4.8. Ubiquitination and degradation of ILK impairs fibroblast migration

ILK is a central scaffold linking integrins with the actin cytoskeleton. It has been shown to be essential for cell migration in fibroblasts as well as several other cell types (Grashoff, Aszodi et al. 2003; Sakai, Li et al. 2003). In recent years also E3 ligases and ubiquitination have been implicated in the regulation of cell adhesion dynamics and migration. It has been demonstrated that various E3 ligases, via ubiquitination of numerous components of focal adhesions and the actin cytoskeleton, can tune the cell migration machinery through regulation of actin polymerization, adhesion dynamics and cell polarization (Huang 2010). Therefore, one of the aims of this study was to investigate the influence of ILK ubiquitination and subsequent degradation on fibroblast migration. To this end migration assays in 3D collagen gels were performed, as these provide more in vivo-like conditions than migration assays performed in 2D (Hakkinen, Harunaga et al. 2011; Harunaga and Yamada 2011). These assays revealed a dramatically reduced migration velocity and distance of ILK -/- fibroblasts compared to ILK fl/fl cells. Interestingly, ILK fl/fl fibroblasts treated with the Hsp90 inhibitor 17AAG displayed a similar migratory defect as the ILK -/- cells. These data clearly demonstrate that inhibition of Hsp90 leads to impaired fibroblast migration. This might occur through destabilization of ILK and subsequent ubiquitination and proteasomal degradation of the protein. At this point it cannot, however, be excluded that destabilization of other Hsp90 clients could also play a role in the observed migration defect.

Interestingly, many adhesion molecules including ILK, are overexpressed in different hematological and solid malignancies (Schmidmaier and Baumann 2008). It has been proposed that this overexpression of adhesion molecules mediates drug resistance (CAM-DR) in certain malignancies such as multiple myelomas, lymphomas, acute and chronic leukemia as well as pancreatic cancer, breast cancer, colorectal carcinoma, neuroblastoma, small cell and non-small cell lung cancer among the solid tumors (Schmidmaier and Baumann 2008). Therefore, destabilizing ILK and the IPP complex by 17AAG would be a very interesting potential anti-adhesion therapy in different

hematopoietic and solid malignancies. ILK plays a role also in fibrosis of the kidney, liver and lung through a process highly resembling the epithelial-mesenchymal transition (EMT) that leads to accumulation of fibroblasts and myofibroblasts in the tissue (Li, Yang et al. 2003; Zhang, Ikegami et al. 2006; Kavvadas, Kypreou et al. 2010). Therefore it might be of interest to explore the antifibrotic effect of 17AAG in these tissues.

5. Curriculum Vitae

Dipl. Mol. Biol. Korana Radovanac

Date of birth: June 10th, 1982

Place of birth: Belgrade, Serbia

Nationality: Serbian

EDUCATION

2007-2012 **PhD Studies** at Ludwig Maximilians University Munich, Germany
PhD work with Prof. Dr. Reinhard Fässler Dept. of Molecular Medicine,
Max Planck Institute of Biochemistry, Martinsried, Germany
PhD Thesis: ``Regulation of Integrin-Linked Kinase (ILK) by Hsp 90 and E3 Ligase CHIP´´

2001-2007 **Diploma Studies** in Molecular Biology and Physiology, University of Belgrade
Faculty of Biology, Course of Experimental Biomedicine
Average grade: 9.26 (lowest passing grade 6, highest 10)
Diploma Thesis work with Dr. Mirjana Brankovic-Magic,
Institute for Oncology and Radiology of Serbia, National Cancer Research Center, Belgrade, Serbia
Diploma Thesis: ``Polymorphisms of p53 tumor-suppressor gene at codon 72 in the patients with cervical cancer´´

1997-2001 **High School Matura** at Tenth Belgrade High School ``Mihajlo Pupin´´, Belgrade, Finished with the highest honors
Matura Thesis: ``Human hereditary diseases´´

PUBLICATIONS

Widmaier M, Rognoni M, Radovanac K, Azimifar SB, Fässler R., Integrin-linked kinase (ILK) at the glance. J Cell Sci. 2012

Wickström SA, Radovanac K, Fässler R., Genetic analyses of integrin signaling. Cold Spring Harb Perspect Biol. 2011 Feb 1; 3(2).

6. References

Adhikari, A. and Z. J. Chen (2009). "Diversity of polyubiquitin chains." Dev Cell **16**(4): 485-486.

Alexandrova, A. Y., K. Arnold, et al. (2008). "Comparative dynamics of retrograde actin flow and focal adhesions: formation of nascent adhesions triggers transition from fast to slow flow." PLoS One **3**(9): e3234.

Alon, R. and K. Ley (2008). "Cells on the run: shear-regulated integrin activation in leukocyte rolling and arrest on endothelial cells." Curr Opin Cell Biol **20**(5): 525-532.

Aoyagi, Y., N. Fujita, et al. (2005). "Stabilization of integrin-linked kinase by binding to Hsp90." Biochem Biophys Res Commun **331**(4): 1061-1068.

Arnaout, M. A., B. Mahalingam, et al. (2005). "Integrin structure, allostery, and bidirectional signaling." Annu Rev Cell Dev Biol **21**: 381-410.

Arndt, V., C. Daniel, et al. (2005). "BAG-2 acts as an inhibitor of the chaperone-associated ubiquitin ligase CHIP." Mol Biol Cell **16**(12): 5891-5900.

Arndt, V., N. Dick, et al. (2010). "Chaperone-assisted selective autophagy is essential for muscle maintenance." Curr Biol **20**(2): 143-148.

Azioune, A., M. Storch, et al. (2009). "Simple and rapid process for single cell micro-patterning." Lab Chip **9**(11): 1640-1642.

Baharloo, B., M. Textor, et al. (2005). "Substratum roughness alters the growth, area, and focal adhesions of epithelial cells, and their proximity to titanium surfaces." J Biomed Mater Res A **74**(1): 12-22.

Ballestrem, C., N. Erez, et al. (2006). "Molecular mapping of tyrosine-phosphorylated proteins in focal adhesions using fluorescence resonance energy transfer." J Cell Sci **119**(Pt 5): 866-875.

Ballestrem, C., B. Hinz, et al. (2001). "Marching at the front and dragging behind: differential alphaVbeta3-integrin turnover regulates focal adhesion behavior." J Cell Biol **155**(7): 1319-1332.

Ballinger, C. A., P. Connell, et al. (1999). "Identification of CHIP, a novel tetratricopeptide repeat-containing protein that interacts with heat shock proteins and negatively regulates chaperone functions." Mol Cell Biol **19**(6): 4535-4545.

Barczyk, M., S. Carracedo, et al. (2010). "Integrins." Cell Tissue Res **339**(1): 269-280.

Baudoin, C., M. J. Goumans, et al. (1998). "Knockout and knockin of the beta1 exon D define distinct roles for integrin splice variants in heart function and embryonic development." Genes Dev **12**(8): 1202-1216.

Beattie, J., L. McIntosh, et al. (2010). "Cross-talk between the insulin-like growth factor (IGF) axis and membrane integrins to regulate cell physiology." J Cell Physiol **224**(3): 605-611.

Behrends, C. and J. W. Harper (2011). "Constructing and decoding unconventional ubiquitin chains." Nat Struct Mol Biol **18**(5): 520-528.

Berrier, A. L. and K. M. Yamada (2007). "Cell-matrix adhesion." J Cell Physiol **213**(3): 565-573.

Bix, G. and R. V. Iozzo (2005). "Matrix revolutions: "tails" of basement-membrane components with angiostatic functions." Trends Cell Biol **15**(1): 52-60.

Bokel, C. and N. H. Brown (2002). "Integrins in development: moving on, responding to, and sticking to the extracellular matrix." Dev Cell **3**(3): 311-321.

Bouvard, D., C. Brakebusch, et al. (2001). "Functional consequences of integrin gene mutations in mice." Circ Res **89**(3): 211-223.

Braun, A., R. Bordoy, et al. (2003). "PINCH2 is a new five LIM domain protein, homologous to PINCHand localized to focal adhesions." Exp Cell Res **284**(2): 239-250.

Broussard, J. A., D. J. Webb, et al. (2008). "Asymmetric focal adhesion disassembly in motile cells." Curr Opin Cell Biol **20**(1): 85-90.

Brown, M. C. and C. E. Turner (2004). "Paxillin: adapting to change." Physiol Rev **84**(4): 1315-1339.

Cabodi, S., M. del Pilar Camacho-Leal, et al. (2010). "Integrin signalling adaptors: not only figurants in the cancer story." Nat Rev Cancer **10**(12): 858-870.

Cabodi, S., L. Moro, et al. (2004). "Integrin regulation of epidermal growth factor (EGF) receptor and of EGF-dependent responses." Biochem Soc Trans **32**(Pt3): 438-442.
Cadwell, K. and L. Coscoy (2005). "Ubiquitination on nonlysine residues by a viral E3 ubiquitin ligase." Science **309**(5731): 127-130.
Calderwood, D. A., Y. Fujioka, et al. (2003). "Integrin beta cytoplasmic domain interactions with phosphotyrosine-binding domains: a structural prototype for diversity in integrin signaling." Proc Natl Acad Sci U S A **100**(5): 2272-2277.
Campbell, I. D. and M. J. Humphries (2011). "Integrin structure, activation, and interactions." Cold Spring Harb Perspect Biol **3**(3).
Carman, C. V. (2012). "Overview: imaging in the study of integrins." Methods Mol Biol **757**: 159-189.
Carragher, N. O., B. Levkau, et al. (1999). "Degraded collagen fragments promote rapid disassembly of smooth muscle focal adhesions that correlates with cleavage of pp125(FAK), paxillin, and talin." J Cell Biol **147**(3): 619-630.
Caswell, P. T., S. Vadrevu, et al. (2009). "Integrins: masters and slaves of endocytic transport." Nat Rev Mol Cell Biol **10**(12): 843-853.
Chao, W. T. and J. Kunz (2009). "Focal adhesion disassembly requires clathrin-dependent endocytosis of integrins." FEBS Lett **583**(8): 1337-1343.
Chen, W. T., E. Hasegawa, et al. (1985). "Development of cell surface linkage complexes in cultured fibroblasts." J Cell Biol **100**(4): 1103-1114.
Chen, W. T. and S. J. Singer (1982). "Immunoelectron microscopic studies of the sites of cell-substratum and cell-cell contacts in cultured fibroblasts." J Cell Biol **95**(1): 205-222.
Chen, X. and X. M. Yin (2011). "Coordination of autophagy and the proteasome in resolving endoplasmic reticulum stress." Vet Pathol **48**(1): 245-253.
Chiswell, B. P., R. Zhang, et al. (2008). "The structural basis of integrin-linked kinase-PINCH interactions." Proc Natl Acad Sci U S A **105**(52): 20677-20682.
Choi, C. K., M. Vicente-Manzanares, et al. (2008). "Actin and alpha-actinin orchestrate the assembly and maturation of nascent adhesions in a myosin II motor-independent manner." Nat Cell Biol **10**(9): 1039-1050.
Chu, H., I. Thievessen, et al. (2006). "gamma-Parvin is dispensable for hematopoiesis, leukocyte trafficking, and T-cell-dependent antibody response." Mol Cell Biol **26**(5): 1817-1825.
Ciechanover, A. (1994). "The ubiquitin-proteasome proteolytic pathway." Cell **79**(1): 13-21.
Ciechanover, A. (2005). "Proteolysis: from the lysosome to ubiquitin and the proteasome." Nat Rev Mol Cell Biol **6**(1): 79-87.
Clague, M. J. and S. Urbe (2010). "Ubiquitin: same molecule, different degradation pathways." Cell **143**(5): 682-685.
Cluzel, C., F. Saltel, et al. (2005). "The mechanisms and dynamics of (alpha)v(beta)3 integrin clustering in living cells." J Cell Biol **171**(2): 383-392.
Conaway, R. C., C. S. Brower, et al. (2002). "Emerging roles of ubiquitin in transcription regulation." Science **296**(5571): 1254-1258.
Dai, Q., C. Zhang, et al. (2003). "CHIP activates HSF1 and confers protection against apoptosis and cellular stress." EMBO J **22**(20): 5446-5458.
Dickey, C. A., C. Patterson, et al. (2007). "Brain CHIP: removing the culprits in neurodegenerative disease." Trends Mol Med **13**(1): 32-38.
Ding, W. X., H. M. Ni, et al. (2007). "Linking of autophagy to ubiquitin-proteasome system is important for the regulation of endoplasmic reticulum stress and cell viability." Am J Pathol **171**(2): 513-524.
Dobreva, I., A. Fielding, et al. (2008). "Mapping the integrin-linked kinase interactome using SILAC." J Proteome Res **7**(4): 1740-1749.
Dourdin, N., A. K. Bhatt, et al. (2001). "Reduced cell migration and disruption of the actin cytoskeleton in calpain-deficient embryonic fibroblasts." J Biol Chem **276**(51): 48382-48388.
Doyle, A. D., M. L. Kutys, et al. (2012). "Micro-environmental control of cell migration - myosin IIA is required for efficient migration in fibrillar environments through control of cell adhesion dynamics." J Cell Sci **125**(Pt 9): 2244-2256.

Doyle, A. D., F. W. Wang, et al. (2009). "One-dimensional topography underlies three-dimensional fibrillar cell migration." J Cell Biol **184**(4): 481-490.

Ezratty, E. J., C. Bertaux, et al. (2009). "Clathrin mediates integrin endocytosis for focal adhesion disassembly in migrating cells." J Cell Biol **187**(5): 733-747.

Ezratty, E. J., M. A. Partridge, et al. (2005). "Microtubule-induced focal adhesion disassembly is mediated by dynamin and focal adhesion kinase." Nat Cell Biol **7**(6): 581-590.

Fielding, A. B., I. Dobreva, et al. (2008). "Beyond focal adhesions: integrin-linked kinase associates with tubulin and regulates mitotic spindle organization." Cell Cycle **7**(13): 1899-1906.

Franco, S. J., M. A. Rodgers, et al. (2004). "Calpain-mediated proteolysis of talin regulates adhesion dynamics." Nat Cell Biol **6**(10): 977-983.

Fukuda, K., S. Gupta, et al. (2009). "The pseudoactive site of ILK is essential for its binding to alpha-Parvin and localization to focal adhesions." Mol Cell **36**(5): 819-830.

Fukuda, K., J. D. Knight, et al. (2011). "Biochemical, proteomic, structural, and thermodynamic characterizations of integrin-linked kinase (ILK): cross-validation of the pseudokinase." J Biol Chem **286**(24): 21886-21895.

Fukuda, T., K. Chen, et al. (2003). "PINCH-1 is an obligate partner of integrin-linked kinase (ILK) functioning in cell shape modulation, motility, and survival." J Biol Chem **278**(51): 51324-51333.

Geiger, B., A. Bershadsky, et al. (2001). "Transmembrane crosstalk between the extracellular matrix--cytoskeleton crosstalk." Nat Rev Mol Cell Biol **2**(11): 793-805.

Geiger, B. and K. M. Yamada (2011). "Molecular architecture and function of matrix adhesions." Cold Spring Harb Perspect Biol **3**(5).

Giancotti, F. G. and E. Ruoslahti (1999). "Integrin signaling." Science **285**(5430): 1028-1032.

Giannone, G., B. J. Dubin-Thaler, et al. (2007). "Lamellipodial actin mechanically links myosin activity with adhesion-site formation." Cell **128**(3): 561-575.

Gimona, M., K. Djinovic-Carugo, et al. (2002). "Functional plasticity of CH domains." FEBS Lett **513**(1): 98-106.

Glading, A., D. A. Lauffenburger, et al. (2002). "Cutting to the chase: calpain proteases in cell motility." Trends Cell Biol **12**(1): 46-54.

Grashoff, C., A. Aszodi, et al. (2003). "Integrin-linked kinase regulates chondrocyte shape and proliferation." EMBO Rep **4**(4): 432-438.

Hakkinen, K. M., J. S. Harunaga, et al. (2011). "Direct comparisons of the morphology, migration, cell adhesions, and actin cytoskeleton of fibroblasts in four different three-dimensional extracellular matrices." Tissue Eng Part A **17**(5-6): 713-724.

Han, J., C. J. Lim, et al. (2006). "Reconstructing and deconstructing agonist-induced activation of integrin alphaIIbbeta3." Curr Biol **16**(18): 1796-1806.

Hanks, S. K. and T. Hunter (1995). "Protein kinases 6. The eukaryotic protein kinase superfamily: kinase (catalytic) domain structure and classification." FASEB J **9**(8): 576-596.

Hannigan, G. E., J. G. Coles, et al. (2007). "Integrin-linked kinase at the heart of cardiac contractility, repair, and disease." Circ Res **100**(10): 1408-1414.

Hannigan, G. E., C. Leung-Hagesteijn, et al. (1996). "Regulation of cell adhesion and anchorage-dependent growth by a new beta 1-integrin-linked protein kinase." Nature **379**(6560): 91-96.

Hannigan, G. E., P. C. McDonald, et al. (2011). "Integrin-linked kinase: not so 'pseudo' after all." Oncogene **30**(43): 4375-4385.

Harunaga, J. S. and K. M. Yamada (2011). "Cell-matrix adhesions in 3D." Matrix Biol **30**(7-8): 363-368.

Hochstrasser, M. (2009). "Origin and function of ubiquitin-like proteins." Nature **458**(7237): 422-429.

Hoege, C., B. Pfander, et al. (2002). "RAD6-dependent DNA repair is linked to modification of PCNA by ubiquitin and SUMO." Nature **419**(6903): 135-141.

Huang, C. (2010). "Roles of E3 ubiquitin ligases in cell adhesion and migration." Cell Adh Migr **4**(1): 10-18.

Huang, C., Z. Rajfur, et al. (2009). "Talin phosphorylation by Cdk5 regulates Smurf1-mediated talin head ubiquitylation and cell migration." Nat Cell Biol **11**(5): 624-630.
Humphries, J. D., A. Byron, et al. (2006). "Integrin ligands at a glance." J Cell Sci **119**(Pt 19): 3901-3903.
Humphries, M. J. (2000). "Integrin structure." Biochem Soc Trans **28**(4): 311-339.
Hurley, J. H. and S. D. Emr (2006). "The ESCRT complexes: structure and mechanism of a membrane-trafficking network." Annu Rev Biophys Biomol Struct **35**: 277-298.
Huttenlocher, A. and A. R. Horwitz (2011). "Integrins in cell migration." Cold Spring Harb Perspect Biol **3**(9): a005074.
Huttenlocher, A., S. P. Palecek, et al. (1997). "Regulation of cell migration by the calcium-dependent protease calpain." J Biol Chem **272**(52): 32719-32722.
Hynes, R. O. (2002). "Integrins: bidirectional, allosteric signaling machines." Cell **110**(6): 673-687.
Hynes, R. O. and A. T. Destree (1978). "Relationships between fibronectin (LETS protein) and actin." Cell **15**(3): 875-886.
Hynes, R. O. and Q. Zhao (2000). "The evolution of cell adhesion." J Cell Biol **150**(2): F89-96.
Ikeda, F., N. Crosetto, et al. (2010). "What determines the specificity and outcomes of ubiquitin signaling?" Cell **143**(5): 677-681.
Ikeda, F. and I. Dikic (2008). "Atypical ubiquitin chains: new molecular signals. 'Protein Modifications: Beyond the Usual Suspects' review series." EMBO Rep **9**(6): 536-542.
Ito, S., Y. Takahara, et al. (2010). "The roles of two distinct regions of PINCH-1 in the regulation of cell attachment and spreading." Mol Biol Cell **21**(23): 4120-4129.
Johnson, M. S., N. Lu, et al. (2009). "Integrins during evolution: evolutionary trees and model organisms." Biochim Biophys Acta **1788**(4): 779-789.
Kaabeche, K., H. Guenou, et al. (2005). "Cbl-mediated ubiquitination of alpha5 integrin subunit mediates fibronectin-dependent osteoblast detachment and apoptosis induced by FGFR2 activation." J Cell Sci **118**(Pt 6): 1223-1232.
Kadrmas, J. L., M. A. Smith, et al. (2004). "The integrin effector PINCH regulates JNK activity and epithelial migration in concert with Ras suppressor 1." J Cell Biol **167**(6): 1019-1024.
Kannouche, P. L., J. Wing, et al. (2004). "Interaction of human DNA polymerase eta with monoubiquitinated PCNA: a possible mechanism for the polymerase switch in response to DNA damage." Mol Cell **14**(4): 491-500.
Kavvadas, P., K. P. Kypreou, et al. (2010). "Integrin-linked kinase (ILK) in pulmonary fibrosis." Virchows Arch **457**(5): 563-575.
Keane, M. M., O. M. Rivero-Lezcano, et al. (1995). "Cloning and characterization of cbl-b: a SH3 binding protein with homology to the c-cbl proto-oncogene." Oncogene **10**(12): 2367-2377.
Kerscher, O., R. Felberbaum, et al. (2006). "Modification of proteins by ubiquitin and ubiquitin-like proteins." Annu Rev Cell Dev Biol **22**: 159-180.
Kirkin, V., T. Lamark, et al. (2009). "A role for NBR1 in autophagosomal degradation of ubiquitinated substrates." Mol Cell **33**(4): 505-516.
Klionsky, D. J., H. Abeliovich, et al. (2008). "Guidelines for the use and interpretation of assays for monitoring autophagy in higher eukaryotes." Autophagy **4**(2): 151-175.
Kraft, C., M. Peter, et al. (2010). "Selective autophagy: ubiquitin-mediated recognition and beyond." Nat Cell Biol **12**(9): 836-841.
Kravtsova-Ivantsiv, Y. and A. Ciechanover (2012). "Non-canonical ubiquitin-based signals for proteasomal degradation." J Cell Sci **125**(Pt 3): 539-548.
Kundrat, L. and L. Regan (2010). "Balance between folding and degradation for Hsp90-dependent client proteins: a key role for CHIP." Biochemistry **49**(35): 7428-7438.
Kundrat, L. and L. Regan (2010). "Identification of residues on Hsp70 and Hsp90 ubiquitinated by the cochaperone CHIP." J Mol Biol **395**(3): 587-594.
LaLonde, D. P., M. C. Brown, et al. (2005). "Actopaxin interacts with TESK1 to regulate cell spreading on fibronectin." J Biol Chem **280**(22): 21680-21688.

LaLonde, D. P., M. Grubinger, et al. (2006). "CdGAP associates with actopaxin to regulate integrin-dependent changes in cell morphology and motility." Curr Biol **16**(14): 1375-1385.

Lammermann, T., B. L. Bader, et al. (2008). "Rapid leukocyte migration by integrin-independent flowing and squeezing." Nature **453**(7191): 51-55.

Lange, A., S. A. Wickstrom, et al. (2009). "Integrin-linked kinase is an adaptor with essential functions during mouse development." Nature **461**(7266): 1002-1006.

Lau, T. L., V. Dua, et al. (2008). "Structure of the integrin alphaIIb transmembrane segment." J Biol Chem **283**(23): 16162-16168.

Lau, T. L., A. W. Partridge, et al. (2008). "Structure of the integrin beta3 transmembrane segment in phospholipid bicelles and detergent micelles." Biochemistry **47**(13): 4008-4016.

Lawson, M. A. and F. R. Maxfield (1995). "Ca(2+)- and calcineurin-dependent recycling of an integrin to the front of migrating neutrophils." Nature **377**(6544): 75-79.

Lee, S., M. S. Kwon, et al. (2011). "Enhanced peptide quantification using spectral count clustering and cluster abundance." BMC Bioinformatics **12**: 423.

Legate, K. R. and R. Fassler (2009). "Mechanisms that regulate adaptor binding to beta-integrin cytoplasmic tails." J Cell Sci **122**(Pt 2): 187-198.

Legate, K. R., E. Montanez, et al. (2006). "ILK, PINCH and parvin: the tIPP of integrin signalling." Nat Rev Mol Cell Biol **7**(1): 20-31.

Legate, K. R., S. A. Wickstrom, et al. (2009). "Genetic and cell biological analysis of integrin outside-in signaling." Genes Dev **23**(4): 397-418.

Lele, T. P., C. K. Thodeti, et al. (2008). "Investigating complexity of protein-protein interactions in focal adhesions." Biochem Biophys Res Commun **369**(3): 929-934.

Li, S., R. Bordoy, et al. (2005). "PINCH1 regulates cell-matrix and cell-cell adhesions, cell polarity and cell survival during the peri-implantation stage." J Cell Sci **118**(Pt 13): 2913-2921.

Li, Y., J. Yang, et al. (2003). "Role for integrin-linked kinase in mediating tubular epithelial to mesenchymal transition and renal interstitial fibrogenesis." J Clin Invest **112**(4): 503-516.

Li, Z., M. K. Delaney, et al. (2010). "Signaling during platelet adhesion and activation." Arterioscler Thromb Vasc Biol **30**(12): 2341-2349.

Linder, S., D. Nelson, et al. (1999). "Wiskott-Aldrich syndrome protein regulates podosomes in primary human macrophages." Proc Natl Acad Sci U S A **96**(17): 9648-9653.

Liu, J., S. M. DeYoung, et al. (2003). "The roles of Cbl-b and c-Cbl in insulin-stimulated glucose transport." J Biol Chem **278**(38): 36754-36762.

Liu, S. and Z. J. Chen (2011). "Expanding role of ubiquitination in NF-kappaB signaling." Cell Res **21**(1): 6-21.

Lobert, V. H., A. Brech, et al. (2010). "Ubiquitination of alpha 5 beta 1 integrin controls fibroblast migration through lysosomal degradation of fibronectin-integrin complexes." Dev Cell **19**(1): 148-159.

Lorenz, K., C. Grashoff, et al. (2007). "Integrin-linked kinase is required for epidermal and hair follicle morphogenesis." J Cell Biol **177**(3): 501-513.

Lorenz, S., I. Vakonakis, et al. (2008). "Structural analysis of the interactions between paxillin LD motifs and alpha-parvin." Structure **16**(10): 1521-1531.

Mackinnon, A. C., H. Qadota, et al. (2002). "C. elegans PAT-4/ILK functions as an adaptor protein within integrin adhesion complexes." Curr Biol **12**(10): 787-797.

Majeski, A. E. and J. F. Dice (2004). "Mechanisms of chaperone-mediated autophagy." Int J Biochem Cell Biol **36**(12): 2435-2444.

Margadant, C., H. N. Monsuur, et al. (2011). "Mechanisms of integrin activation and trafficking." Curr Opin Cell Biol **23**(5): 607-614.

Margadant, C. and A. Sonnenberg (2010). "Integrin-TGF-beta crosstalk in fibrosis, cancer and wound healing." EMBO Rep **11**(2): 97-105.

McDonald, P. C., A. B. Fielding, et al. (2008). "Integrin-linked kinase--essential roles in physiology and cancer biology." J Cell Sci **121**(Pt 19): 3121-3132.

McDonough, H. and C. Patterson (2003). "CHIP: a link between the chaperone and proteasome systems." Cell Stress Chaperones **8**(4): 303-308.

Min, J. N., R. A. Whaley, et al. (2008). "CHIP deficiency decreases longevity, with accelerated aging phenotypes accompanied by altered protein quality control." Mol Cell Biol **28**(12): 4018-4025.

Mishima, W., A. Suzuki, et al. (2004). "The first CH domain of affixin activates Cdc42 and Rac1 through alphaPIX, a Cdc42/Rac1-specific guanine nucleotide exchanging factor." Genes Cells **9**(3): 193-204.

Montanez, E., S. Ussar, et al. (2008). "Kindlin-2 controls bidirectional signaling of integrins." Genes Dev **22**(10): 1325-1330.

Montanez, E., S. A. Wickstrom, et al. (2009). "Alpha-parvin controls vascular mural cell recruitment to vessel wall by regulating RhoA/ROCK signalling." EMBO J **28**(20): 3132-3144.

Morishima, Y., A. M. Wang, et al. (2008). "CHIP deletion reveals functional redundancy of E3 ligases in promoting degradation of both signaling proteins and expanded glutamine proteins." Hum Mol Genet **17**(24): 3942-3952.

Moser, M., M. Bauer, et al. (2009). "Kindlin-3 is required for beta2 integrin-mediated leukocyte adhesion to endothelial cells." Nat Med **15**(3): 300-305.

Moser, M., K. R. Legate, et al. (2009). "The tail of integrins, talin, and kindlins." Science **324**(5929): 895-899.

Moser, M., B. Nieswandt, et al. (2008). "Kindlin-3 is essential for integrin activation and platelet aggregation." Nat Med **14**(3): 325-330.

Murata, S., T. Chiba, et al. (2003). "CHIP: a quality-control E3 ligase collaborating with molecular chaperones." Int J Biochem Cell Biol **35**(5): 572-578.

Nikolopoulos, S. N. and C. E. Turner (2000). "Actopaxin, a new focal adhesion protein that binds paxillin LD motifs and actin and regulates cell adhesion." J Cell Biol **151**(7): 1435-1448.

Nikolopoulos, S. N. and C. E. Turner (2001). "Integrin-linked kinase (ILK) binding to paxillin LD1 motif regulates ILK localization to focal adhesions." J Biol Chem **276**(26): 23499-23505.

Nikolopoulos, S. N. and C. E. Turner (2002). "Molecular dissection of actopaxin-integrin-linked kinase-Paxillin interactions and their role in subcellular localization." J Biol Chem **277**(2): 1568-1575.

Nobes, C. D. and A. Hall (1995). "Rho, rac, and cdc42 GTPases regulate the assembly of multimolecular focal complexes associated with actin stress fibers, lamellipodia, and filopodia." Cell **81**(1): 53-62.

Nyamsuren, O., D. Faggionato, et al. (2007). "A mutation in CHN-1/CHIP suppresses muscle degeneration in Caenorhabditis elegans." Dev Biol **312**(1): 193-202.

Olski, T. M., A. A. Noegel, et al. (2001). "Parvin, a 42 kDa focal adhesion protein, related to the alpha-actinin superfamily." J Cell Sci **114**(Pt 3): 525-538.

Osley, M. A. (2006). "Regulation of histone H2A and H2B ubiquitylation." Brief Funct Genomic Proteomic **5**(3): 179-189.

Pankov, R., E. Cukierman, et al. (2000). "Integrin dynamics and matrix assembly: tensin-dependent translocation of alpha(5)beta(1) integrins promotes early fibronectin fibrillogenesis." J Cell Biol **148**(5): 1075-1090.

Parsons, J. T., A. R. Horwitz, et al. (2010). "Cell adhesion: integrating cytoskeletal dynamics and cellular tension." Nat Rev Mol Cell Biol **11**(9): 633-643.

Patterson, C. and S. Ronnebaum (2009). "Breast cancer quality control." Nat Cell Biol **11**(3): 239-241.

Pickart, C. M. and D. Fushman (2004). "Polyubiquitin chains: polymeric protein signals." Curr Opin Chem Biol **8**(6): 610-616.

Piper, R. C. and P. J. Lehner (2011). "Endosomal transport via ubiquitination." Trends Cell Biol **21**(11): 647-655.

Ponti, A., M. Machacek, et al. (2004). "Two distinct actin networks drive the protrusion of migrating cells." Science **305**(5691): 1782-1786.

Pratt, W. B., Y. Morishima, et al. (2010). "Proposal for a role of the Hsp90/Hsp70-based chaperone machinery in making triage decisions when proteins undergo oxidative and toxic damage." Exp Biol Med (Maywood) **235**(3): 278-289.

Ravid, T. and M. Hochstrasser (2004). "NF-kappaB signaling: flipping the switch with polyubiquitin chains." Curr Biol **14**(20): R898-900.
Ravid, T. and M. Hochstrasser (2007). "Autoregulation of an E2 enzyme by ubiquitin-chain assembly on its catalytic residue." Nat Cell Biol **9**(4): 422-427.
Rhee, S. (2009). "Fibroblasts in three dimensional matrices: cell migration and matrix remodeling." Exp Mol Med **41**(12): 858-865.
Riedl, J., A. H. Crevenna, et al. (2008). "Lifeact: a versatile marker to visualize F-actin." Nat Methods **5**(7): 605-607.
Rinnerthaler, G., B. Geiger, et al. (1988). "Contact formation during fibroblast locomotion: involvement of membrane ruffles and microtubules." J Cell Biol **106**(3): 747-760.
Sakai, T., S. Li, et al. (2003). "Integrin-linked kinase (ILK) is required for polarizing the epiblast, cell adhesion, and controlling actin accumulation." Genes Dev **17**(7): 926-940.
Santala, P. and J. Heino (1991). "Regulation of integrin-type cell adhesion receptors by cytokines." J Biol Chem **266**(34): 23505-23509.
Schmidmaier, R. and P. Baumann (2008). "ANTI-ADHESION evolves to a promising therapeutic concept in oncology." Curr Med Chem **15**(10): 978-990.
Schulman, B. A. and Z. J. Chen (2005). "Protein ubiquitination: CHIPping away the symmetry." Mol Cell **20**(5): 653-655.
Schwartz, M. A. and M. H. Ginsberg (2002). "Networks and crosstalk: integrin signalling spreads." Nat Cell Biol **4**(4): E65-68.
Shi, F., J. Harman, et al. (2010). "Collagen I matrix turnover is regulated by fibronectin polymerization." Am J Physiol Cell Physiol **298**(5): C1265-1275.
Shi, F. and J. Sottile (2008). "Caveolin-1-dependent beta1 integrin endocytosis is a critical regulator of fibronectin turnover." J Cell Sci **121**(Pt 14): 2360-2371.
Small, J. V. and I. Kaverina (2003). "Microtubules meet substrate adhesions to arrange cell polarity." Curr Opin Cell Biol **15**(1): 40-47.
Stanchi, F., C. Grashoff, et al. (2009). "Molecular dissection of the ILK-PINCH-parvin triad reveals a fundamental role for the ILK kinase domain in the late stages of focal-adhesion maturation." J Cell Sci **122**(Pt 11): 1800-1811.
Stankiewicz, M., R. Nikolay, et al. (2010). "CHIP participates in protein triage decisions by preferentially ubiquitinating Hsp70-bound substrates." FEBS J **277**(16): 3353-3367.
Strieter, E. R. and D. A. Korasick (2012). "Unraveling the complexity of ubiquitin signaling." ACS Chem Biol **7**(1): 52-63.
Suetsugu, S., T. Tezuka, et al. (2004). "Regulation of actin cytoskeleton by mDab1 through N-WASP and ubiquitination of mDab1." Biochem J **384**(Pt 1): 1-8.
Tagawa, A., A. Mezzacasa, et al. (2005). "Assembly and trafficking of caveolar domains in the cell: caveolae as stable, cargo-triggered, vesicular transporters." J Cell Biol **170**(5): 769-779.
Taipale, M., D. F. Jarosz, et al. (2010). "HSP90 at the hub of protein homeostasis: emerging mechanistic insights." Nat Rev Mol Cell Biol **11**(7): 515-528.
Takenawa, T. and H. Miki (2001). "WASP and WAVE family proteins: key molecules for rapid rearrangement of cortical actin filaments and cell movement." J Cell Sci **114**(Pt 10): 1801-1809.
Tarone, G., D. Cirillo, et al. (1985). "Rous sarcoma virus-transformed fibroblasts adhere primarily at discrete protrusions of the ventral membrane called podosomes." Exp Cell Res **159**(1): 141-157.
Thrower, J. S., L. Hoffman, et al. (2000). "Recognition of the polyubiquitin proteolytic signal." EMBO J **19**(1): 94-102.
Tripathi, V., A. Ali, et al. (2007). "CHIP chaperones wild type p53 tumor suppressor protein." J Biol Chem **282**(39): 28441-28454.
Tu, Y., Y. Huang, et al. (2001). "A new focal adhesion protein that interacts with integrin-linked kinase and regulates cell adhesion and spreading." J Cell Biol **153**(3): 585-598.
van der Flier, A. and A. Sonnenberg (2001). "Function and interactions of integrins." Cell Tissue Res **305**(3): 285-298.

Vaynberg, J., T. Fukuda, et al. (2005). "Structure of an ultraweak protein-protein complex and its crucial role in regulation of cell morphology and motility." Mol Cell **17**(4): 513-523.

Vicente-Manzanares, M. and A. R. Horwitz (2011). "Adhesion dynamics at a glance." J Cell Sci **124**(Pt 23): 3923-3927.

Vicente-Manzanares, M., M. A. Koach, et al. (2008). "Segregation and activation of myosin IIB creates a rear in migrating cells." J Cell Biol **183**(3): 543-554.

Vinogradova, O., T. Haas, et al. (2000). "A structural basis for integrin activation by the cytoplasmic tail of the alpha IIb-subunit." Proc Natl Acad Sci U S A **97**(4): 1450-1455.

Vinogradova, O., A. Velyvis, et al. (2002). "A structural mechanism of integrin alpha(IIb)beta(3) "inside-out" activation as regulated by its cytoplasmic face." Cell **110**(5): 587-597.

Wang, H. R., Y. Zhang, et al. (2003). "Regulation of cell polarity and protrusion formation by targeting RhoA for degradation." Science **302**(5651): 1775-1779.

Wang, H. V., L. W. Chang, et al. (2008). "Integrin-linked kinase stabilizes myotendinous junctions and protects muscle from stress-induced damage." J Cell Biol **180**(5): 1037-1049.

Wang, X., K. Fukuda, et al. (2008). "The structure of alpha-parvin CH2-paxillin LD1 complex reveals a novel modular recognition for focal adhesion assembly." J Biol Chem **283**(30): 21113-21119.

Wang, X., R. A. Herr, et al. (2007). "Ubiquitination of serine, threonine, or lysine residues on the cytoplasmic tail can induce ERAD of MHC-I by viral E3 ligase mK3." J Cell Biol **177**(4): 613-624.

Wayne, N., P. Mishra, et al. (2011). "Hsp90 and client protein maturation." Methods Mol Biol **787**: 33-44.

Wegener, K. L. and I. D. Campbell (2008). "Transmembrane and cytoplasmic domains in integrin activation and protein-protein interactions (review)." Mol Membr Biol **25**(5): 376-387.

Wegener, K. L., A. W. Partridge, et al. (2007). "Structural basis of integrin activation by talin." Cell **128**(1): 171-182.

Wehrle-Haller, B. (2007). "Analysis of integrin dynamics by fluorescence recovery after photobleaching." Methods Mol Biol **370**: 173-202.

Welchman, R. L., C. Gordon, et al. (2005). "Ubiquitin and ubiquitin-like proteins as multifunctional signals." Nat Rev Mol Cell Biol **6**(8): 599-609.

Wickstrom, S. A., A. Lange, et al. (2010). "Integrin-linked kinase controls microtubule dynamics required for plasma membrane targeting of caveolae." Dev Cell **19**(4): 574-588.

Widmaier, M., E. Rognoni, et al. (2012). "Integrin-linked kinase at a glance." J Cell Sci **125**(Pt 8): 1839-1843.

Wolfenson, H., A. Lubelski, et al. (2009). "A role for the juxtamembrane cytoplasm in the molecular dynamics of focal adhesions." PLoS One **4**(1): e4304.

Wong, E. and A. M. Cuervo (2010). "Integration of clearance mechanisms: the proteasome and autophagy." Cold Spring Harb Perspect Biol **2**(12): a006734.

Xie, P., Y. Fan, et al. (2009). "CHIP represses myocardin-induced smooth muscle cell differentiation via ubiquitin-mediated proteasomal degradation." Mol Cell Biol **29**(9): 2398-2408.

Xiong, J. P., T. Stehle, et al. (2001). "Crystal structure of the extracellular segment of integrin alpha Vbeta3." Science **294**(5541): 339-345.

Yamada, K. M., R. Pankov, et al. (2003). "Dimensions and dynamics in integrin function." Braz J Med Biol Res **36**(8): 959-966.

Yamaguchi, K., O. Ohara, et al. (2008). "Smurf1 directly targets hPEM-2, a GEF for Cdc42, via a novel combination of protein interaction modules in the ubiquitin-proteasome pathway." Biol Chem **389**(4): 405-413.

Yamaji, S., A. Suzuki, et al. (2002). "Possible role of ILK-affixin complex in integrin-cytoskeleton linkage during platelet aggregation." Biochem Biophys Res Commun **297**(5): 1324-1331.

Yamaji, S., A. Suzuki, et al. (2001). "A novel integrin-linked kinase-binding protein, affixin, is involved in the early stage of cell-substrate interaction." J Cell Biol **153**(6): 1251-1264.

Yang, Y., X. Wang, et al. (2009). "Structural basis of focal adhesion localization of LIM-only adaptor PINCH by integrin-linked kinase." J Biol Chem **284**(9): 5836-5844.

Yuan, L., M. J. Fairchild, et al. (2010). "Analysis of integrin turnover in fly myotendinous junctions." J Cell Sci **123**(Pt 6): 939-946.

Zaidel-Bar, R., C. Ballestrem, et al. (2003). "Early molecular events in the assembly of matrix adhesions at the leading edge of migrating cells." J Cell Sci **116**(Pt 22): 4605-4613.

Zaidel-Bar, R. and B. Geiger (2010). "The switchable integrin adhesome." J Cell Sci **123**(Pt 9): 1385-1388.

Zaidel-Bar, R., R. Milo, et al. (2007). "A paxillin tyrosine phosphorylation switch regulates the assembly and form of cell-matrix adhesions." J Cell Sci **120**(Pt 1): 137-148.

Zamir, E. and B. Geiger (2001). "Molecular complexity and dynamics of cell-matrix adhesions." J Cell Sci **114**(Pt 20): 3583-3590.

Zamir, E., B. Geiger, et al. (2008). "Quantitative multicolor compositional imaging resolves molecular domains in cell-matrix adhesions." PLoS One **3**(4): e1901.

Zamir, E., M. Katz, et al. (2000). "Dynamics and segregation of cell-matrix adhesions in cultured fibroblasts." Nat Cell Biol **2**(4): 191-196.

Zervas, C. G., S. L. Gregory, et al. (2001). "Drosophila integrin-linked kinase is required at sites of integrin adhesion to link the cytoskeleton to the plasma membrane." J Cell Biol **152**(5): 1007-1018.

Zhang, M., M. Windheim, et al. (2005). "Chaperoned ubiquitylation--crystal structures of the CHIP U box E3 ubiquitin ligase and a CHIP-Ubc13-Uev1a complex." Mol Cell **20**(4): 525-538.

Zhang, Y., L. Guo, et al. (2002). "A critical role of the PINCH-integrin-linked kinase interaction in the regulation of cell shape change and migration." J Biol Chem **277**(1): 318-326.

Zhang, Y., T. Ikegami, et al. (2006). "Involvement of integrin-linked kinase in carbon tetrachloride-induced hepatic fibrosis in rats." Hepatology **44**(3): 612-622.

Zhong, C., M. Chrzanowska-Wodnicka, et al. (1998). "Rho-mediated contractility exposes a cryptic site in fibronectin and induces fibronectin matrix assembly." J Cell Biol **141**(2): 539-551.

Zhou, P., N. Fernandes, et al. (2003). "ErbB2 degradation mediated by the co-chaperone protein CHIP." J Biol Chem **278**(16): 13829-13837.

Zhu, J., B. H. Luo, et al. (2008). "Structure of a complete integrin ectodomain in a physiologic resting state and activation and deactivation by applied forces." Mol Cell **32**(6): 849-861.